museum

SERVICE GEOLOGIQUE DE BELGIQUE
BELGISCHE GEOLOGISCHE DIENST

Geological Survey of Belgium

Rue Jenner 13 - 1000 Bruxelles
Jennerstraat 13 - 1000 Brussel

ISSN 0378-0902

KONINKLIJK BELGISCH INSTITUUT VOOR NATUURWETENSCHAPPEN

INSTITUT ROYAL DES SCIENCES NATURELLES DE BELGIQUE

ROYAL BELGIAN INSTITUTE OF NATURAL SCIENCES

GEOLOGICAL SURVEY OF BELGIUM
PROFESSIONAL PAPER 2006/1 – N. 302

PETROGRAPHIC ATLAS OF THE POTENTIALLY ALKALI-REACTIVE ROCKS IN EUROPE

G. LORENZI, J. JENSEN, B. WIGUM, R. SIBBICK,
M. HAUGEN, S. GUÉDON, U. ÅKESSON

KONINKLIJK BELGISCH INSTITUUT VOOR NATUURWETENSCHAPPEN

INSTITUT ROYAL DES SCIENCES NATURELLES DE BELGIQUE

ROYAL BELGIAN INSTITUTE OF NATURAL SCIENCES

GEOLOGICAL SURVEY OF BELGIUM PROFESSIONAL PAPER
2006/1 - N.302

Petrographic atlas of the potentially alkali-reactive rocks in Europe *

G. LORENZI, J. JENSEN, B. WIGUM, R. SIBBICK,
M. HAUGEN, S. GUÉDON, U. ÅKESSON

Gabriel Lorenzi, ISSeP, Institut Scientifique de Service public, rue du Chéra 200, B-4000 Liège (Belgium) – ga.lorenzi@issep.be
Jørn Jensen, PC Laboratoriet A/S, Maagevej 7, DK-9690 Fjerritslev (Denmark) - jcj@pclab.dk
Børge Wigum, Hönnun, Grensásvegur 1, 108 Reykjavik (Iceland) - wigum@honnun.is
Richard Sibbick, formerly BRE (UK) now W.R. Grace & Co, Cambridge, MA (USA) – richard.sibbick@grace.com
Marit Haugen, SINTEF, Civil and Environmental Engineering Cement and Concrete, N-7565 Trondheim (Norway) – marit.haugen@sintef.no
Sylvine Guédon, LCPC, Laboratoire Central des Ponts et Chaussées, Boulevard Lefèbvre 58, F-75732 Paris Cedex 15 – guedon@lcpc.fr
Urban Åkesson, SP, Swedish National Testing and Research Institute, Box 857, SE-501 15 Borås (Sweden) – urban.akesson@sp.se

*FP5 - PARTNER-project-GRD1-CT-2001-40103

(63 pages, 192 photographs)

Cover illustration: Mylonite from Norway showing a strong ductile deformation. Cross-polarized light with gypsum plate inserted. Picture is 2,9 mm wide.

CONTENT

Foreword 1
Introduction 2
Method 2
1. Sedimentary rocks 3
 1.1. Siliceous rocks 3
  1.1.1. Flint – chert 3
  1.1.2. Sandstone 3
  1.1.3. Siltstone 4
  1.1.4. Greywacke 4
 1.2. Carbonate rocks 5
  1.2.1. Limestone 6
2. Metamorphic rocks 6
  2.1. Gneiss 7
  2.2. Metaquartzite – metagreywacke 7
  2.3. Phyllite 8
  2.4. Mylonite 9
  2.5. Cataclasite 9
  2.6. Hornfels 10
3. Igneous rocks 10
  3.1. Basalts and volcanic glass 10
  3.2. Rhyolite 10
  3.3. Granite – granophyre 11
  3.4. Porphyritic diorite 11
4. Regional experience – some examples 12
  4.1. Belgium 12
  4.2. Denmark 12
  4.3. Norway 13
  4.4. Sweden 13
Acknowledgements 14
References 15
Photoplates 15
  Flint – chert 16
  Sandstone 16
  Siltstone 21
  Greywacke 24
  Limestone 25
  Gneiss 29
  Metaquartzite - metagreywacke 35
  Phyllite 37
  Mylonite 40
  Cataclasite 42
  Hornfels 45
  Basalts and volcanic glass 46
  Rhyolite 48
  Granite - granophyre 49
  Porphyritic diorite 51
  Belgium 52
  Denmark 53
  Norway 56
  Sweden 58
Colofon 62

64

FOREWORD

A wide variety of concrete aggregate types in common use across Europe, particularly those with a siliceous composition, can be vulnerable to attack by the alkaline pore fluid in concrete; this reaction is so named "the alkali-silica reaction (ASR)". This reaction can cause, in wet conditions, the deterioration of the concrete: the reaction product is an alkali-silica gel which expands by absorbing water and consequently provokes the development of microcracks initially within the reactive aggregate particle, but eventually throughout the concrete, if the reaction is severe, leading to its expansion and disruption. The reaction generally takes 2-3 years to 10-15 years to start and develop, depending on various parameters including the aggregate reactivity. The mechanism of the reaction is complex, but, schematically, this reaction needs chemical interaction between alkali hydroxides, reactive silica and water. The alkalinity of the pore solution is a normal result of the hydration of Portland cement (the alkali content of the cement and the cement content will primarily determine the level of alkalinity); alkalis from other sources such as additions (slag, fly ash,...), de-icing salts, etc., can also influence the pore solution alkalinity. The reactive silica is usually derived from the aggregates: it is widely accepted that the siliceous minerals susceptible to the alkalis significantly enough to cause severe degradation include: opal, chalcedony, micro-cryptocrystalline quartz, tridymite, cristobalite, strained quartz and some siliceous glasses. The reactivity of an aggregate in a particular concrete will finally depend on the cement type used, on the alkali content in the concrete and the presence and source of water, combined with the exposure effects of the structural design. It will also depend on the content of the reactive rock type in the aggregate. The alkali-silica reaction can be written as follows:

SiO_2 (reactive silica in aggregates) + $[Na, K, Ca]_{sol.}$ cement/external + H_2O → swelling AS gel

Alkali-reactive aggregates have been investigated for many years and as a result different test methods have been developed. Unfortunately, such tests are, in some cases, only relevant for specific materials within a country.

The **PARTNER project** (contract n° GRD1-CT-2001-40103), supported by the fifth European Framework Program, has mapped the known types of reactive aggregates throughout Europe, based on laboratory and field experience.

During the project a state of the art report has been produced and several testing methods have been evaluated such as: the RILEM AAR-1 petrographic method, RILEM AAR-2 accelerated mortar bar test, the RILEM AAR-3 and AAR-4 concrete tests. These laboratory tests have been validated by field tests under different climates. Overall, the project provides the basis for a unified European testing methodology to evaluate and classify the alkali reactivity of aggregates in concrete.

This petrographic atlas, which covers the European alkali silica reactive concrete aggregates, has been produced as part of the **PARTNER project**.
The project involved 24 partners from 14 countries covering most of Europe, from Iceland to Greece :

BRE - Building Research Establishment (United Kingdom)
PC Laboratoriet A/S - Ltd company in materials technology (Denmark)
SINTEF - Civil and Environmental Engineering Cement (Norway)
SP - Swedish National Testing and Research Institute (Sweden)
RAMBOLL - Consulting Engineers company (Denmark)
ISSeP - Institut Scientifique de Service Public (Belgium)
LCPC - Laboratoire Central des Ponts et Chaussées (France)
VDZ - German Cement Works Association (Germany)
TITAN Cement Company, S.A (Greece)
LABEIN - Technological research and innovation centre (Spain)
CRIC - Centre national de Recherche Scientifique et Technique pour l'Industrie Cimentière (Belgium)
IMBiGS - Instytut Mechanizacji Budownictwa I Gornictwa (Poland)
NORCEM A.S - Norwegian cement - Heidelberger Cement Group (Norway)
CESI - Centro Elettrotecnico Sperimentale Italiano (Italy)
VÖZ - Research Institute of the Austrian Cement industry (Austria)
IBRI - Icelandic Building Research Institute (Iceland)
STATS Ltd - Consulting Engineers company (United Kingdom)
NCC Construction Sweden AB (Sweden)
DTI - Danish Technological Institute (Denmark)
AIDICO - Construction technology Institute (Spain)
ANEFA - National Association of Spanish aggregate producers (Spain)
CEMEX - Central laboratory (Spain)
HOLCIM AGGREGATE - Holderbank Group (Belgium)
HÖNNUN - Consulting Engineers company (Iceland)

INTRODUCTION

The aim of this petrographic atlas of the potentially alkali-reactive rocks in Europe is to assist geologists who work in the field of the concrete degradations and in particular in the field of the alkali-silica reactions.

It is not possible, in only one atlas, to describe every type of concrete alkali-reactive aggregate from Europe. In particular, some aggregates like the sands and the gravels, often contain several different rock types. For these reasons, this atlas has been based on the parent rocks rather than on the aggregates.

In this atlas, the rocks are firstly classified according to their genetic origin (sedimentary, metamorphic or igneous) using the international nomenclatures; secondly, they have been grouped as families of similar species. For each rock family, a general description is given in the header, including the most particular characteristics of the different rock species from different countries. The reactive components are emphasized within the descriptions and, when possible, within the pictures which illustrate the type of aggregate. Despite the fact that this atlas is not exhaustive, it is nevertheless representative of the majority of the European alkali-reactive rocks.

Concerning the aggregates, it is important to emphasize additional points:
- Firstly, if some rock types are reactive, it does not necessary mean that all rocks of the same family are reactive too.
- Secondly, some aggregate types exhibit a pessimum effect: actually, when a certain amount of reactive aggregate is reached in the concrete the expansion is at its maximum, whereas below and above this particular value less or even no expansion is observed. Because of the pessimum effect a greater proportion of a particular reactive rock type may not necessarily lead to greater reactivity.

METHOD

Petrography, the systematic description of rocks (and concretes) in thin sections, is a basic investigative tool for geologists worldwide. Thin sections are slices of rock/concrete ground down to a thickness of about 30 microns. Usually, the size of the sample to be studied is 50 x 40 x 0,030 mm but larger thin-sections can be prepared. The 30 microns thickness is standard and is necessary for the minerals to become translucent and in order to study the birefringence of the minerals by which they can be identified. The thin sections can be studied under a polarized microscope in varying modes of transmitted light: plane polarized light (PPL), cross-polarized light (XPL), cross-polarized light with gypsum plate inserted (XPLG) and fluorescent light (FL).

The fluorescent mode is obtained by first vacuum-impregnating the sample with an epoxy resin containing a yellow fluorescent dye, and then inserting two filters in the light path of a halogen lamp: an excitation band pass filter (with a maximum transmission of 400 nm) and a suppression long pass filter (with a maximum transmission of 500-550 nm). This mode makes the petrographic technique especially suitable for the study of porosities and microcracking. The result, in PPL view, is a sample embedded in a impregnation resin coloured in yellow, and, in FL view, a sample showing a differential porosity: the more porous the sample, the more intense the yellow-green colour (the non porous particles are nearly black or opaque).

1. Sedimentary rocks

1.1. Siliceous rocks

1.1.1. Flint – chert

The term **flint** is generally used as a synonym of chert. They are rocks consisting of silica in the form of micro- or cryptocrystalline quartz. Primary flint or chert is mainly composed of silica derived from siliceous organisms such as siliceous sponges, diatoms and radiolaria, and secondary flint or chert, which replaces calcite minerals in the limestones with silica.

Dense flint may contain varying amounts of carbonates, which range from small to larger crystals, occurring either individually or within specific areas of the rock. The fluorescence microscopy technique (FL) doesn't reveal any porosity within this rock type.

Chalcedony is another form of silica found in flint, which consists of feathered crystals of microquartz.

The porosity of the **porous chalcedony and porous flints** is revealed easily using fluorescent microscopy.

Opaline flint consists of isotropic hydrated silica (**opal**) associated with varying amounts of carbonates. When the carbonate is the major constituent of the rock, it makes the identification of the opaline flint phase difficult in such rock types. However the fluorescent microscopy technique can help by revealing the higher porosity of the opaline flint material. The opaline flint in these rocks is constantly isotropic (black) in XPL and bordeaux red in XPL with gypsum plate inserted.

1, 2, 3. *Dense flint composed of cryptocrystalline quartz (center of the photo). The grains of sand are embedded in a yellow impregnation epoxy resin.*
(PPL, XPL, XPLGx20, pictures are 5,8 mm wide).

4. Same view as picture 1. Fluorescent light reveals the lack of porosity.
(FLx20, picture is 5,8 mm wide).

5. Porous flint composed of cryptocrystalline quartz.
(PPLx40, picture is 2,9 mm wide).

6, 7. *Same view as picture 5 revealing the potentially reactive cryptocrystalline quartz.*
(XPL, XPLGx40, pictures are 2,9 mm wide).

8. Same view as picture 5. FL reveals a high porosity.
(FLx40, picture is 2,9 mm wide).

9, 10*. Grain of opaline flint.*
(PPL, XPLx40, pictures are 2,9 mm wide)

11. *Same view as picture 9, under cross-polarized light with gypsum plate, showing the particular bordeaux interference colour.*
(XPLGx40, picture is 2,9 mm wide).

12*. Same view as picture 9. FL reveals a high porosity.*
(FLx40, picture is 2,9 mm wide).

13, 14. *Flints containing varying amounts of carbonates.*
(PPL, XPLx40, pictures are 2,9 mm wide).

15. *Other flints containing varying amounts of carbonates.*
(PPLx40, picture is 2,9 mm wide).

16*. Same view as picture 15: carbonates show creamy interference colours.*
(XPLx40, picture is 2,9 mm wide).

17, 18, 19. *Chalcedonic flint with the particular feathered crystals of micro-cryptocrystalline quartz .*
(PPL, XPL, XPLGx40, pictures are 2,9 mm wide).

20. *Same view as picture 17: FL reveals no porosity.*
(FLx40, picture is 2,9 mm wide).

1.1.2. Sandstone

Sandstones are terrigenous rocks derived from clastic sediments formed after the weathering of pre-existing rocks. These rocks are largely composed of quartz, feldspar and rock fragments. A matrix makes up the cementing agent for the particles; this latter can be fine-grained and composed of clay minerals or it may be a secondary cement, such as silica, iron or carbonates. Sandstones are classified according to the amount of these various clastic components, the amount of the matrix material (greater or less than 15 %) and the grain size.

The main reactive sandstones found in Europe are sandstones with an argillaceous matrix. The recrystallisation of particular minerals (e.g. secondary biotite) and the lineation of some areas of the clayey matrix suggest some degree of low-grade metamorphism affecting all these rocks. It is widely accepted that the reactive components are mainly the very fine-grained sedimentary quartz (micro-cryptocrystalline grains) embedded within the clayey matrix.
Particular sandstones with an opaline component to the matrix have also been found to be reactive.

21. *Fine sandstone with rounded grains cemented partly with recrystallized silica and partly with a cryptocrystalline matrix.*
(PPLx40, picture is 2,9 mm wide).

22. *Detail showing the cryptocrystalline cement.*
(XPLx100, picture is 1,15 mm wide).

23. *Same view as picture 22 showing the matrix with the potentially reactive cryptocrystalline quartz.*
(XPLGx100, picture is 1,15 mm wide).

24. *Very fine sandstone with spots of secondary biotite resulting from a low-grade metamorphism; the grains are cemented with a very thin argillaceous matrix.*
(PPLx40, picture is 2,9 mm wide).

25. *Same view as picture 24. The argillaceous matrix acts as a support framework to the potentially micro- to cryptocrystalline quartz.*
(XPLx40, picture is 2,9 mm wide).

26, 27. *Detail of picture 24 showing the thin matrix and biotites.*
(PPL, XPLx100, pictures are 1,15 mm wide).

28, 29. *Medium-grained sandstone with rounded clastic grains cemented with a cryptocrystalline clayey matrix.*
(PPL, XPLx20, pictures are 5,8 mm wide).

30. *Sand grain of opaline sandstone. The grain is embedded in a yellow impregnation epoxy resin.*
(PPLx20, picture is 5,8 mm wide).

31. *Same view as picture 30, under fluorescent light showing a high porosity.*
(FLx20, picture is 5,8 mm wide).

32, 33. *Close-up detail of picture 30 showing the different components: siliceous needles, other silica sponge debris and glauconite in an opaline matrix.*
(PPL, XPLx40, pictures are 2,9 mm wide).

34. *Same view as picture 32 revealing opal and cryptocrystalline quartz.*
(XPLGx40, picture is 2,9 mm wide).

1.1.3. Siltstone

Siltstones are terrigenous rocks derived from fine-grained clastic sediments, in which the grain size ranges between 0,0039 and 0,0625mm. They are generally enriched in clay minerals. As with the sandstones and greywackes, it is widely accepted that the reactive components are mainly the very fine-grained quartz embedded within the clayey matrix.

35, 36. *Siltstone: fine grains of quartz and altered feldspars embedded in a dark argillaceous matrix enriched with opaque minerals.*
(PPL, XPLx40, pictures are 2,9 mm wide).

37, 38. *Another siltstone containing quartz, chlorite, pyrite, muscovite, calcite and clay minerals (sericite), all cemented together by fine silica and a little calcite.*
(PPL, XPLx40, pictures are 2,9 mm wide).

1.1.4. Greywacke

Greywackes are sandstones containing more than 15 % of fine-grained matrix. Many of them are related to the mode of formation "Turbidite sequences" (Tucker, 2001); they are generally a complete jumble of particle types with different sizes and shapes cemented within a clayey matrix and like for the sandstone and siltstones, it is widely accepted that the reactive components are mainly the very fine-grained quartz embedded within the clayey matrix.

39, 40. *Fine-grained greywacke showing potentially reactive fine quartz and a lot of secondary biotite grains embedded within a clayey matrix.*
(PPL, XPLx40, pictures are 2,9 mm wide).

41. *Poorly sorted greywacke.*
(PPLx40, picture is 2,9 mm wide).

42. *Same view as picture 41 showing the rocks particles embedded within a cryptocrystalline matrix containing the potentially very fine-grained quartz.*
(XPLx40, picture is 2,9 mm wide).

43. *Fine-grained greywacke partly cemented with calcite*
(PPLx40, picture is 2,9 mm wide).

44. *Same view as picture 43 : calcite shows pinkish interference colours.*
(XPLx40, picture is 2,9 mm wide).

45. *Grain of fine greywacke embedded in a yellow epoxy resin and showing cleavage.*
(PPLx20, picture is 5,8 mm wide).

46. *Detailed view of previous picture.*
(PPLx40, picture is 2,9 mm wide).

47. *Same view as picture 46 showing the uniform orientation of the clay minerals composing the matrix.*
(XPLGx40, picture is 2,9 mm wide).

48. *Poorly sorted greywacke with coarse quartz and altered feldspar grains (sericite) and showing a cleavage.*
(PPLx20, picture is 5,8 mm wide).

49. *Same view as the previous picture showing the sericite grains.*
(XPLx20, picture is 5,8 mm wide).

50. *Close-up view of picture 49 showing the microcrystalline matrix and the sericite.*
(XPLx100, picture is 1,15 mm wide).

51. *Medium sorted greywacke with very fine to medium coarse grains embedded within the clayey matrix.*
(PPLx20, picture is 5,8 mm wide).

52. *Same view as previous picture emphasizing the secondary biotite (reddish interference colours).*
(XPLx20, picture is 5,8 mm wide).

1.2. Carbonate rocks

1.2.1. Limestone

Limestones are sedimentary rocks consisting mainly of calcite with variable amounts of dolomite and other minor impurities. They are primarily made up of allochems (ooids, bioclasts, peloids,...) and terrigenous elements (quartz, clays, rock debris). They are classified by comparing the proportions of carbonate matrix, either mud (micrite), or sparry calcite (sparite), and the allochems.

The alkali-reactive limestones can be divided into two groups:
- The **silicified limestones**: these rocks are usually packstones, wackestones or mudstones; they are mostly fine dark-grey argillaceous limestones often including fossil debris, some detrital quartz grains and showing some silicification. The reactive silica is found in the form of diagenetic micro-cryptocrystalline quartz or chalcedony and usually partially replaces the calcite within the fossils; it can also be found as discrete cryptocrystalline masses within the matrix, or as an infilling to some voids. Often, this limestone type shows some dolomitization. The dark colour is usually due to the presence of organic matter. White varieties of such a type of rocks, with less organic matter, are however found to be reactive too.
- **Non-silicified limestones**: this rock type is similar to the silicified limestone (fine dark-grey argillaceous limestone often with fossil debris and dolomitization), but showing no silicification. The reactive silica is found, after a specific type of chemical attack, as very fine detrital quartz grains embedded within the argillaceous matrix. Of course, this type of very fine detrital quartz dust can also be found within the silicified limestones.

53. *Silicified wackestone with many fossil debris such as echinoids, brachiopods, with very thin layers of dark organic matter and clays.*
(PPLx 20, picture is 5,8 mm wide).

54. *Same limestone: coarse piece of shell completely silicified.*
(PPLx 20, picture is 5,8 mm wide).

55, 56. *Same views as picture 54: the calcite of the shell is replaced by potentially reactive microquartz which is revealed by its low first-order interference colours.*
(XPL, XPLGx20, pictures are 5,8mm wide).

57. *Grain of a silicified micritic limestone: the grain is embedded in a yellow impregnation epoxy resin.*
(PPLx20, picture is 5,8 mm wide).

58. *Detailed view of previous picture showing microfossils embedded in a micritic matrix.*
(PPLx40, picture is 2,9 mm wide).

59, 60. *Same views as picture 58 showing the potentially reactive microsilica within the matrix (low first order interference colours).*
(XPL, XPLGx40, pictures are 2,9 mm wide).

61. *Grain of a silicified sparitic limestone with a white area of silica.*
(PPLx20, picture is 5,8 mm wide).

62. *Same view as picture 61showing the silicification with some chalcedony.*
(XPLx20, picture is 5,8 mm wide).

63. *Same view as 62 with gypsum plate inserted.*
(XPLGx20, picture is 5,8 mm wide).

64. *Silicified micritic limestone with spherulites embedded in a fine matrix.*
(PPLx40, picture is 2,9 mm wide).

65. *Same view as picture 64 showing the silicification of the spherulites.*
(XPLGx40, picture is 2,9 mm wide).

66. *Silicified packestone with a lot of coarse fossil debris now partly silicified.*
(PPLx20, picture is 5,8 mm wide).

67. *Same view as picture 66 showing silicification.*
(XPLx20, picture is 5,8 mm wide).

68. *Micritic microfacies of the same limestone with fine sized silicification.*
(PPLx20, picture is 5,8 mm wide).

69, 70. *Detailed views revealing silicification impregnating the matrix.*
(XPL, XPLGx20, pictures are 5,8 mm wide).

71. *Silicified wackestone with lighter coloured uniform areas of silica.*
(PPLx20, picture is 5,8 mm wide).

72, 73. *Same views showing chalcedony.*
(XPL, XPLGx20, pictures are 5,8 mm wide).

74. *View under the SEM of the polished surface of a silicified limestone gently attacked with diluted hydrochloric acid: a fine net of reactive diagenetic silica is clearly visible. To be compared with picture 78.*
(Picture is 180 µm wide).

75, 76, 77. *Different microfacies of a highly reactive limestone without silicifications.*
(PPLx20, x40, x20, pictures are respectively 5,8; 2,9; 5,8mm wide).

78. *View under the SEM of the polished surface of a reactive non-silicified limestone which has been gently attacked with diluted hydrochloric acid: there is no diagenetic silica net, but only small amounts of clay are visible. To be compared with picture 74.*
(Picture is 160 µm wide).

2. Metamorphic rocks

2.1. Gneiss

The term "gneiss" covers a multitude of banded rocks formed during high-grade regional metamorphism of either sedimentary or igneous rocks. These rocks contain a large number of different minerals in variable amounts, but often they are composed largely of quartz, feldspars, micas and mafic minerals. Generally, gneisses are not reactive, but when micro- or cryptocrystalline quartz are present, they might be potentially reactive. Often strained quartz is a sign of potential reactivity. This might be caused by its association with more complex metamorphic suturing on the crystal boundaries and thus the development of separated microquartz crystals at these boundaries, which are potentially reactive.

79, 80. *General view of a grain of gneiss embedded in a yellow epoxy resin.*
(PPL, XPLx40, pictures are 2,9 mm wide).

81. *Other gneiss : view of an area with micro- cryptocrystalline quartz.*
(XPLx100, picture is 1,15 mm wide).

82. *General view of micro- cryptocrystalline quartz and strained quartz.*
(XPLx40, picture is 2,9 mm wide).

83. *Detailed view of micro- cryptocrystalline quartz and strained quartz.*
(XPLx100 picture is 1,15 mm wide).

84. *Another grain of gneiss: general view of microcrystalline quartz and strained quartz.*
(XPLx40, picture is 2,9 mm wide).

***85.** Detailed view of micro- cryptocrystalline quartz and strained quartz.*
(XPLx100, picture is 1,15 mm wide).

***86.** Another area in the same gneiss.*
(XPLx40, picture is 2,9 mm wide).

***87.** Microquartz in a layer of mica.*
(XPLx100, picture is 1,15 mm wide).

2.2. Metaquartzite – metagreywacke

Metaquartzite (or quartzite) is a hard metamorphic rock, which was originally a sandstone. Under conditions of metamorphism, the original grains have recrystallized along with the former cementing material to form an interlocking mosaic of crystals, mainly quartz and feldspars. Minor amounts of the former cementing materials, iron oxide, carbonate and clay, are often recrystallized and migrate under the pressure to form streaks and lenses within the quartzite. All original textures and structures have usually been erased by the metamorphism. Often, quartzite shows stress features, such as foliation, strained quartz,etc. Generally, quartzite is not reactive but when substantial amounts of micro- or cryptocrystalline quartz are present they might be reactive. The terms orthoquartzite / quartzite are also used to refer to quartz-arenite (sandstone with more than 95 % of quartz) cemented primarily with secondary silica giving a well-imbricated grains structure.

Metagreywacke has also been found to be reactive. A metagreywacke is a metamorphic rock, which was originally a greywacke.

***88, 89.** General view of a fine quartzite.*
(PPL, XPLx40, pictures are 2,9 mm wide).

***90, 91.** Detailed view showing the strained quartz embedded in a matrix of potentially reactive microquartz and mica.*
(XPL, XPLGx100, pictures are 1,15 mm wide).

***92.** General view of a metaquartzite grain showing strained quartz intergrown with microquartz.,*
(XPLx40, picture is 2,9 mm wide).

***93.** Detail of the previous photo.*
(XPLx100, picture is 1,15 mm wide).

***94.** General view of another metaquartzite grain showing strained and deformed quartz and microquartz.*
(XPLx40, picture is 2,9 mm wide).

***95.** Detailed view of the previous photo.*
(XPLx100, picture is 1,15 mm wide).

***96.** General view of a fine quartzite.*
(XPLx40, picture is 2,9 mm wide).

***97.** Another view of the same sample.*
(XPLGx40, picture is 2,9 mm wide).

***98.** Detailed view showing the elongated quartz and the potentially reactive microquartz, with some associated layers of muscovite.*
(XPLx100, picture is 1,15 mm wide).

***99.** Metagreywacke with finely grained clastic quartz and feldspar components within a dark-grey microcrystalline siliceous matrix, considered as potentially reactive. The argillaceous brown-reddish layers form a less pronounced cleavage.*
(XPLx200, picture is 0,60 mm wide).

2.3. Phyllite

Phyllite is a metamorphic rock, intermediate between slate and schist; the individual mineral grains are not clearly discernable to the naked eye. It is characterized by a lustreous sheen and usually shows a well-developed cleavage. The rock is often wavy / folded in appearance with a lot of micas, which are nearly parallel oriented and give the rock a cleavage. Sometimes, the rock has a high content of quartz, and when the quartz grain size is on average less than 60 μm, the rock is considered as potentially reactive. Carbonate is sometimes visible in this rock type too.

100. *Phyllite: the rock is wavy / foliated with a large proportion of micas and chlorites.*
(PPLx40, picture is 2,9 mm wide).

101, 102. *Detailed view of picture 100 showing the potentially reactive micro- cryptocrystalline quartz.*
(PPL, XPLx100, pictures are 1,2 mm wide).

103, 104. *Quartz-phyllite: this wavy / foliated rock contains a large amount of fine and micro-cryptocrystalline quartz grains.*
(PPL, XPLx40, pictures are 3,2 mm wide).

105. *Detailed view of picture 104 showing the potentially reactive micro-cryptocrystalline quartz.*
(XPLx100, picture is 1,2 mm wide).

2.4. Mylonite

Mylonite is a foliated (and usually lineated) fine-grained dynamic metamorphic rock which shows evidence for strong ductile deformation. The term is purely structural and gives no indication of the mineralogy of the rock. Thus, a mylonite can be compositionally derived from any rock type and mylonite zones can be found in rocks of all ages and can be found on almost any scale.

Mylonites have two types of constituents, matrix and porphyroclasts. The matrix is composed of the more ductile elements of the rock and of micro- cryptocrystalline minerals, such as quartz minerals. This part of the rock appears almost fluid while the porphyroclasts are the more brittle elements of the rock. A true mylonite will be composed of 10-50 % porphyroclasts.

The different mylonite types are classified in the literature as followed: primary, secondary, protomylonite, ultramylonite, blastomylonite, layered mylonite and hyalomylonite. The classification is based mainly on the degree of metamorphism and secondarily on the matrix / porphyroclasts ratio. The reactive minerals are crypto-microcrystalline quartz and stressed quartz grains of different sizes within the matrix.

106. *General view of a mylonite : deformed rock with stressed porphyroclasts of feldspars and quartz.*
(XPLx20, picture is 5,8 mm wide).

107, 108. *Detailed view of porphyroclasts embedded in a micro-cryptocrystalline matrix including the potentially reactive quartz.*
(XPL, XPLGx40, pictures are 2,9 mm wide).

109. *Other view of the porphyroclasts and thin layers of mica within the matrix.*
(XPLx40, picture is 2,9 mm wide).

110, 111. *Sericitic gneiss-mylonite with heterogeneous deformation under retrograde metamorphic conditions of green schist facies. Center: strongly deformed quartz with sutured grain boundaries and undulatory extinction; bottom right: microshear zone with fine granoblastic quartz grains; upper half: sericitic lenses formed from instable plagioclase; dark central grain: potassic feldspar.*
(XPL, XPLGx40, pictures are 3.9 mm wide).

112, 113. *Another mylonite grain embedded in a yellow epoxy resin: general view showing the porphyroclasts of different sizes.*
(PPL, XPL x40, pictures are 2,9 mm wide).

114. *Detailed view of the porphyroclasts and the micro-cryptocrystalline matrix including the potentially reactive quartz grains.*
(XPLx100, picture is 1,15 mm wide).

115, 116, 117. *General view of another type of mylonite (mylonite / cataclasite) : deformed porphyroclasts embedded in a micro-cryptocrystalline matrix. The dark zones are enriched in organic matter which has migrated under the pressure.*
(PPL, XPL, XPLGx20, pictures are 5,8 mm wide).

118, 119. *Detailed view of the porphyroclasts and the recrystallized clayey matrix including the potentially reactive cryptocrystalline quartz.*
(XPL, XPLGx100, pictures are 1,15 mm wide).

2.5. Cataclasite

A **cataclasite** is a rock, which only has undergone mechanical breakage without showing the plastic deformation and flowage as seen in the mylonites. The rock is brittle deformed and contains randomly distributed and oriented clasts of assorted size derived from the original rock embedded in a matrix of crypto- to microcrystalline minerals. This fine matrix material contains varying amounts of quartz from which the reactivity potential of the rock is derived.

120, 121. *General view of a cataclasite: coarse sized rock debris embedded in a fine-grained matrix.*
(PPL, XPLx20, pictures are 5,8 mm wide).

122, 123. *Detailed view of rocks debris of different sizes embedded within a micro-cryptocrystalline matrix rich in potentially reactive quartz.*
(XPL, XPLGx40, pictures are 2,9 mm wide).

2.6. Hornfels

Hornfels is a fine-grained rock formed by contact metamorphism. It is characterised by a fine-grained matrix without preferred orientation, in which phenocrysts or clasts can be embedded.
Reactive hornfels is found as a rock where the matrix is now composed largely of sericite and including potentially reactive micro-cryptocrystalline quartz grains and some feldspars.

124, 125. *Hornfels: general view showing elongated brownish biotite minerals in a very fine-grained groundmass.*
(PPL, XPLx20, pictures are 5,2 mm wide).

126. *Detailed view: the rock mainly consists of quartz, feldspar, biotite and pyroxene.*
(XPLx100, picture is 1,2 mm wide).

127, 128. *Another view of the same hornfels showing a zonation. Due to the very fine grains, the minerals are hard to be identified.*
(PPL, XPLx20, pictures are 5,2 mm wide).

129. *Detailed view showing some potentially reactive micro- and cryptocrystalline quartz grains. The blue minerals are chlorites.*
(XPLx100, picture is 1,2 mm wide).

3. Igneous rocks

3.1. Basalt and volcanic glass

Basalts are generally dark-coloured and fine-grained basic extrusive igneous rocks. They are mainly composed of augite and plagioclase with opaque minerals. Basalts can be subdivided into tholeiitic basalts and alkali olivine basalts depending on the presence or absence of accessory olivine, quartz and low-Ca pyroxenes. As far as the alkali-silica reaction is concerned, the first basalt type "tholeiite" is the most interesting as it is oversaturated with silica, which is present as cristobalite, tridymite and quartz within the glassy groundmass. It is often impossible to detect these minerals by optical microscopy, and XRD analysis is generally required. According to Katayama et al (1996), it is believed that the high reactivity of some basalts is due to the presence of secondary opal or chalcedony, in combination with the primary cristobalite and rhyolitic glass. Moreover, basaltic rock is usually non-reactive when it is glassy and contains fresh basaltic glass, but may show a potential reactivity when it contains rhyolitic interstitial glass as a residual melt.

130, 131. *Tholeiitic basalt: fine elongated plagioclase crystals embedded within a brown glassy groundmass (palagonite). The glass is potentially alkali-reactive.*
(PPL, XPLx100, pictures are 1,37 mm wide).

132, 133. *Tholeiitic basalt: elongated plagioclase crystals and larger crystals of clinopyroxene embedded within a altered-brown glassy groundmass (palagonisation), which is the potentially alkali-reactive constituent.*
(PPL, XPLx100, pictures are 1,37 mm wide).

134, 135. *Volcanic glass: palagonite with minor amounts of feldspar phenocrysts. The altered glass is potentially reactive.*
(PPL, XPLx200, pictures are 0,69 mm wide).

3.2. Rhyolite

A rhyolite is an acid volcanic rock with phenocrysts of quartz and alkali feldspar embedded in a glassy or cryptocrystalline groundmass. Rhyolites can contain a high proportion of glass. It is the extrusive igneous equivalent of granite. The glass and cryptocrystalline quartz can be considered as alkali-reactive components.

136, 137. *Rhyolite:* fine-grained groundmass containing potentially reactive glass and cryptocrystalline quartz.
(PPL, XPLx200, pictures are 0,69 mm wide).

138. *Another rhyolite type : general view.*
(PPLx20, picture is 6,3 mm wide).

139. *Same view as the previous one: feldspar phenocrysts embedded within a cryptocrystalline groundmass, which is mainly composed of quartz and feldspars. The cryptocrystalline quartz is potentially reactive.*
(XPLx20, picture is 6,3 mm wide).

140. *Another rhyolite type showing a flow texture.*
(PPLx40; picture is 3,2 mm wide).

141. *Same view as the previous picture: the groundmass is mainly composed of cryptocrystalline feldspar and quartz. The cryptocrystalline quartz is potentially reactive. Some other accessory minerals are also present, like fine mica flakes and dark minerals (opaques, amphiboles, pyroxenes).*
(XPLx40; picture is 3,2 mm wide).

3.3. Granite - granophyre

Granite is a plutonic igneous rock composed mainly of quartz and feldspar crystals with accessory biotite, hornblende and muscovite. It is the coarse-grained equivalent to rhyolite. Granitic rocks should in general not be regarded as alkali reactive. However, microstructural properties due to deformation such as strain lamellas and sub-grain development, may enhance the potential for reaction. It is also believed that Myrmekite, which is becoming commonly recognized in deformed rocks may enhance the potential for reaction. The unsteady state of the quartz component in the Myrmekite, and the probably low crystallinity have to be considered when assessing a potentially reactive aggregate containing this mineral.

Granophyre is a fine-grained igneous rock of granitic composition characterized by a porphyritic texture showing coarse phenocrysts embedded within a cryptocrystalline groundmass. This latter contains the potentially alkali-reactive quartz grains.

142. *Granite with myrmekitic texture.*
(XPLx100, picture is 1,37 mm wide).

143. *Granite with strain lamellas.*
(XPLx100, picture is 1,37 mm wide).

144. *Granite* with sub-grain development.
(XPLx100, picture is 1,37 mm wide).

145. *Granophyre:* cryptocrystalline groundmass with larger crystals embedded.
(PPLx50, picture is 2,75 mm wide)

146. Same view as the previous one.
(XPLx50, picture is 2,75 mm wide).

3.4. Porphyritic microdiorite

Porphyritic quartz-rich microdiorite (or dacitic/andesitic metaporphyry): intrusive rock showing a porphyritic texture with coarse crystals of less than 1 cm size embedded within a fine matrix. The main coarse crystals are plagioclases phenocrysts often weathered into epidotes and/or secondary clay minerals. The chlorites minerals are secondary minerals coming from amphiboles transformation. All these minerals are embedded in a fine-grained matrix composed of micro-cryptocrystalline potentially reactive quartz and feldspars.

147, 148. *Porphyritic quartz-rich microdiorite showing phenocrysts of plagioclases weathered into epidotes and embedded in a fine-grained matrix including potentially reactive micro-cryptocrystalline quartz.*
(PPL, XPLx20, pictures are 6 mm wide).

149, 150. *Porphyritic quartz-rich microdiorite. Additional view showing green spots of secondary chlorite and plagioclase altered to sericite, all embedded in a cryptocrystalline matrix.*
(PPL, XPLx20, pictures are 6 mm wide)

4. Regional experience: examples of reactive aggregates as they appear within the concretes in some countries

4.1. Belgium

151. *ASR with a dense flint.*
(PPLx40, picture is 3,1 mm wide).

152. *Same view, under fluorescent light: the reactive flint does not yet show any porosity but is strongly cracked.*
(FLx40, picture is 3,1 mm wide).

153. *ASR with a porphyritic quartz-rich microdiorite.*
(PPLx20, picture is 6,2 mm wide).

154:. *Same view, XPL.*
(x20, picture is 6,2 mm wide).

155. *Detailed view showing the cracks passing through the porphyry grain and filled with ASR gel.*
(PPLx100, picture is 1,2 mm wide).

156. *ASR with a Lower Carboniferous silicified limestone.*
(PPLx20, picture is 6,2 mm wide).

157. *Detailed view of the ASR gel.*
(PPLx100, picture is 1,2 mm wide).

158. *ASR with two reactive aggregate particles: a siltstone (on the right) and a porphyry (on the left).*
(PPLx40, picture is 3,1 mm wide).

159. *Same view under XPL.*
(x40, picture is 3,1 mm wide).

160. *Detailed view showing cracks filled with AS gel and going from the reactive grain through the surrounding cement paste.*
(PPLx100, picture is 1,2 mm wide).

161. *ASR within a lightly metamorphic sandstone.*
(PPLx100, picture is 1,2 mm wide).

162. *Same view, XPLG.*
(x100, picture is 1,2 mm wide).

4.2. Denmark

163. *Opaline flint, which has reacted and caused cracking of the surrounding concrete.*
(PPLx20, picture is 5,3 mm wide).

164. *Same view as picture 163 showing the high porosity of the opaline flint.*
(FLx20, picture is 5,3 mm wide).

165. *Opaline flint, which has reacted and caused internal cracking and filling of adjacent pores with alkali-silica gel from ASR.*
(PPLx20, picture is 5,3 mm wide).

166. *Same view as picture 165 showing the high porosity of the reactive opaline flint.*
(FLx20, picture is 5,3 mm wide).

167, 168. *Dense flint with porous area that has reacted.*
(PPL, FLx20, pictures are 5,3 mm wide).

169. *Detailed view of the same flint.*
(XPLx40, picture is 2,7 mm wide).

170. *Other opaline flint with strong cracking and filling of cracks with alkali-silica gel.*
(PPLx20, picture is 5,3 mm wide).

171. *Same view as the picture 170.*
(FLx20, picture is 5,3 mm wide).

4.3. Norway

172. *ASR with a mylonite aggregate which has caused cracks through the cement paste and the aggregates and containing AS gel.*
(PPLx20, picture is 4,7 mm wide).

173. *Same view as picture 172 showing the potentially reactive micro- to cryptocrystalline matrix.*
(PPLx20, picture is 4,7 mm wide).

174. *Detailed view of previous picture showing the AS gel filling cracks at the edge of the aggregate.*
(PPLx100, picture is 0,9 mm wide).

175. *ASR within sandstone aggregates: the cement paste and the aggregates are cracked.*
(PPLx20, picture is 4,7 mm wide).

***176.** Detailed view of the previous picture: the cracks are filled with AS gel.*
(PPLx100, picture is 0,9 mm wide).

***177.** Other detailed view showing the potentially reactive micro-cryptocrystalline quartz cement surrounding the larger clastic grains.*
(PPLx20, picture is 5,5 mm wide).

***178, 179.** ASR with a greywacke aggregate: air voids with AS gel.*
(PPL, XPLx20, pictures are 4,7 mm wide).

***180.** Detailed view: fine cracks through the upper part of the greywacke aggregate, containing AS gel.*
(PPLx40, picture is 2,4 mm wide).

***181.** Same view, under cross-polarized light, highlighting the potentially reactive micro-cryptocrystalline matrix of the greywacke.*
(XPLx20, picture is 4,7 mm wide).

***182.** ASR with a rhyolite aggregate: strong cracking through the aggregate; the cracks contain AS gel at the edge of the aggregate.*
(PPLx20, picture is 4,7 mm wide).

***183.** Same view under cross-polarized light showing the very fine-grained matrix with some large crystals of feldspars embedded (left side).*
(XPLx20, picture is 4,7 mm wide).

***184.** Detailed view showing the AS gel filling cracks at the edge of the aggregate.*
(PPLx100, picture is 0,9 mm wide).

4.4. Sweden

***185.** ASR with a sandstone aggregate which has caused a strong cracking through the aggregate and cement paste; AS gel is found at the upper edge of the aggregate.*
(PPLx20, picture is 6,3 mm wide).

***186.** Same view as the picture 185, under cross-polarized light, showing a poorly sorted sandstone with a thin clayey matrix and with some veins of quartz.*
(XPLx20, picture is 6,3 mm wide).

***187.** Detailed view : the cracks going through the aggregate and the cement paste are filled with AS gel.*
(PPLx40, picture is 3,2 mm wide).

***188.** Detailed view of the cracks filled with AS gel.*
(PPLx100, picture is 1,2 mm wide).

***189.** Detailed view of the AS gel partly recrystallized (brownish) and partly amorphous (transparent).*
(PPLx200, picture is 0,6 mm wide).

***190.** Same view as the previous photo, under cross-polarized light with gypsum plate inserted : the amorphous gel is characterized by its purple interference colours.*
(XPLGx200, picture is 0,6 mm wide).

***191.** Other detailed view showing air pores filled with AS gel and fine cracks going through the concrete.*
(PPLx100, picture is 1,2 mm wide).

***192.** Same view as the previous picture, under cross-polarized light with gypsum plate inserted : the typical interference colour of the amorphous AS gel is purple.*
(XPLGx100, picture is 1,2 mm wide).

Acknowledgements.

This work was supported by the European Commission, under the fifth European Framework Program, contract n° "Partner-project-GRD1-CT-2001-40103". The authors are grateful to their colleagues and partners who have been involved within this project, for their collaboration and discussions: Philip Nixon (BRE, UK), Björn Schouenborg and Lotta Carlsson (SP, SE), Elke Schäfer, Eberhardt Siebel (VDZ, D) and Jürgen Bokern (formerly VDZ, now VÖZ, A), Bent Grelk and Lene Pedersen (Rambøll, DK), Jan Lindgaard (SINTEF, N), Mario Berra and Enrico Rondena (CESI, I), Terje Rönning and Sigrun Bremseth (Norcem AS, N), Katerina Paulou (Titan Cement Company, GR), Anne-Marie Marion (B), Jacques Vecoven (Holcim, B), Hákon Ólafsson (IBRI, IS), Angel Lopez Buendia (AIDICO, E) and Stefan Goralczyk (IMBiGS, P). We acknowledge also Christine Merz from TFB (Switzerland) for her participation to this work. We would like to thank in particular the persons who have prepared the numerous thin sections used in this work : Atli Hjartarson (IBRI, IS), Lasse Jacobsen (PC Laboratoriet, DK), Simon Lane and Neil Gape (BRE, UK), Dany Leclercq (ISSeP, B) and François Martineau (LCPC, F).

References

ADAMS, A.E., MACKENZIE, W.S. & GUILFORD, C., 1994. Atlas of sedimentary rocks under the microscope. Longman, Harlow. 104 p.

BATES, R. L. & JACKSON, J.A., 1980. Glossary of Geology, American Geological Institute, Virginia. 751 p.

HOINKES, G., HAUZENBERGER, C. A. & R. SCHMID, 2005. Metamorphic rocks. Classification, nomenclature and formation, *in Encyclopedia of Geology*, vol. 3, pp. 386-417, Elsevier, Oxford.

KATAYAMA, T., HELGASON, T.S. & OLAFSSON, H., 1996. Petrography and Alkali-Reactivity of some Volcanic Aggregates from Iceland. Proceedings of the 10th International Conference on Alkali-Aggregate reactions in Concrete. Melbourne, Australia, pp. 377-384.

LORENZI, G., GUEDON-DUBIED, S. & ANTENUCCI, D., 2001. The status of the reactive silica in the limestones susceptible to the alkali-silica reaction: contribution of petrographic and SEM techniques. Proceedings of the 8th Euroseminar on Microscopy applied to Building Materials; pp 205-212; Athens, Greece.

MACKENZIE, W.S., DONALDSON, C.H. & GUILFORD, C., 1982. Atlas of the igneous rocks and their textures. Longman, Harlow. 148 p.

MACKENZIE, W.S. & GUILFORD, C., 1986. Atlas of rock-forming minerals in thin section. Longman, Harlow. 98 p.

RILEM recommended test method TC 106-2 , 2000. Detection of potential alkali-reactivity of aggregates – The ultra-accelerated mortar-bar test. Material and Structures, vol. 33, n° 229, June 2000, pp. 283-289. Cachan, France.

RILEM recommended test method TC 106-3 , 2000. Detection of potential alkali-reactivity of aggregates – Method for aggregate combinations using concrete prisms. Material and Structures, vol. 33, n° 229, June 2000, pp. 290-293. Cachan, France.

RILEM recommended test method AAR-1 , 2003. Detection of potential alkali-reactivity of aggregates – Petrographic method. Material and Structures, vol. 36, n° 261, August - September 2003, pp. 480-496. Cachan, France.

TUCKER, M.E., 2001. Sedimentary Petrology. An Introduction to the Origin of Sedimentary Rocks. Blackwell Science Edit., third Edition, 262p.

SWAMY, R.N., editor, 1992. The alkali-silica reaction in concrete. Blackie, Glasgow. 333 p.

YARDLEY, B.W.D., MACKENZIE, W.S. & GUILFORD, C., 1990. Atlas of the metamorphic rocks and their textures. Longman, Harlow. 120 p.

Manuscript received 18.10.2006 and accepted for publication 24.11.2006.

1

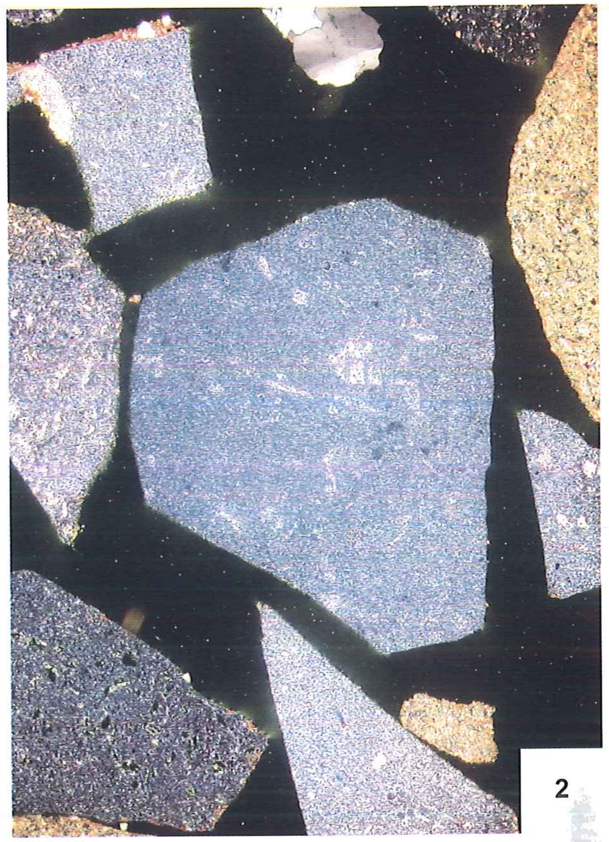

2

3

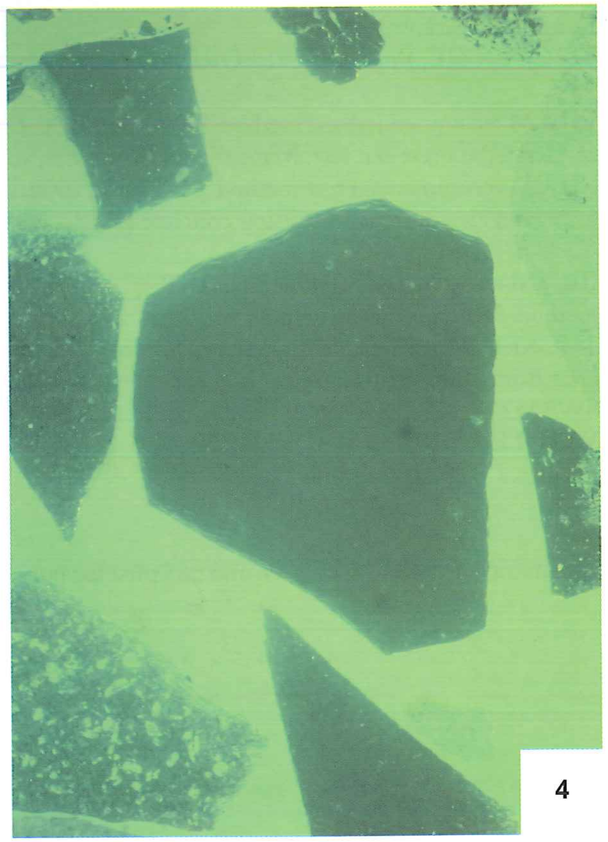

4

5

6

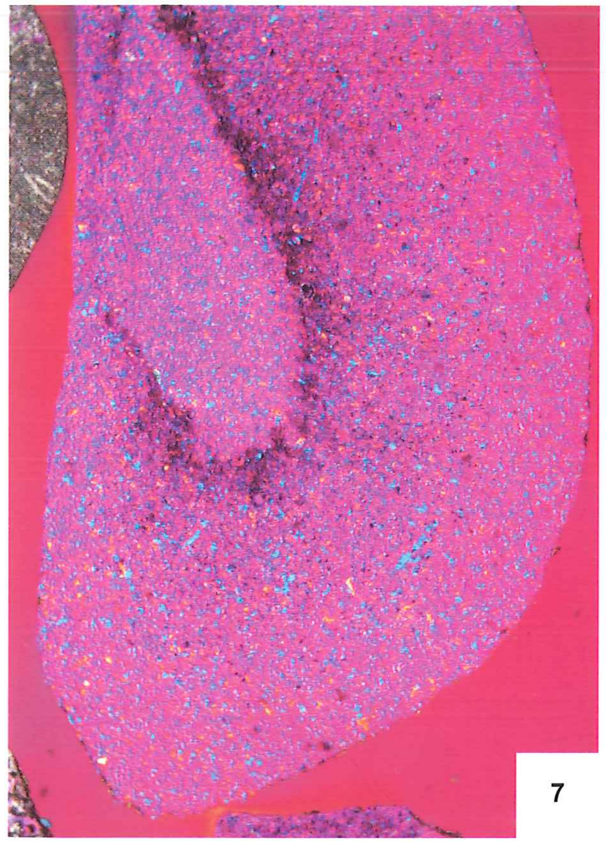

7

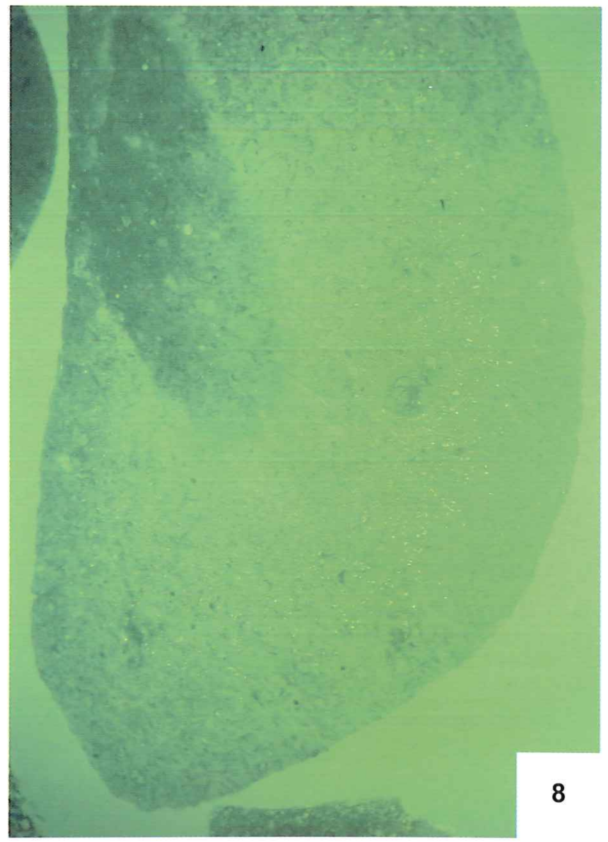

8

9

10

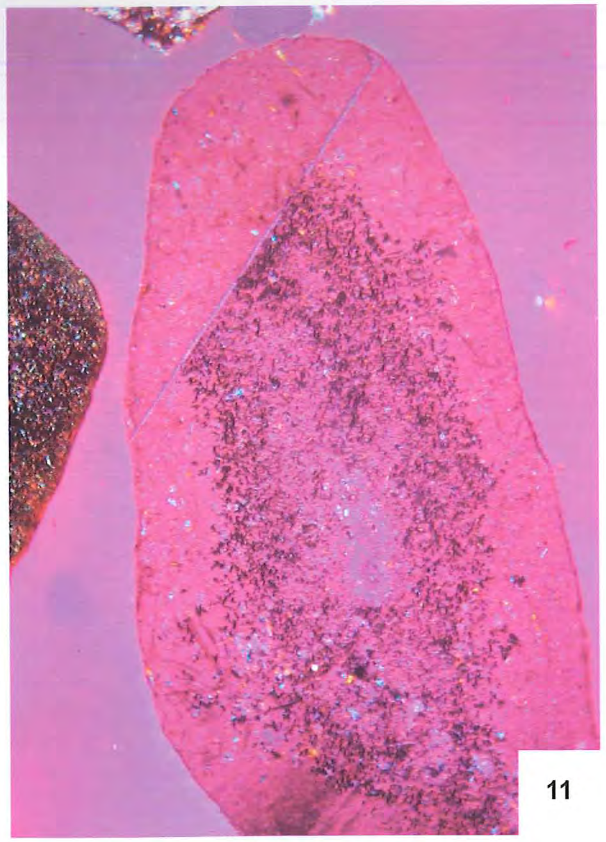

11

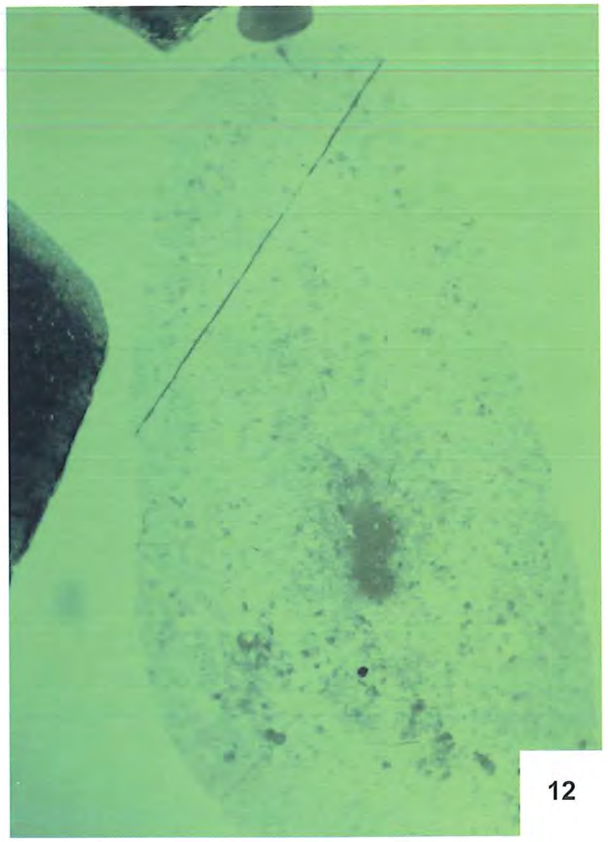

12

13

14

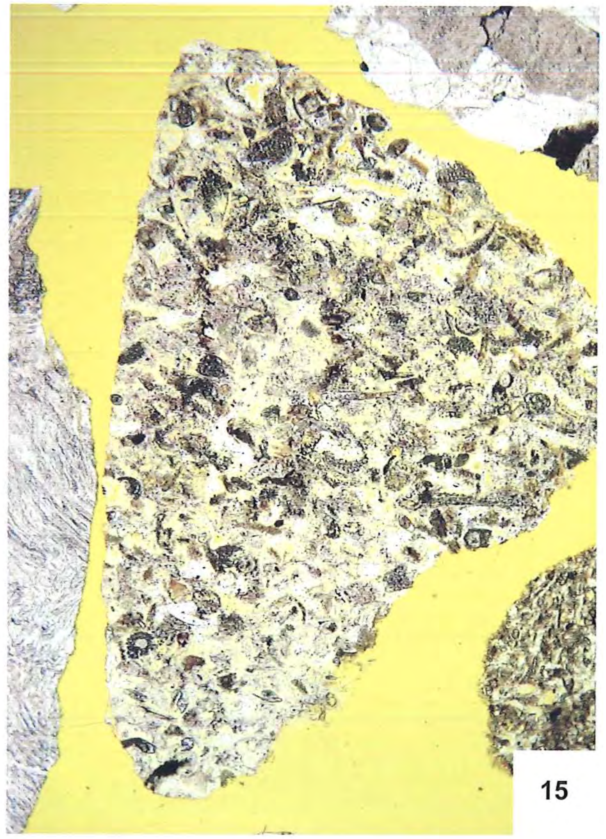

15

16


17


18

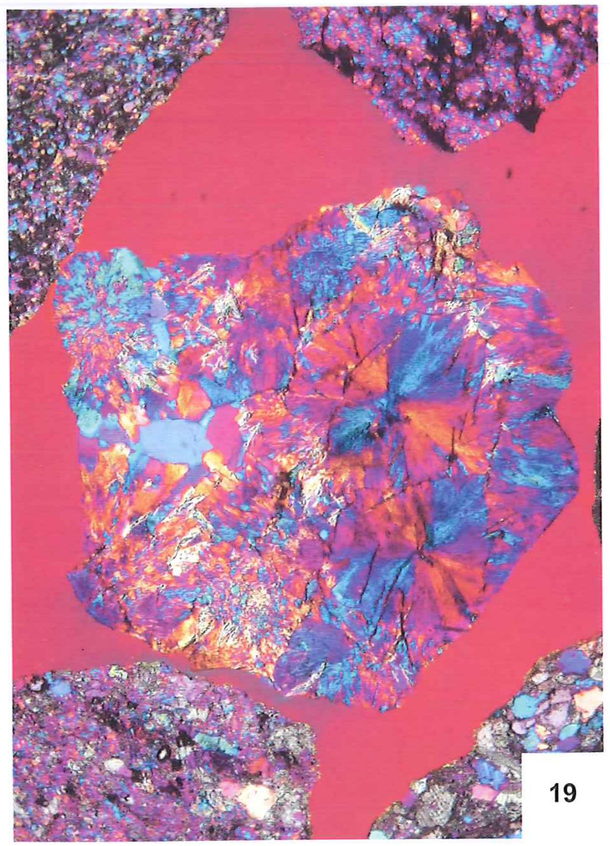
19

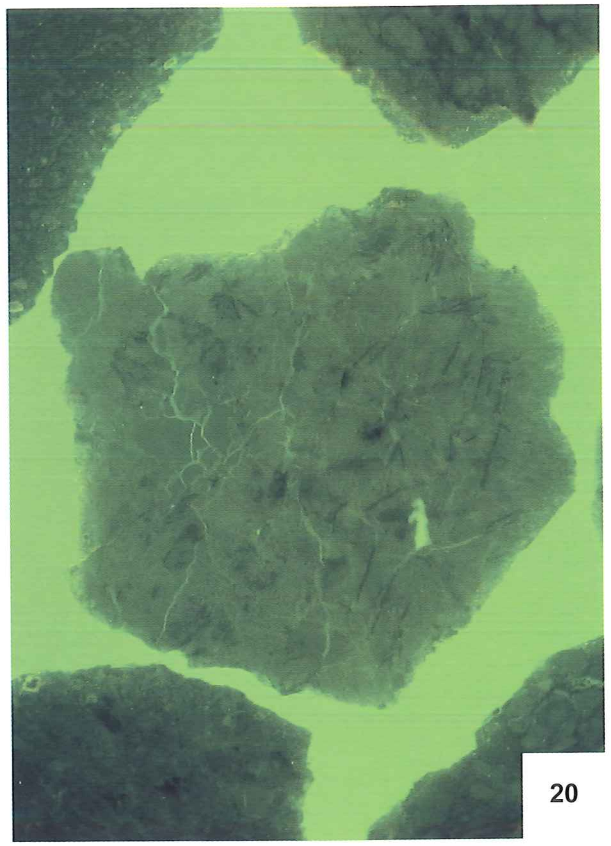
20

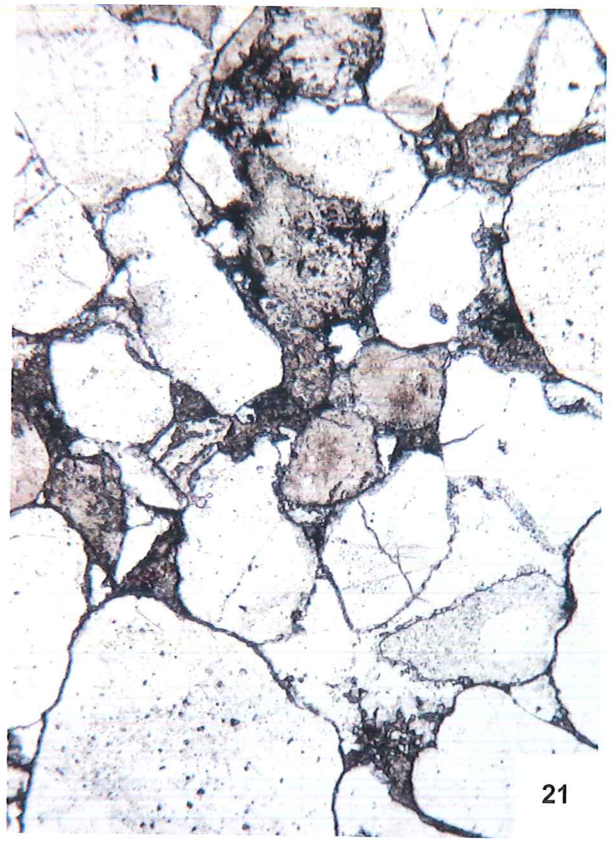
21

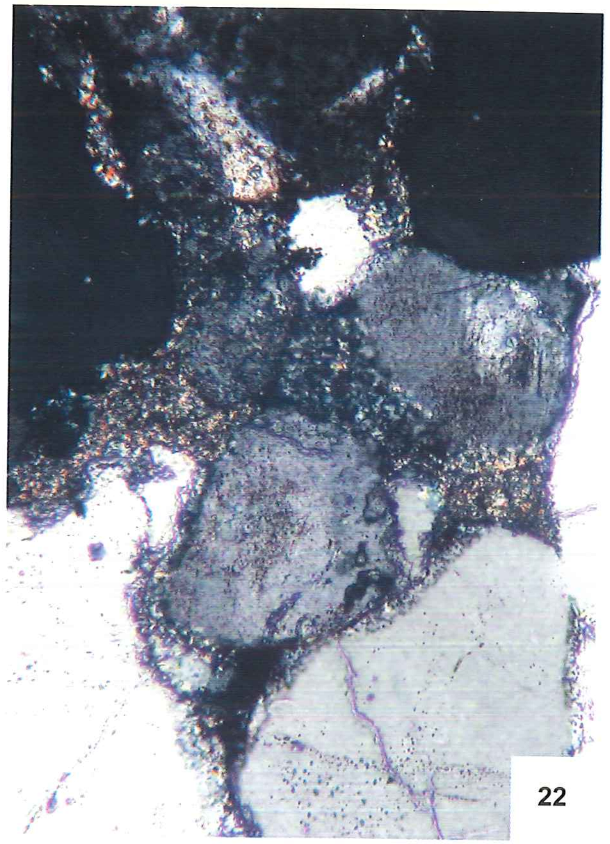
22

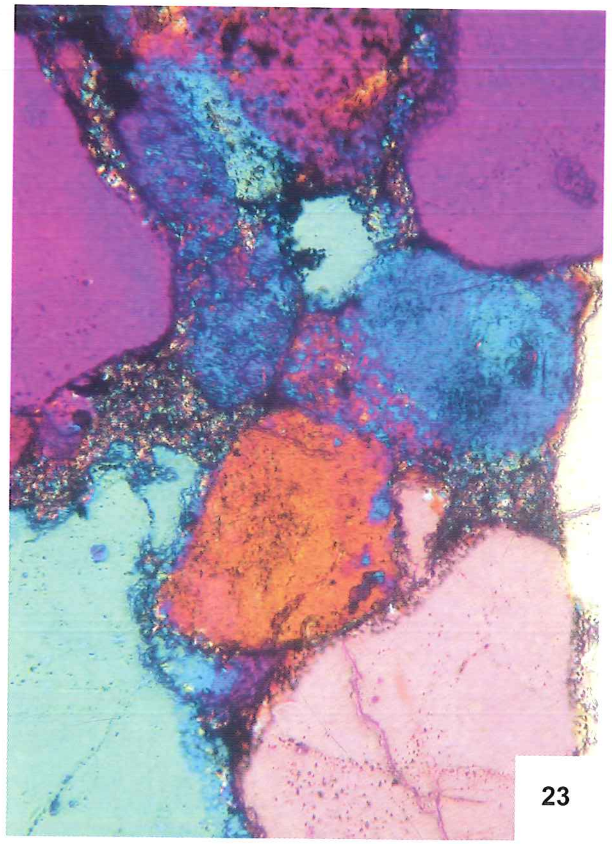
23

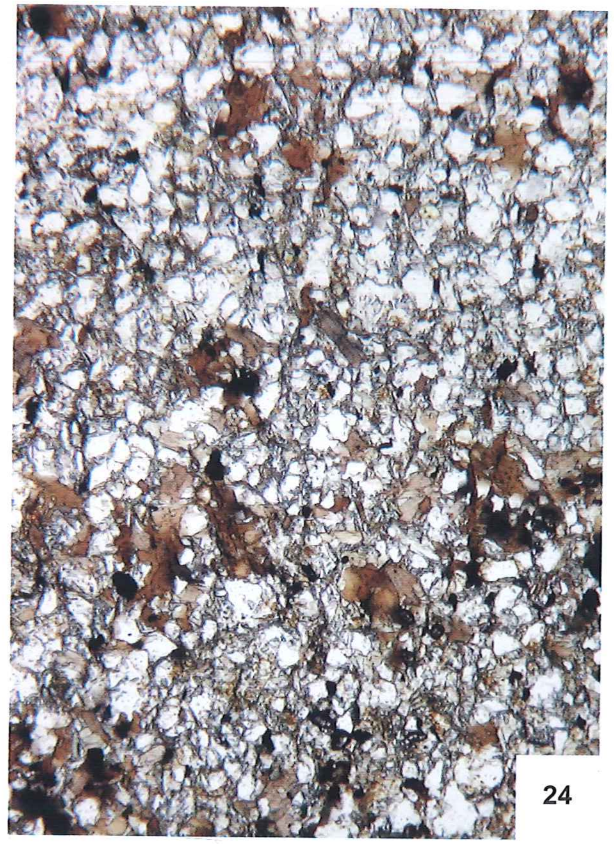
24

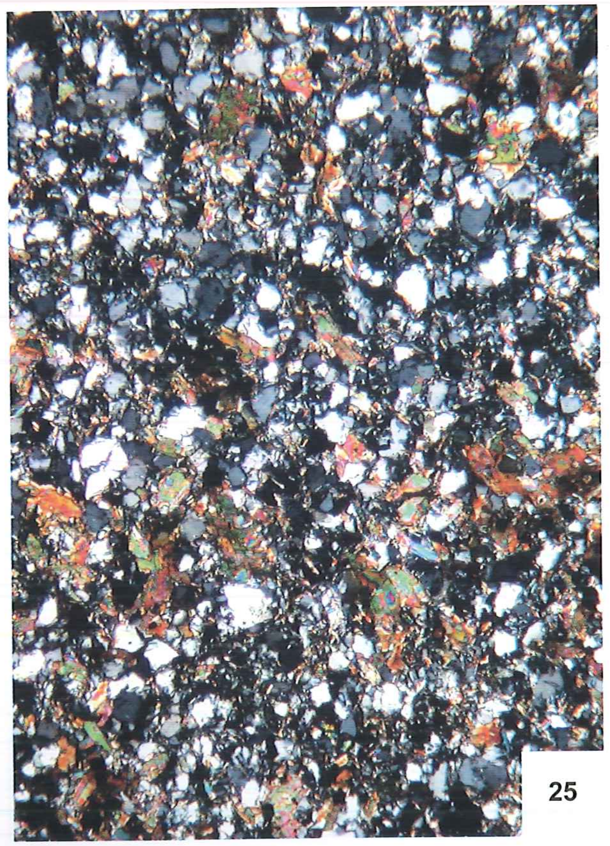

25

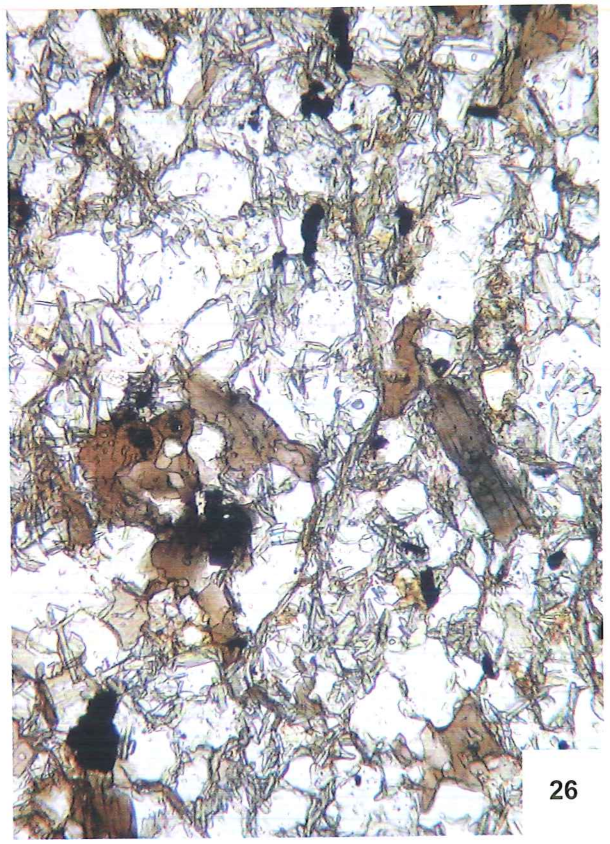

26

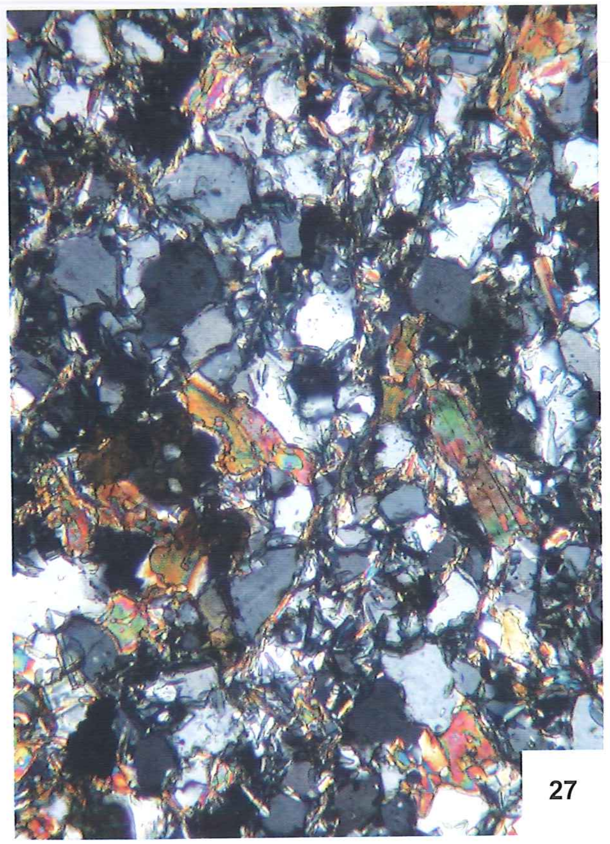

27

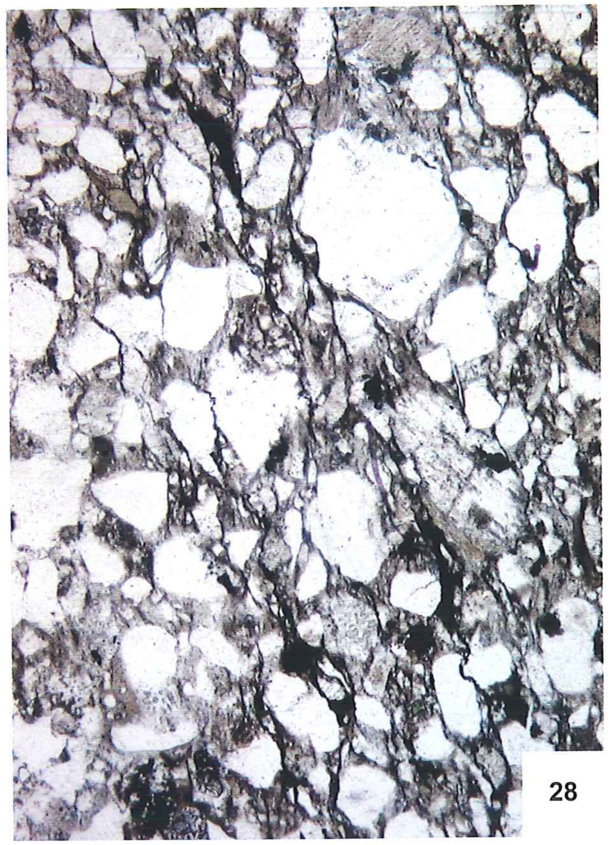

28

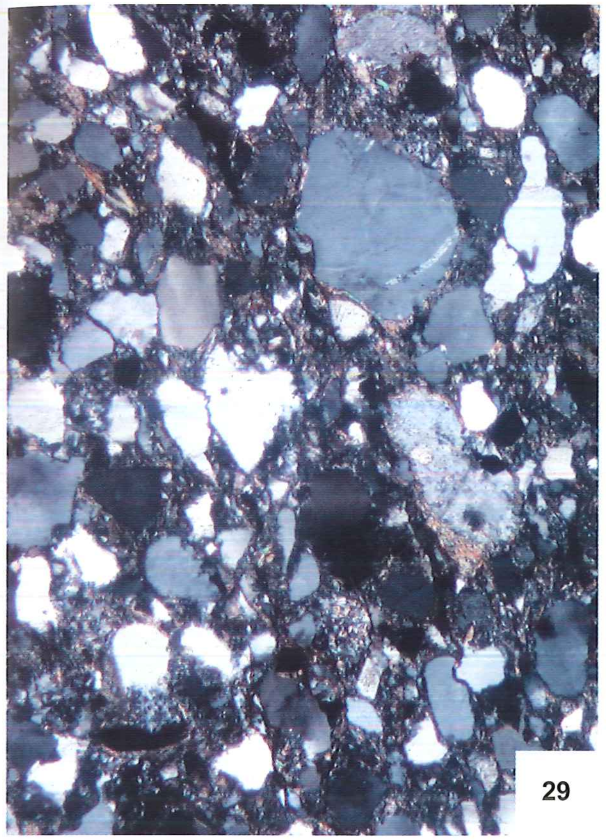

29

30

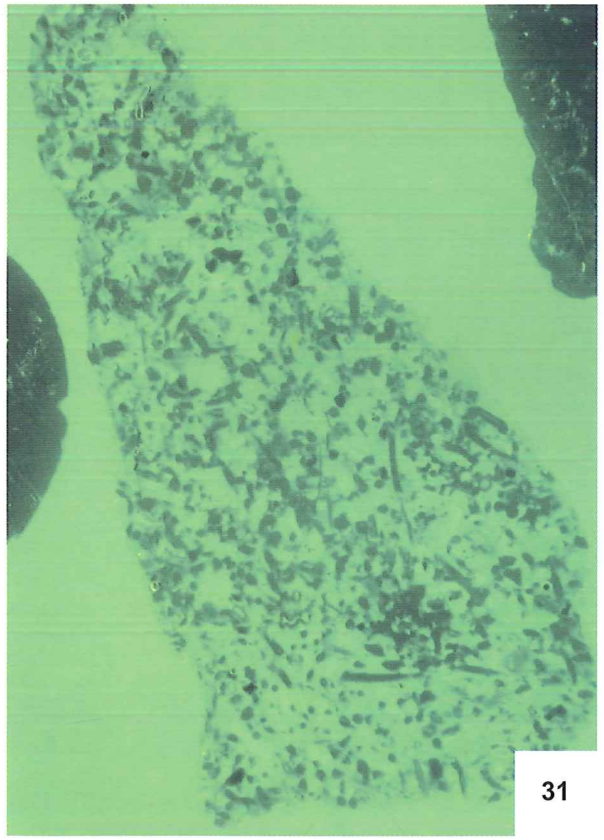

31

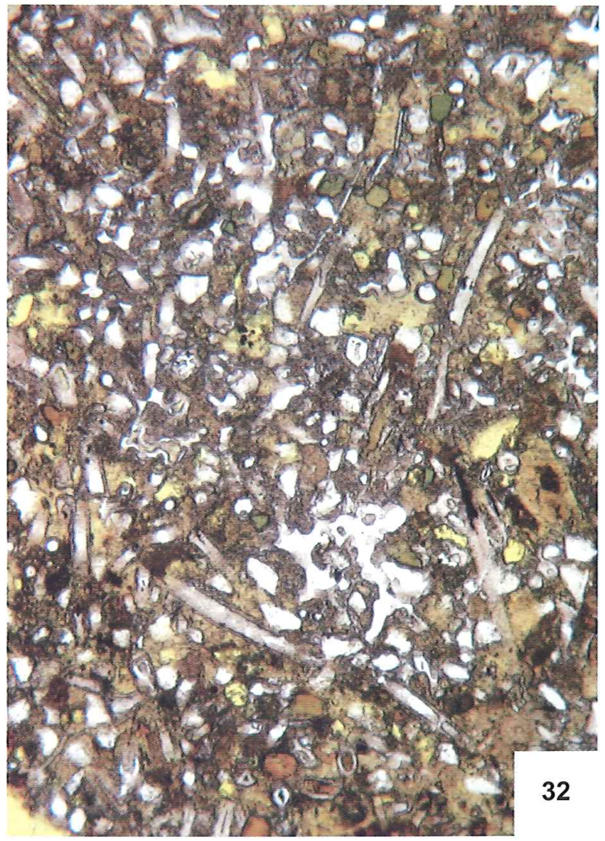

32

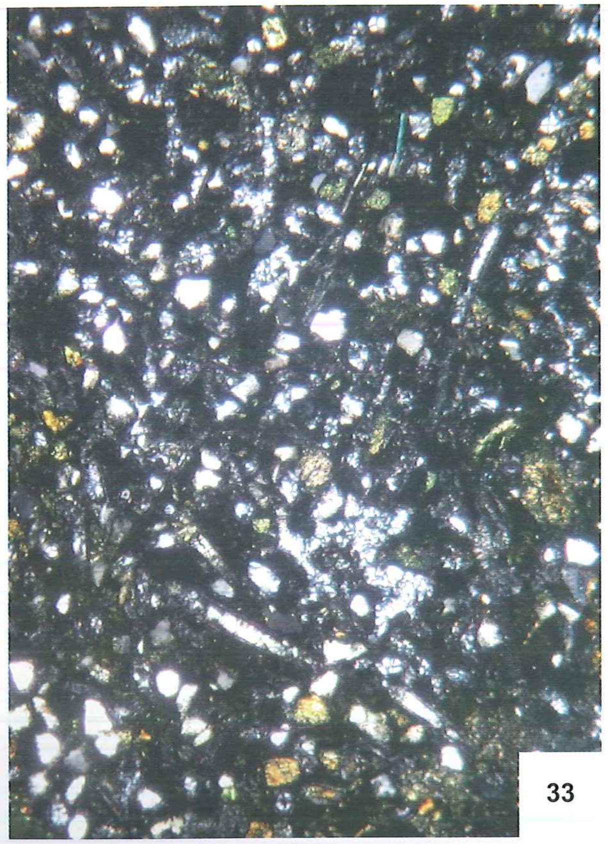

33

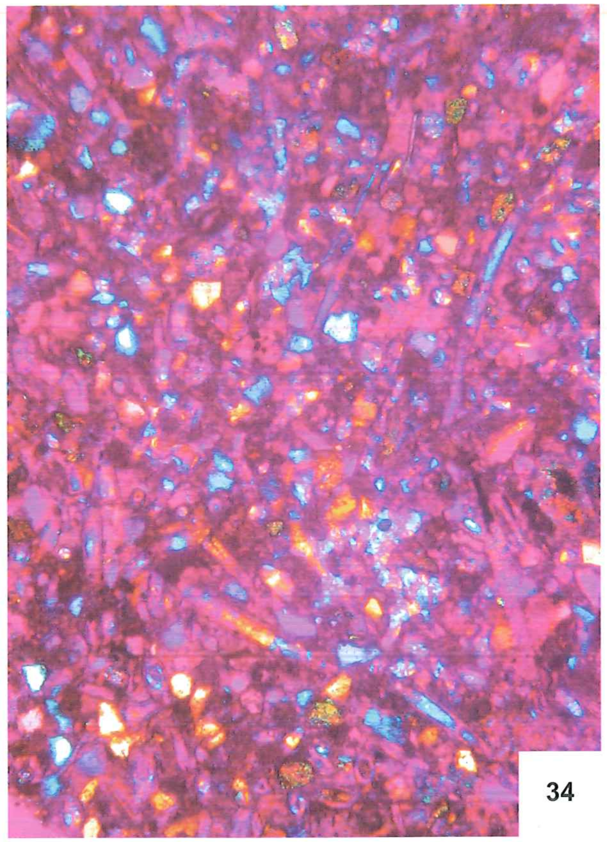

34

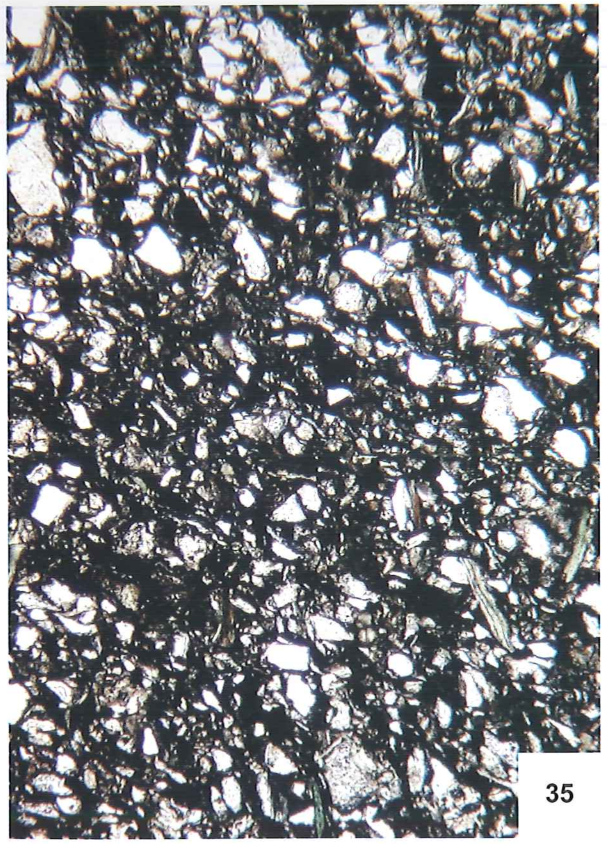

35

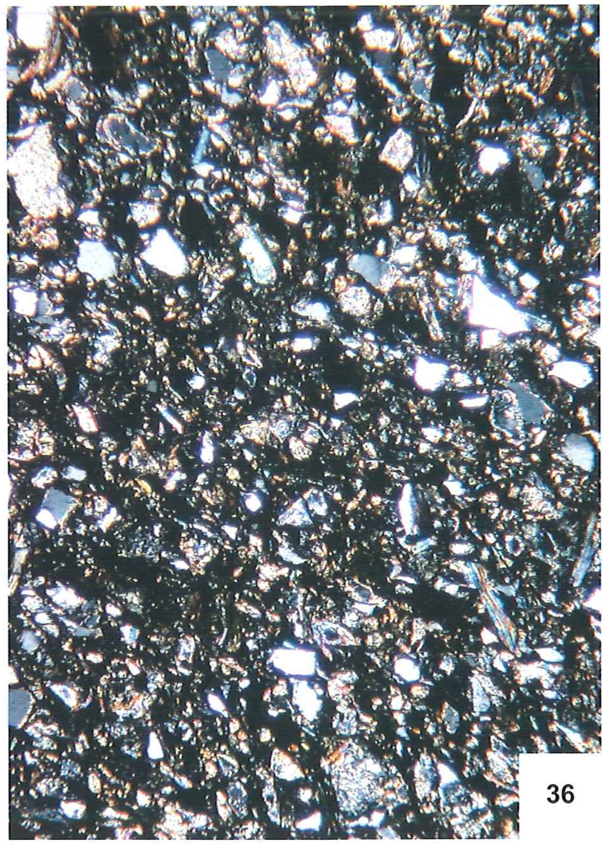

36

37

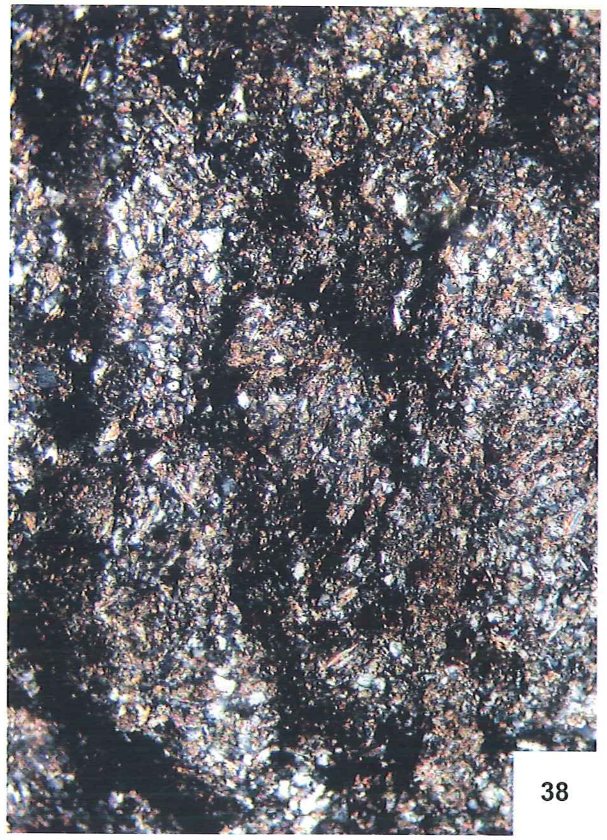

38

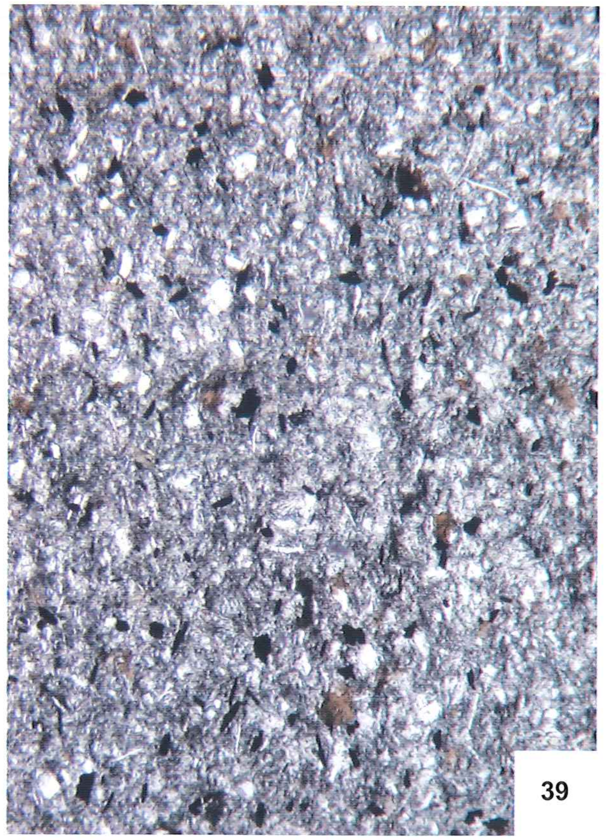

39

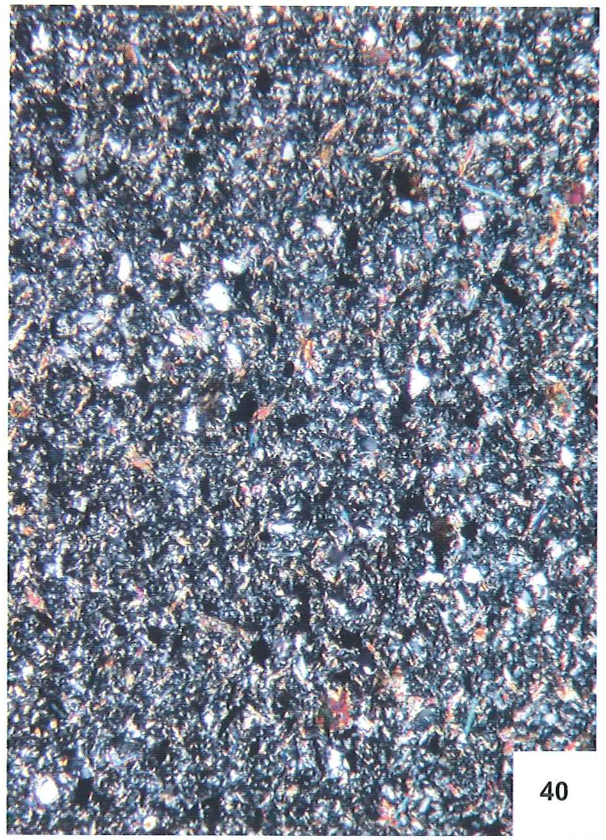

40

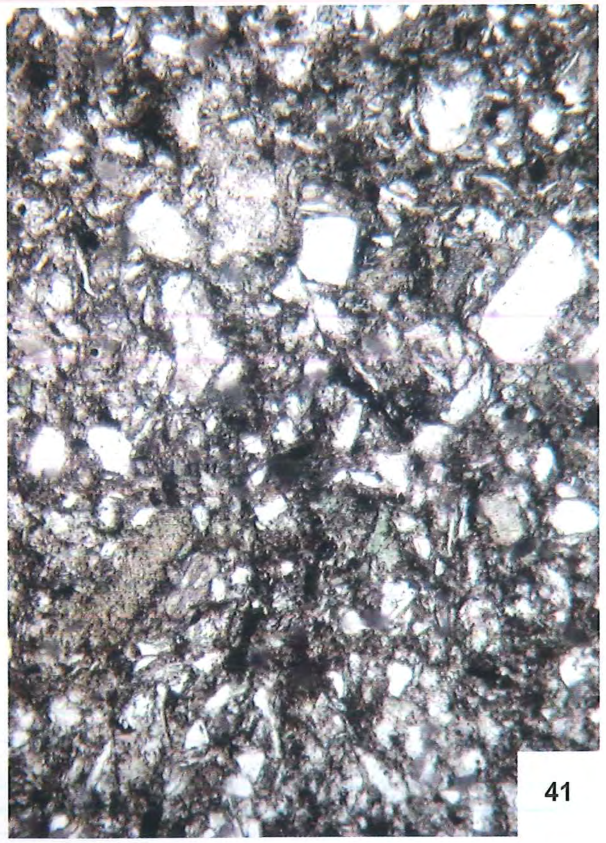
41

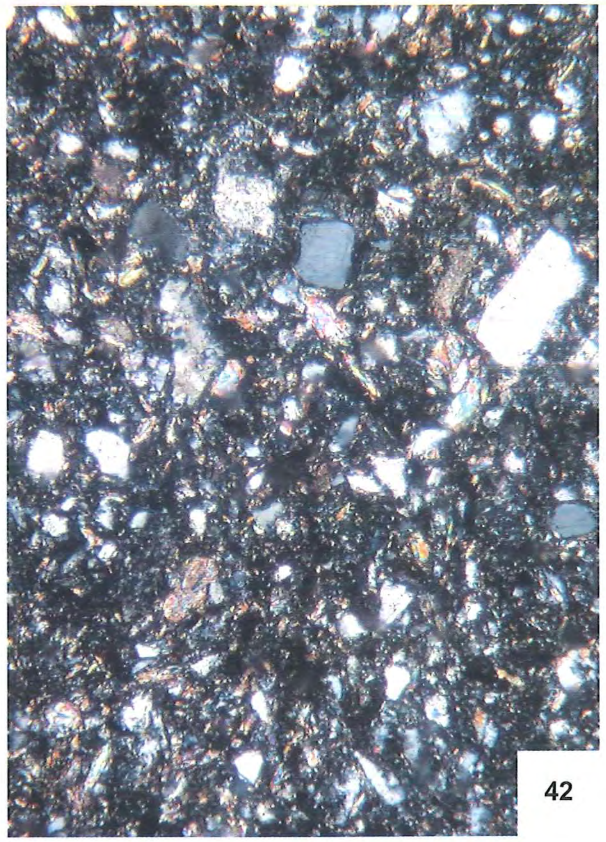
42

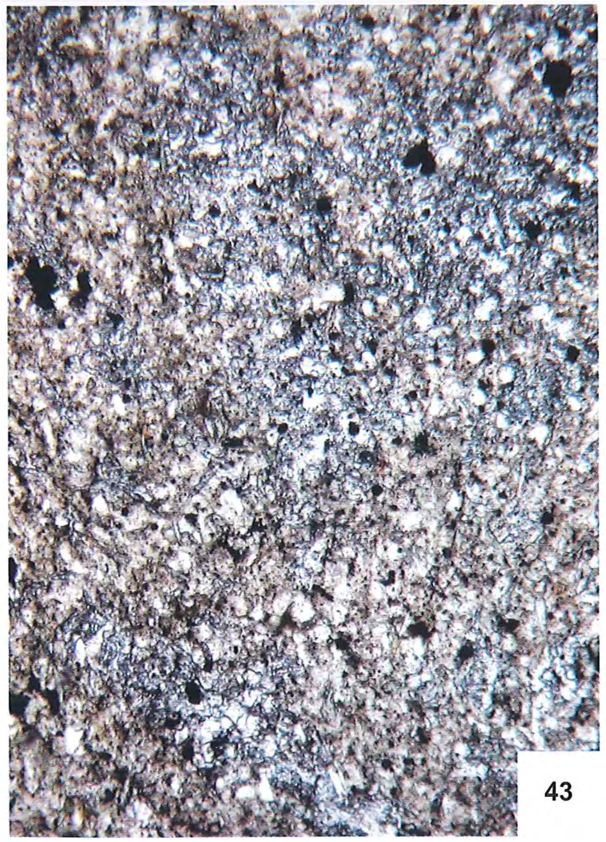
43

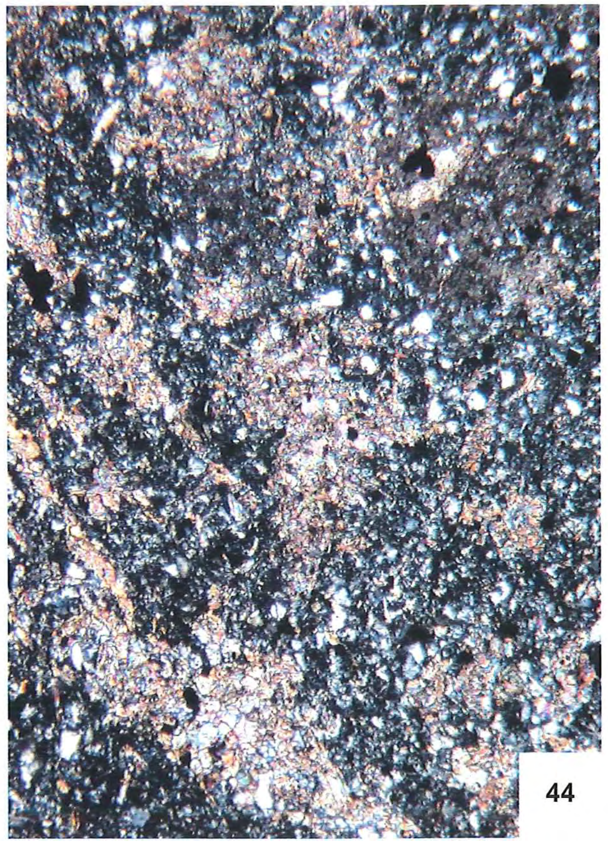
44

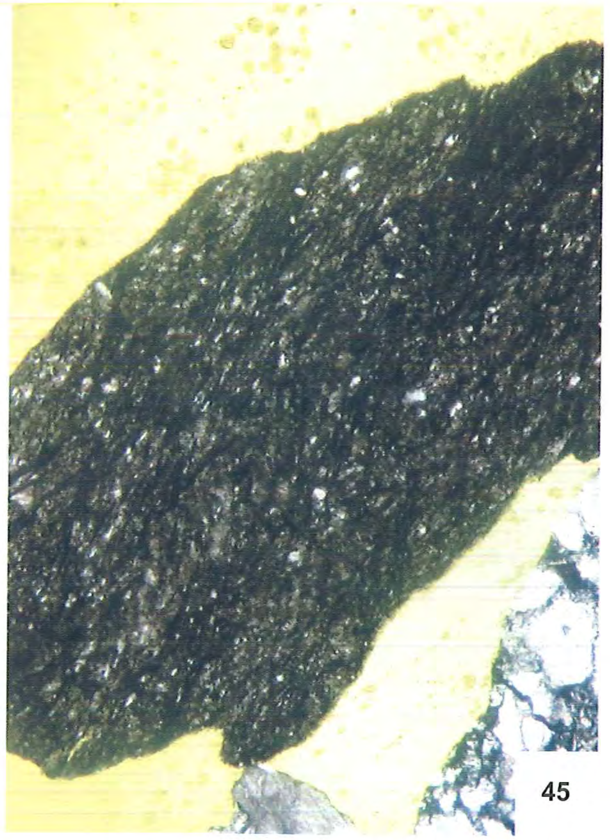
45

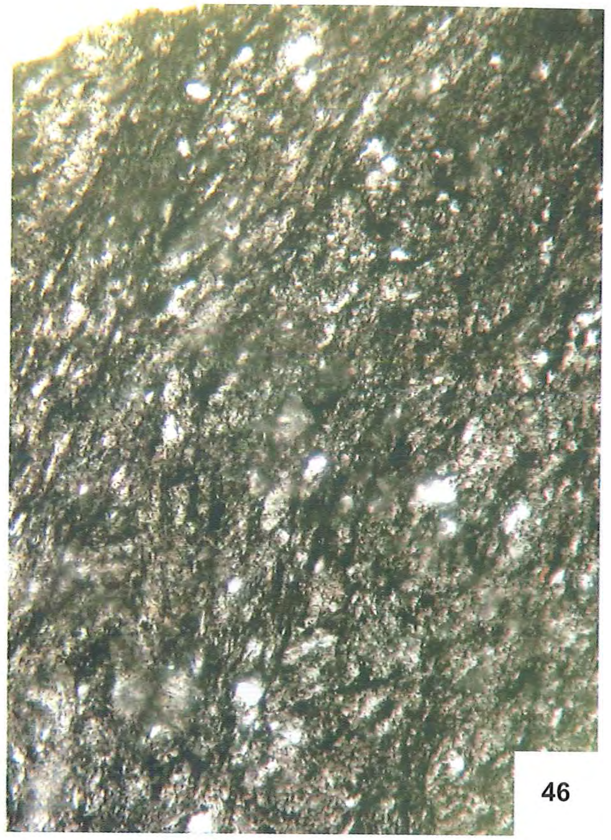
46

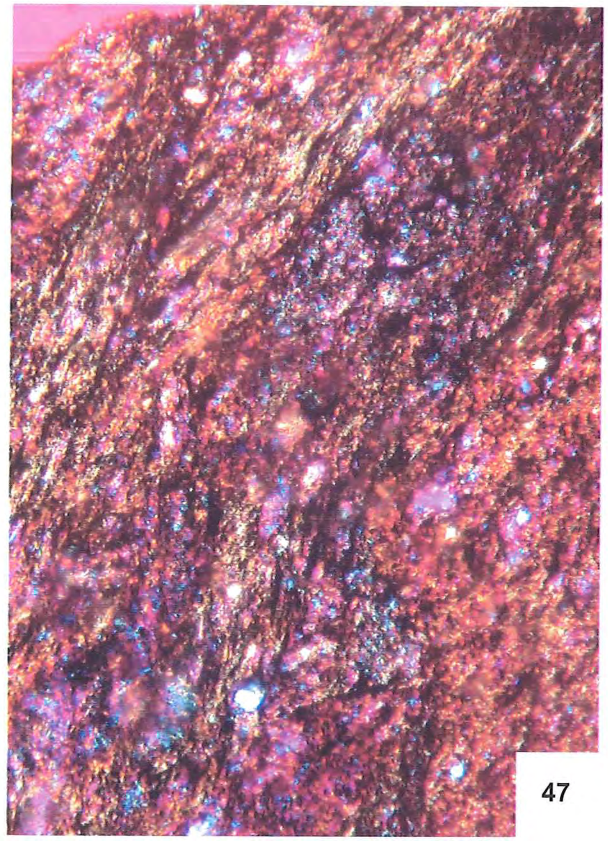
47

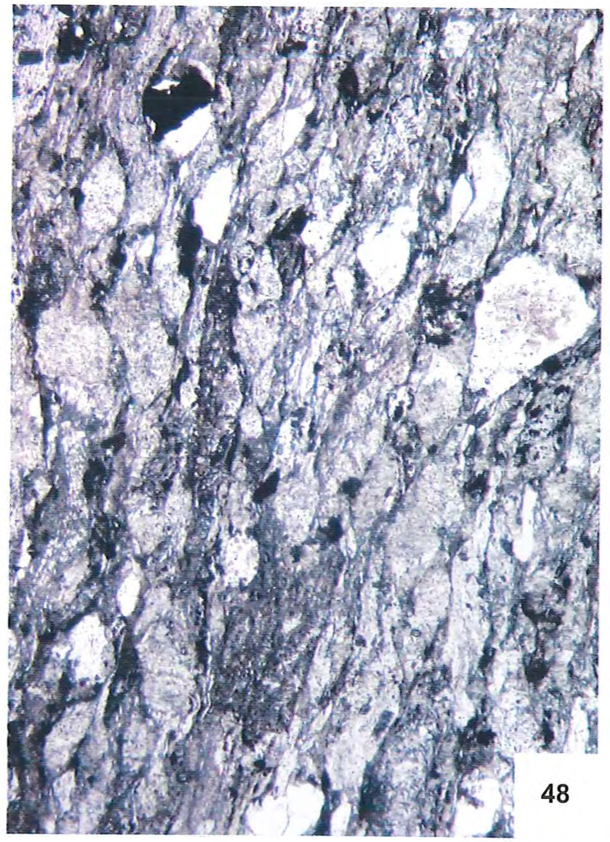
48


49

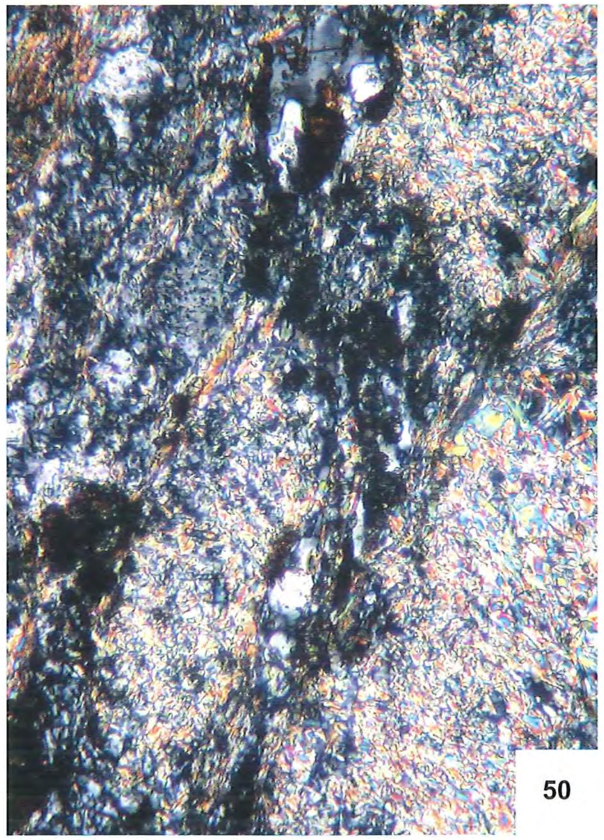
50

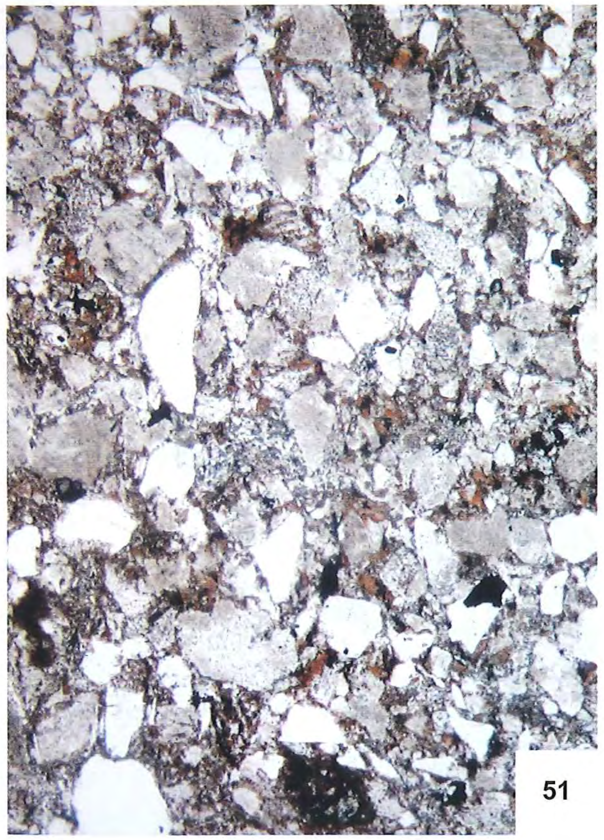
51

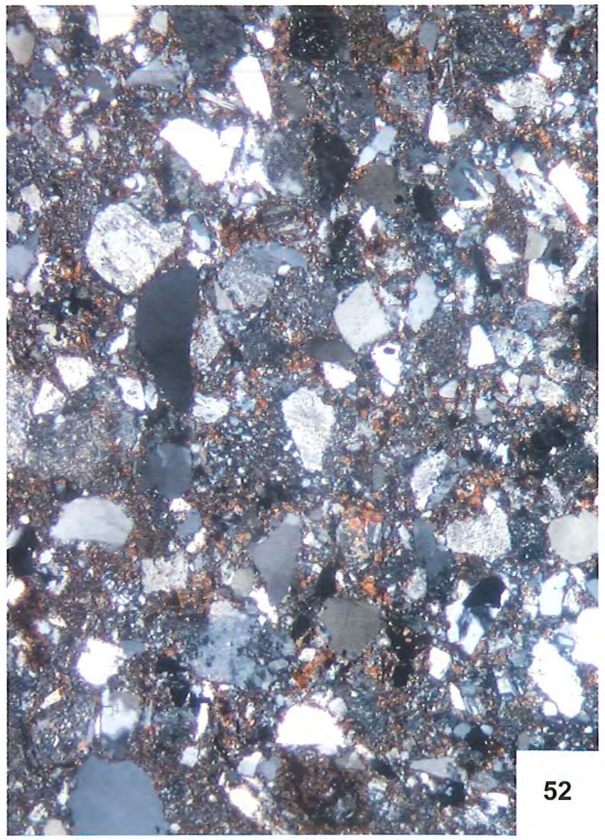
52


53


54

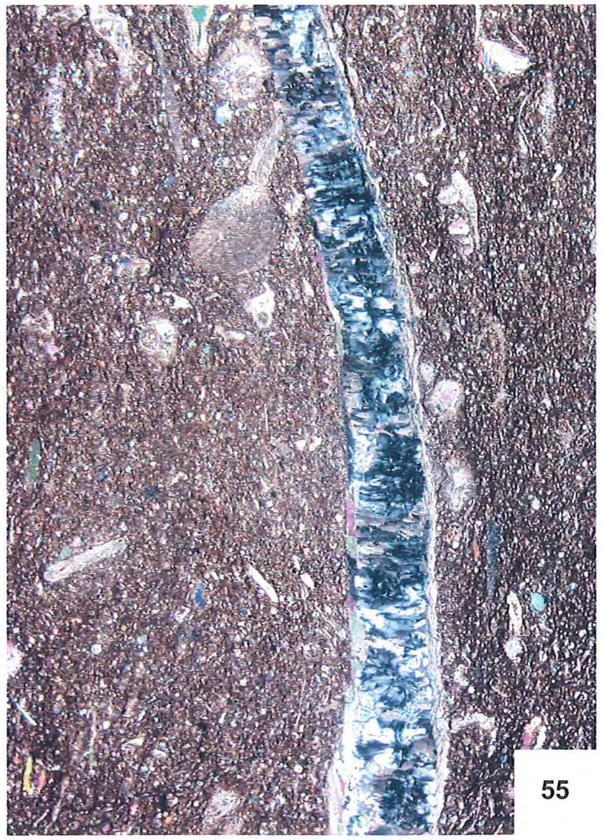
55

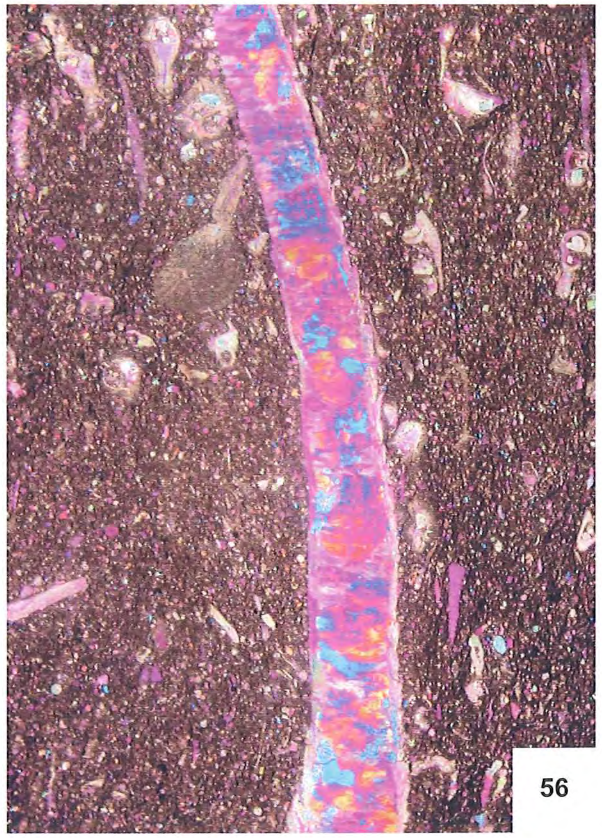
56

57

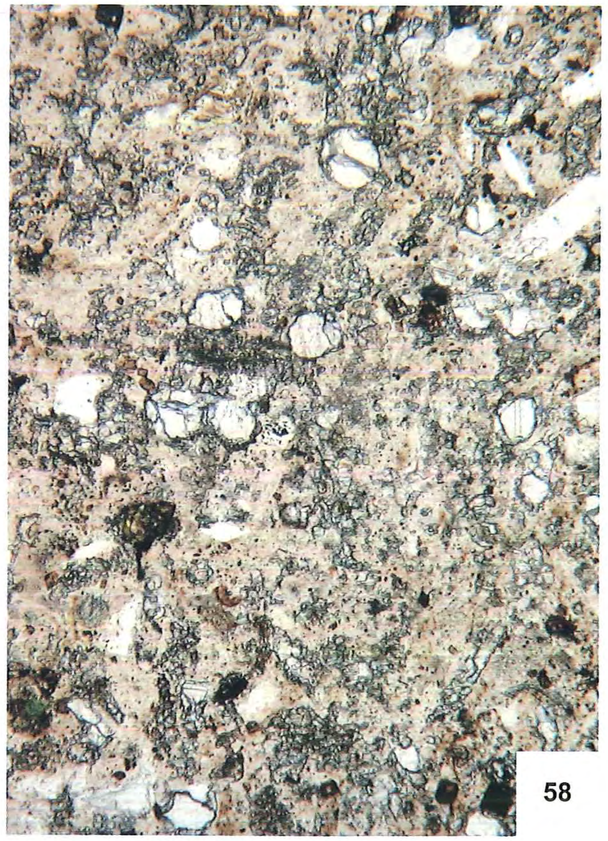

58

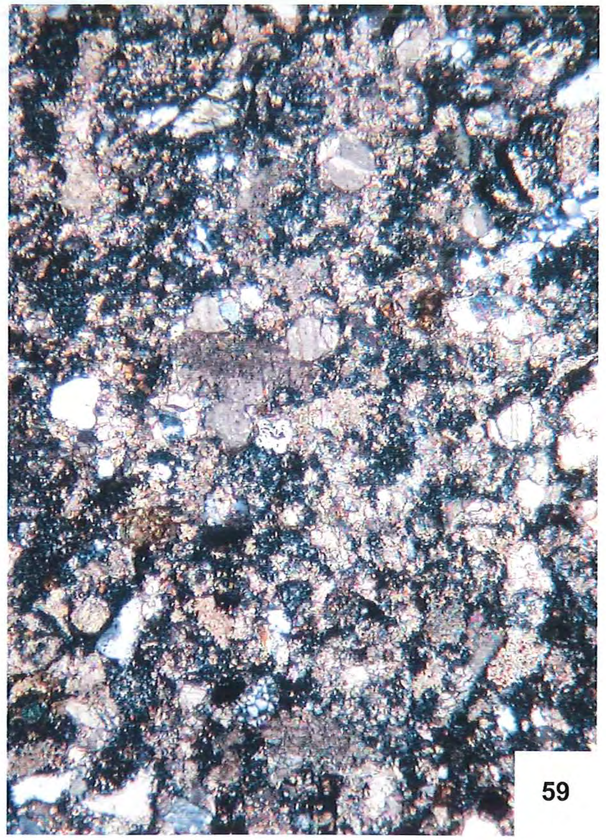

59

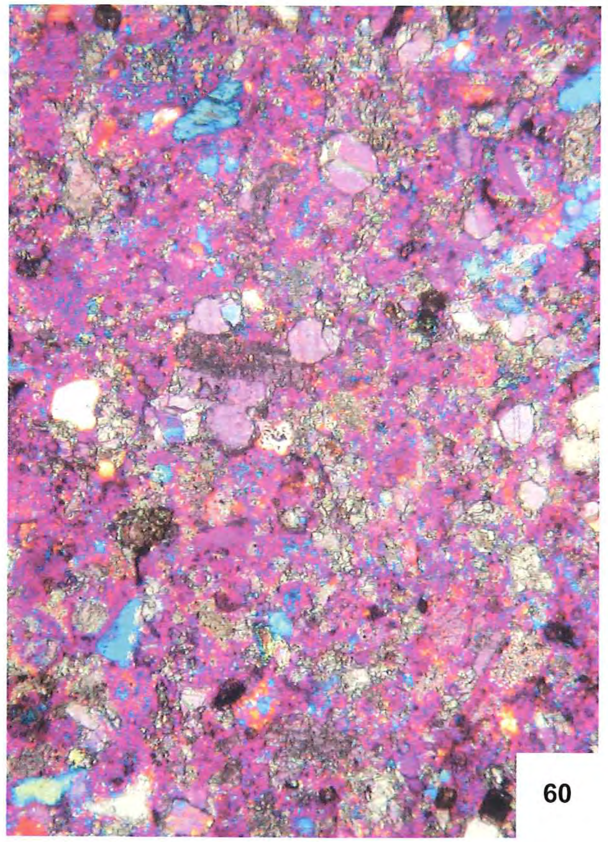

60

61

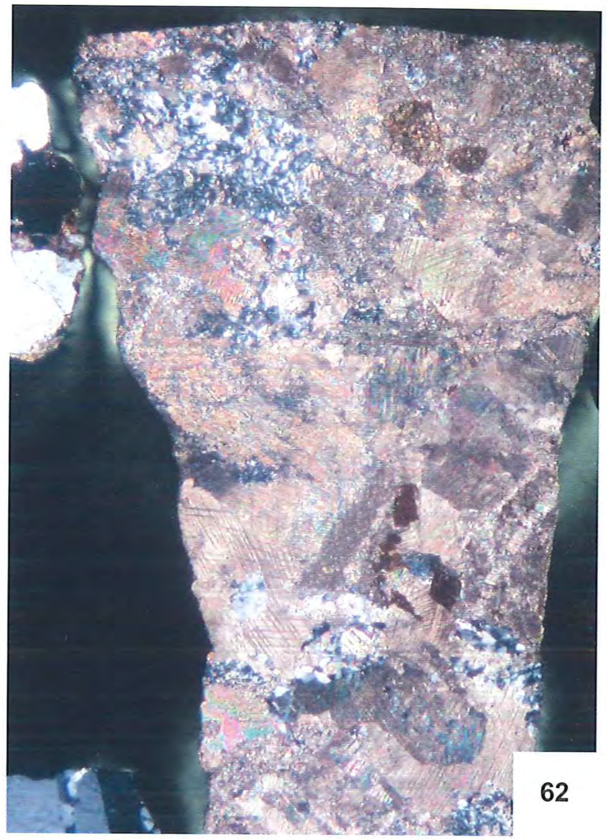

62

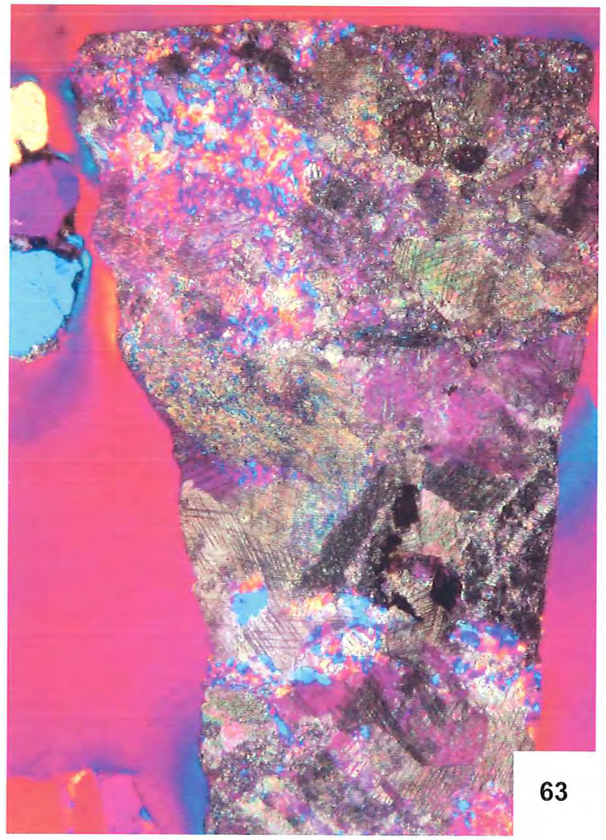

63

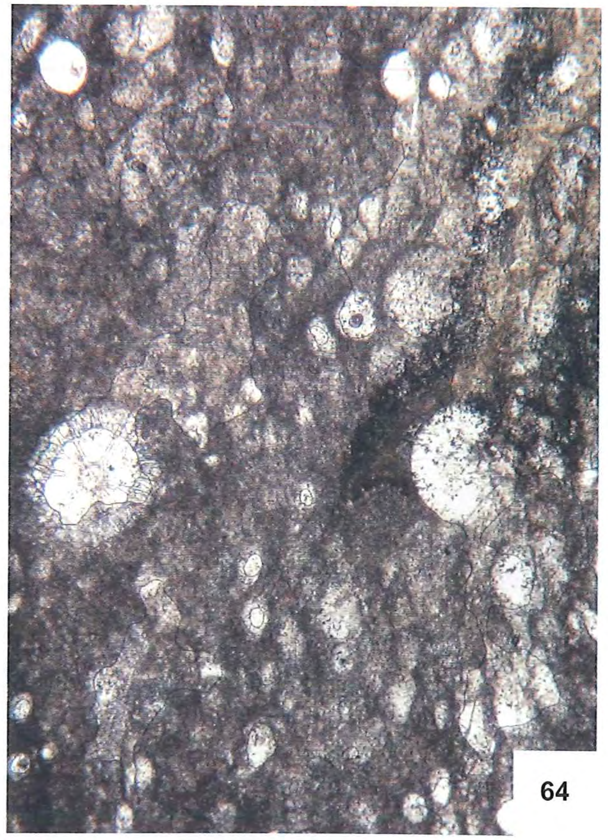

64

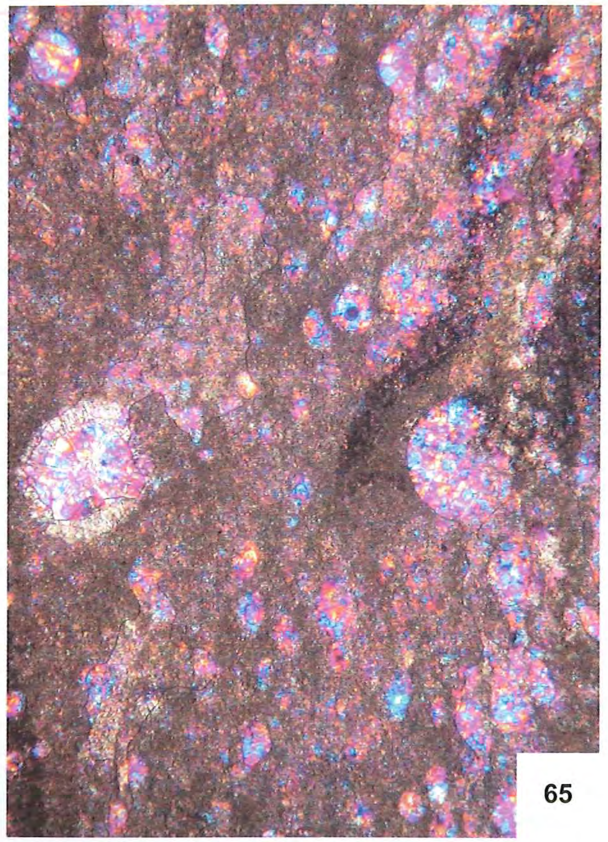
65


66

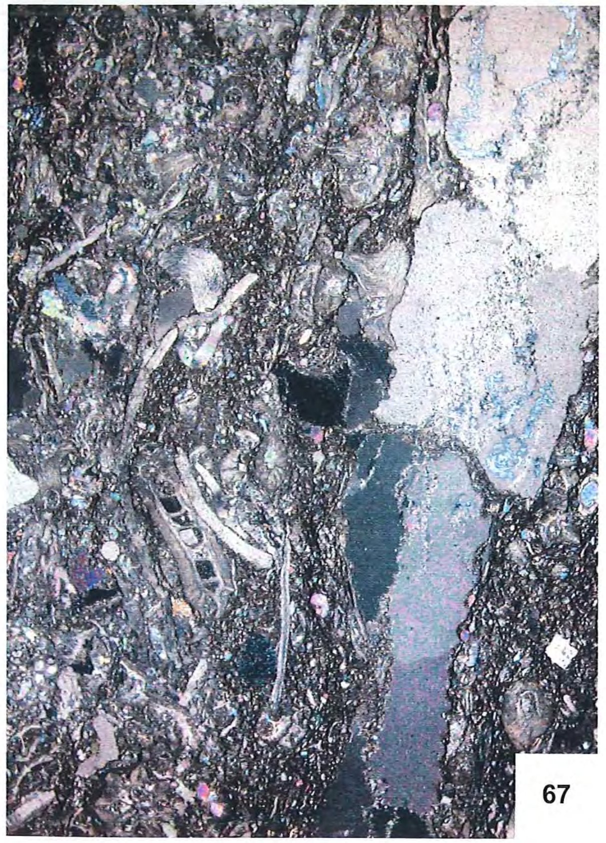
67


68

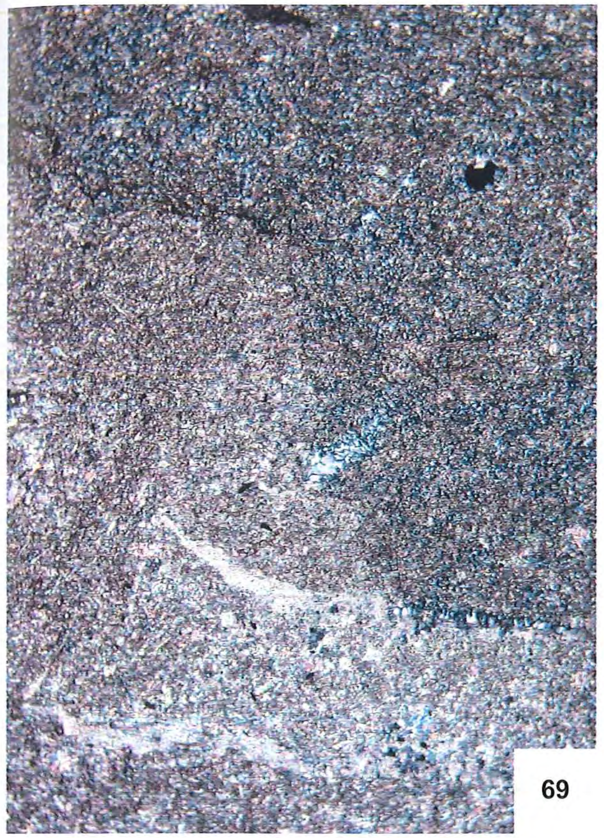
69

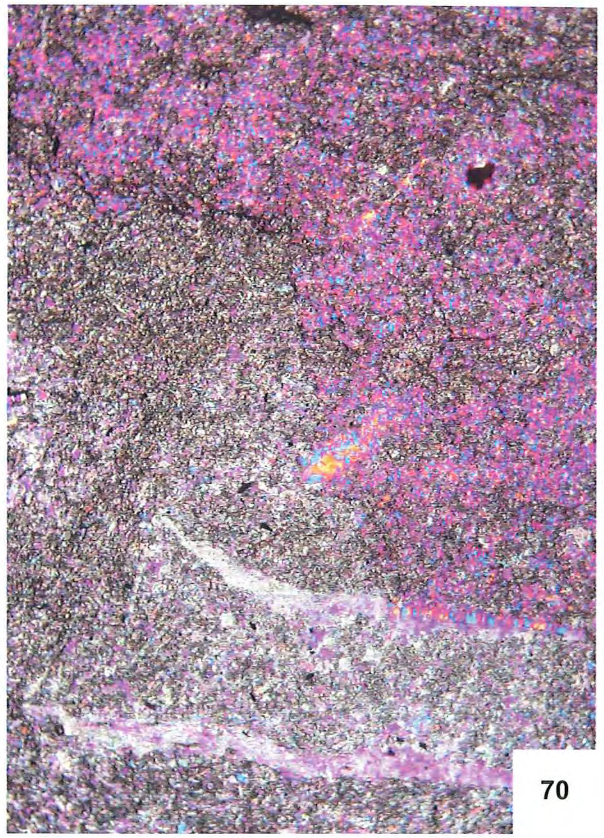
70

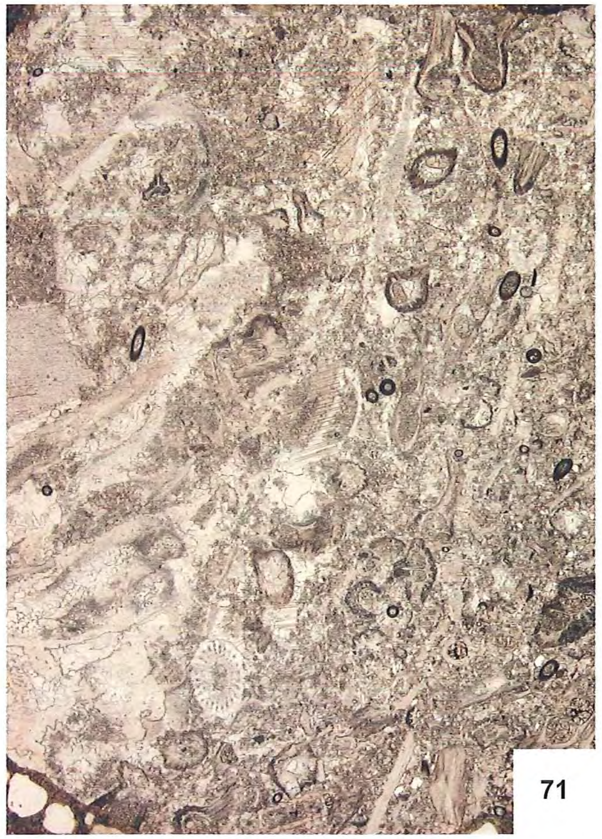
71

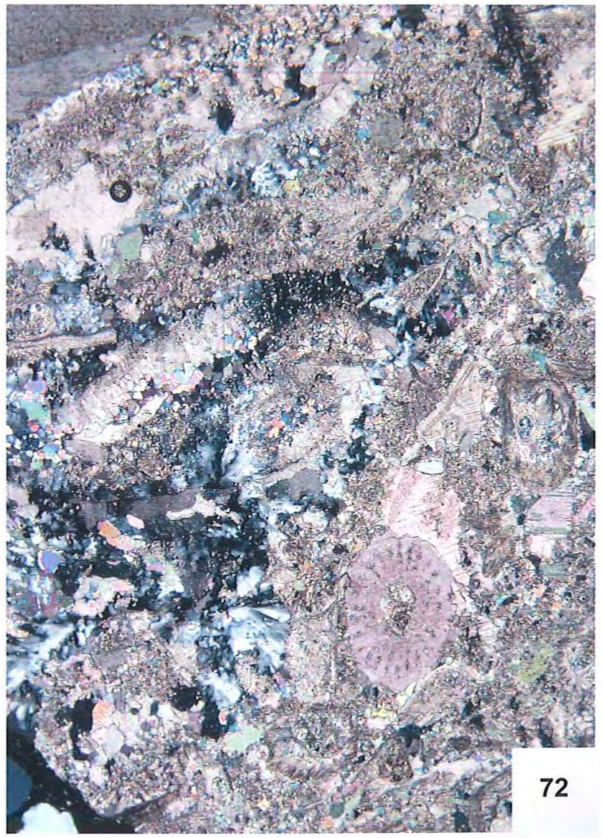
72

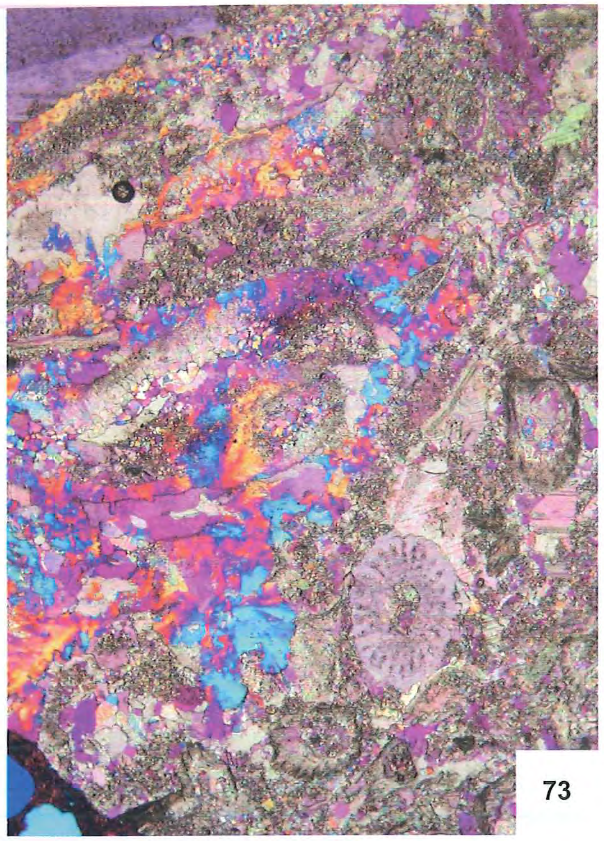
73

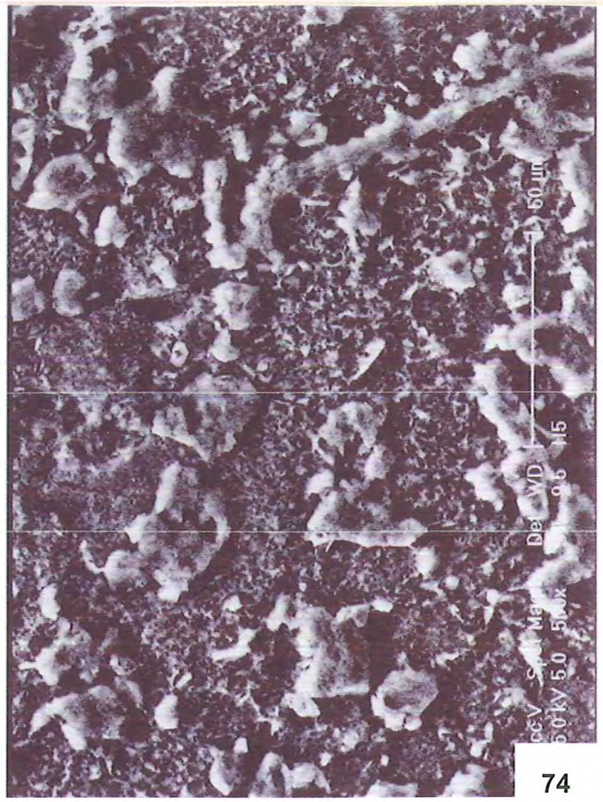
74

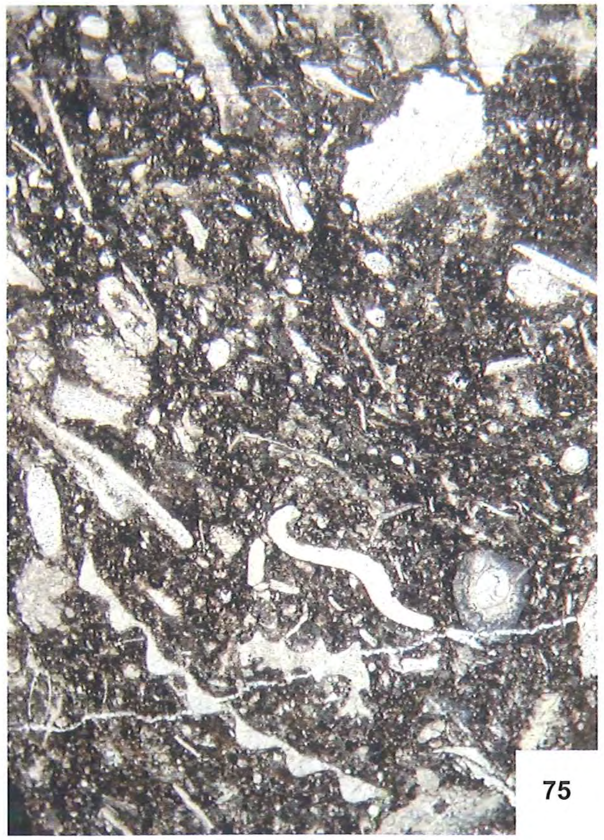
75


76

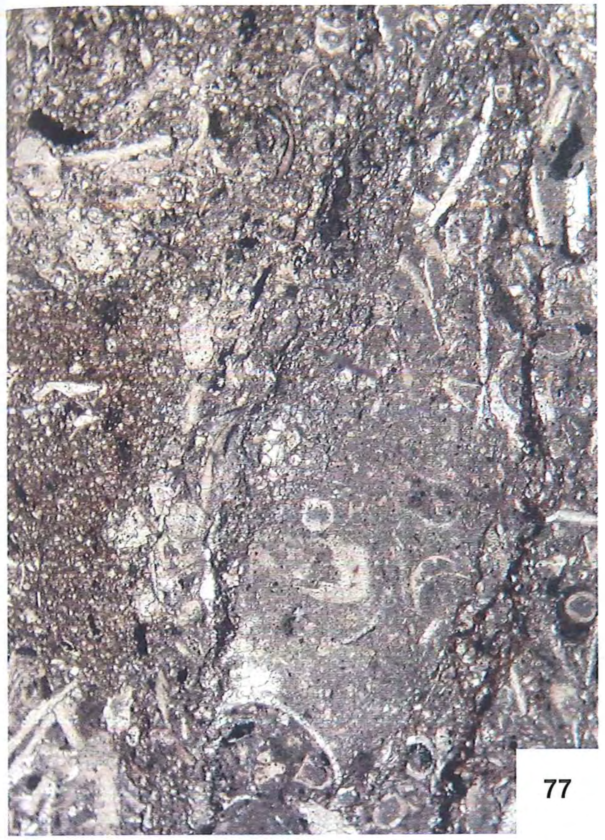
77

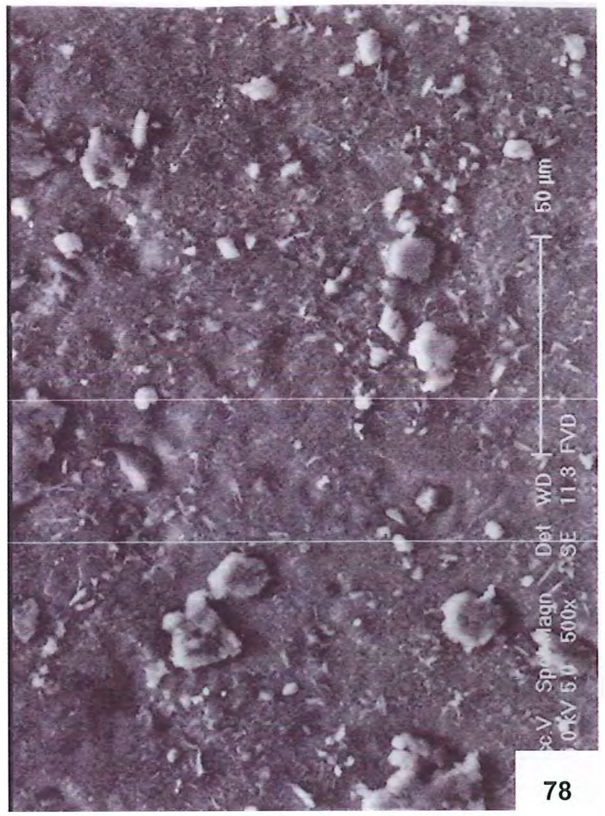
78


79

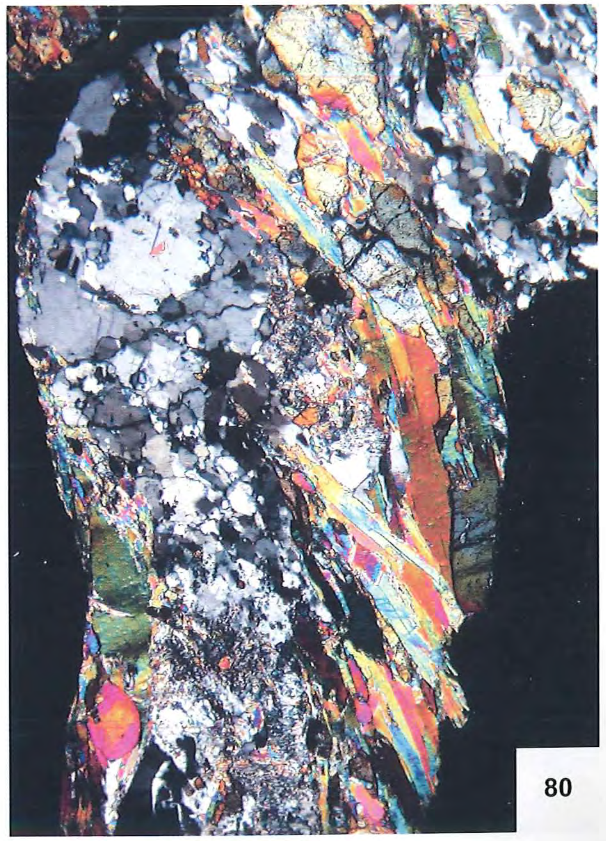
80

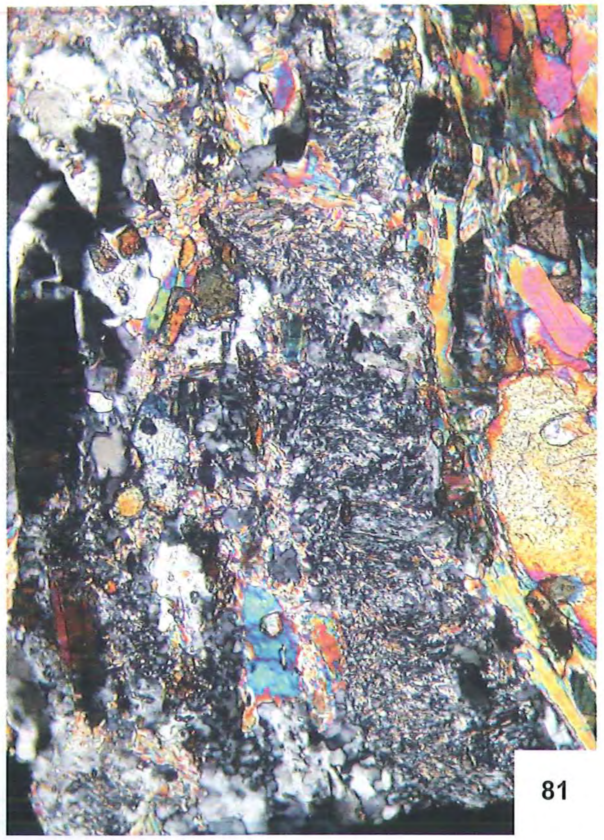
81

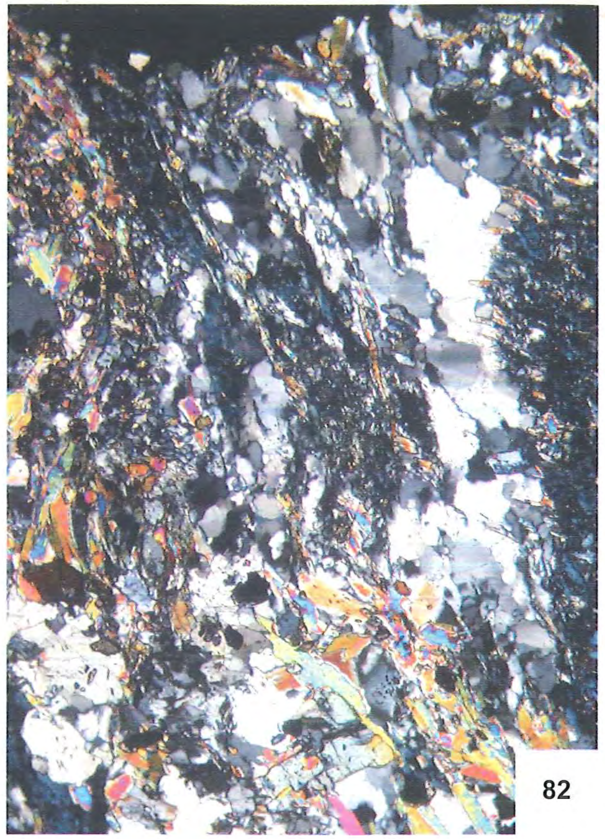
82

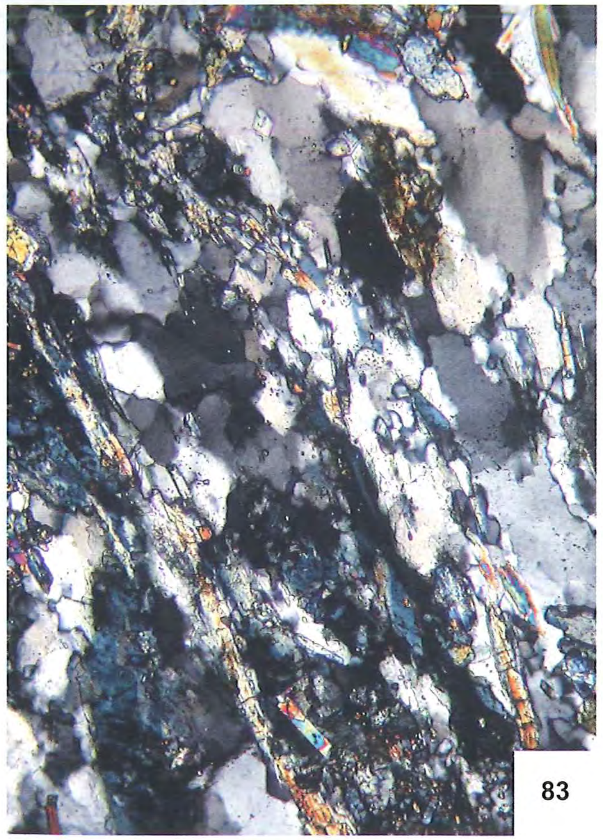
83


84

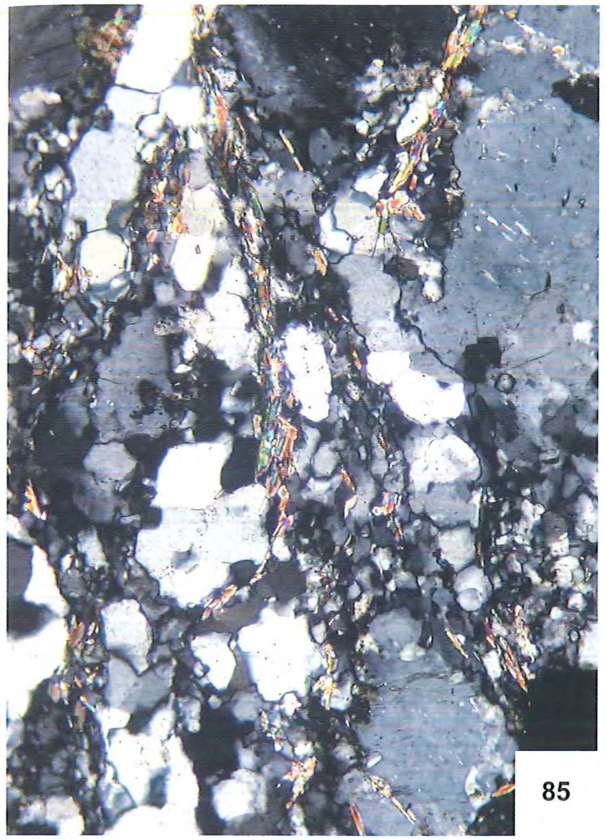
85

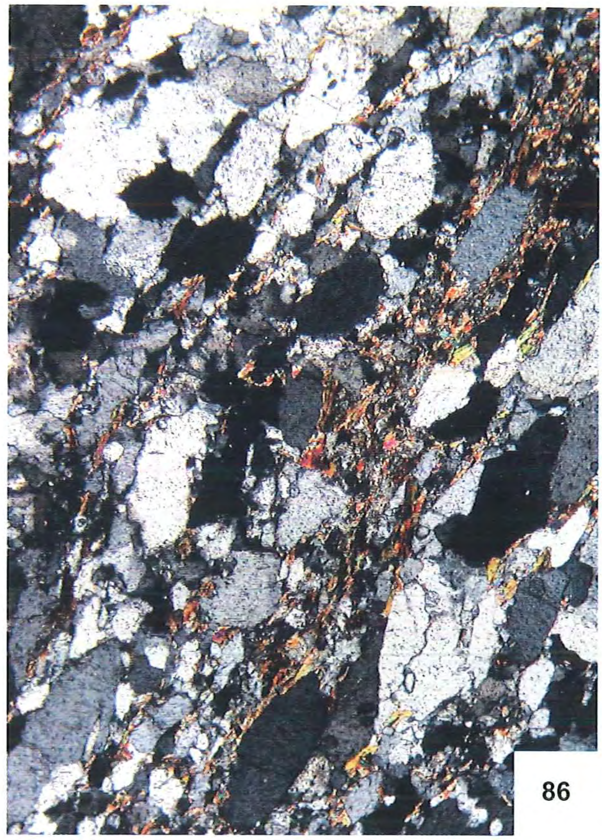
86

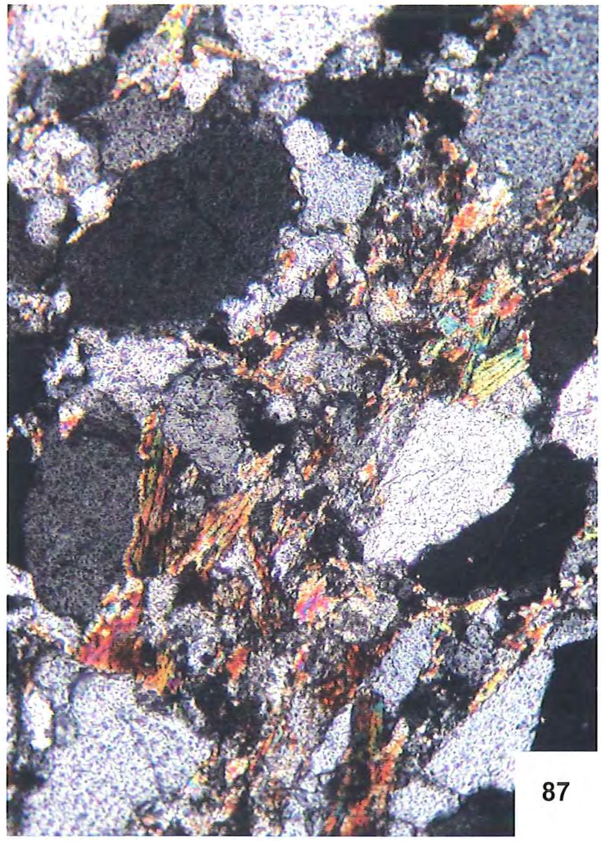
87


88

89

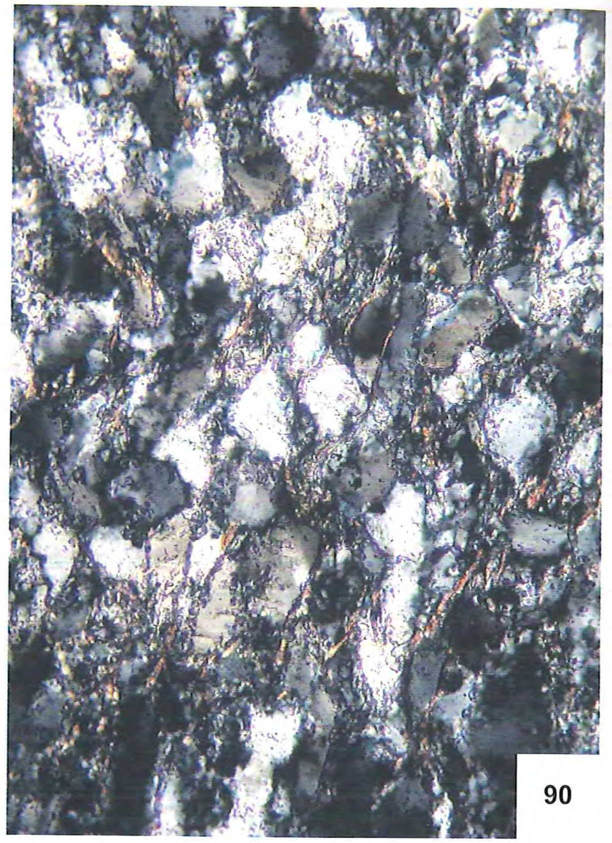

90

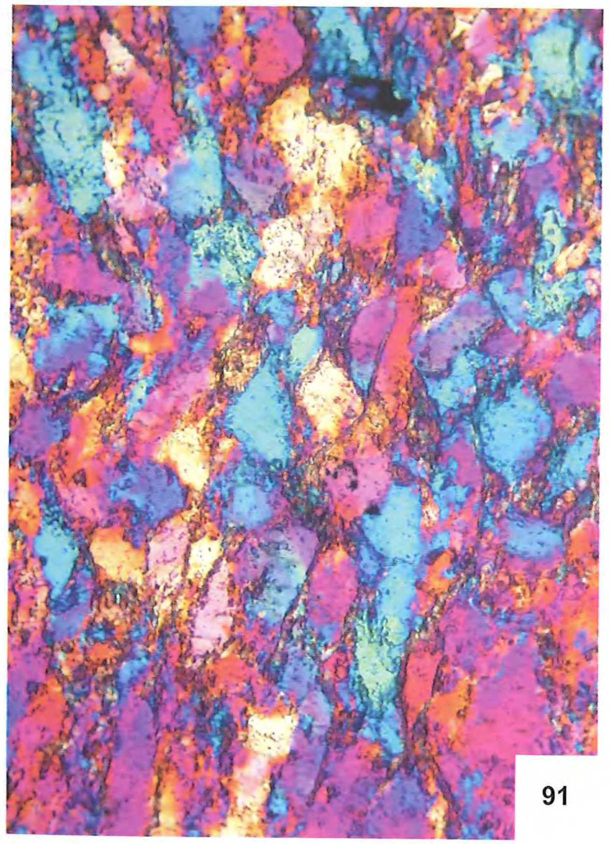

91

92

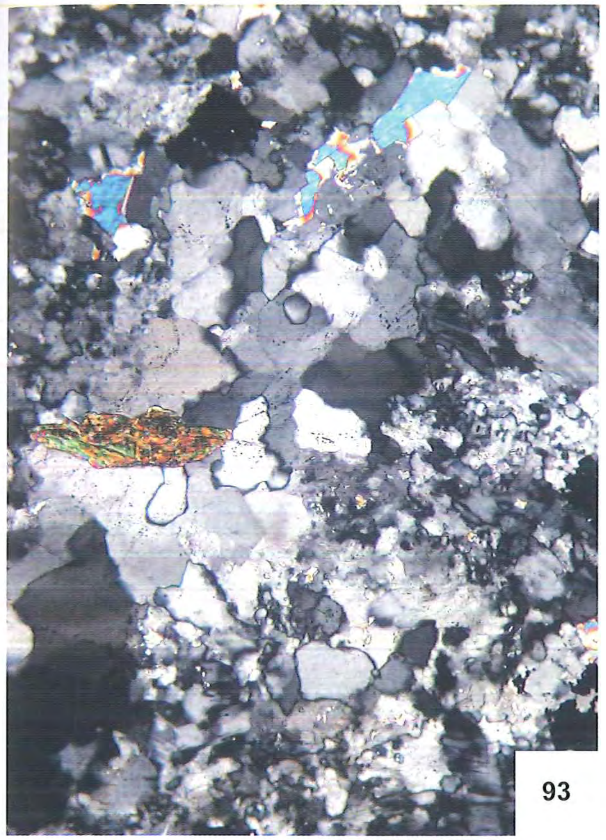

93

94

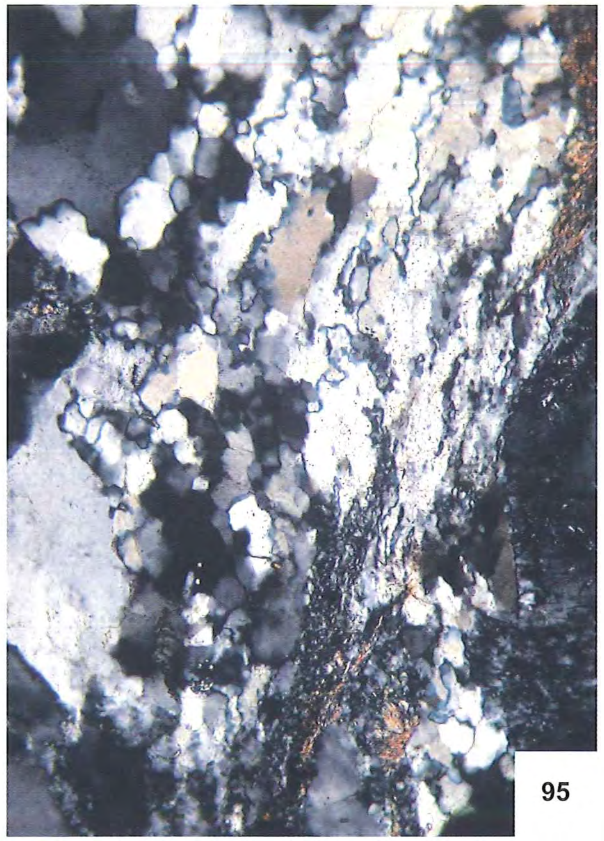

95

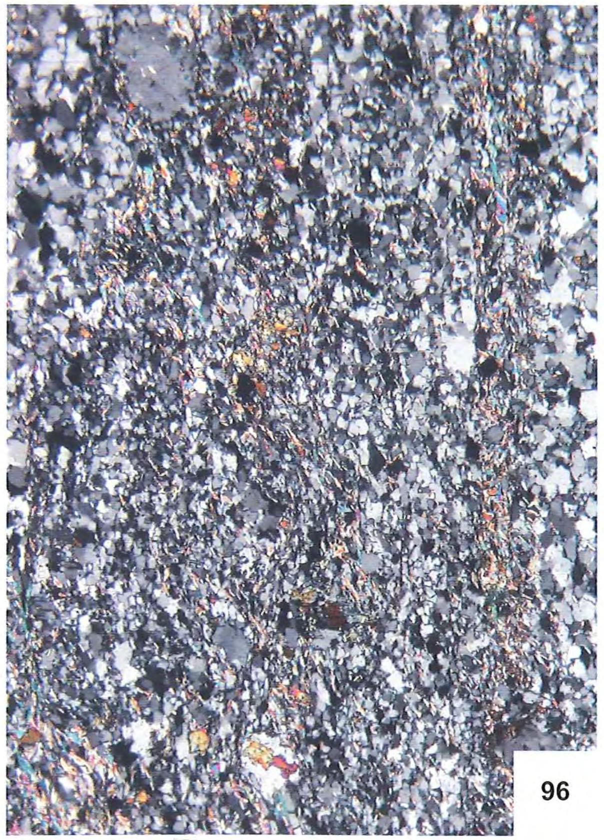

96

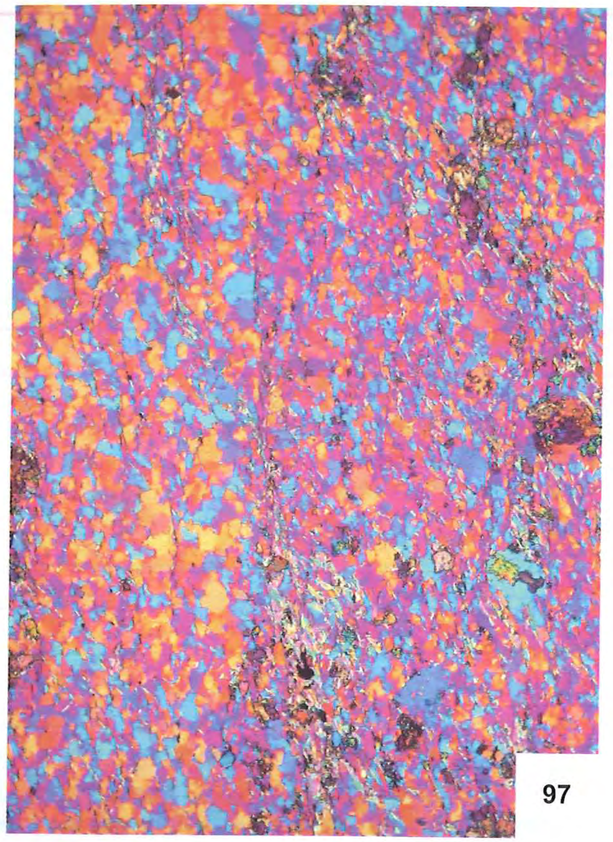
97

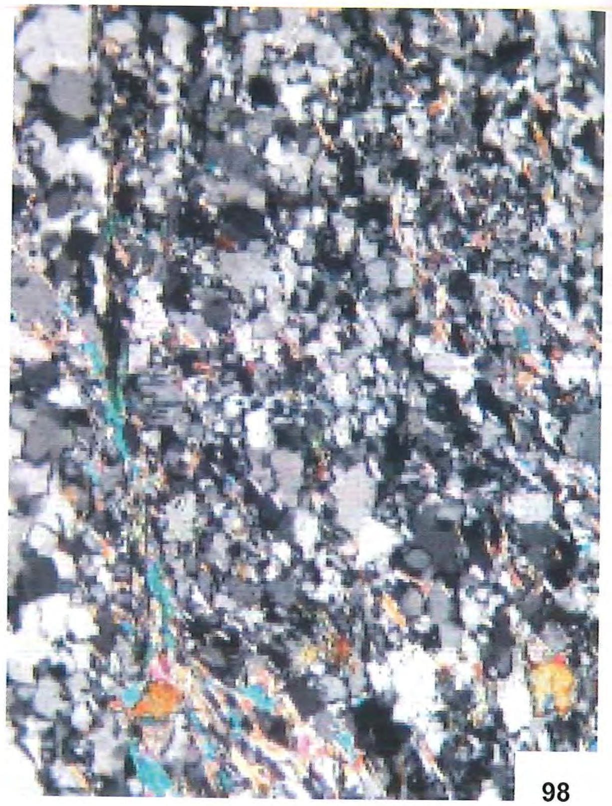
98

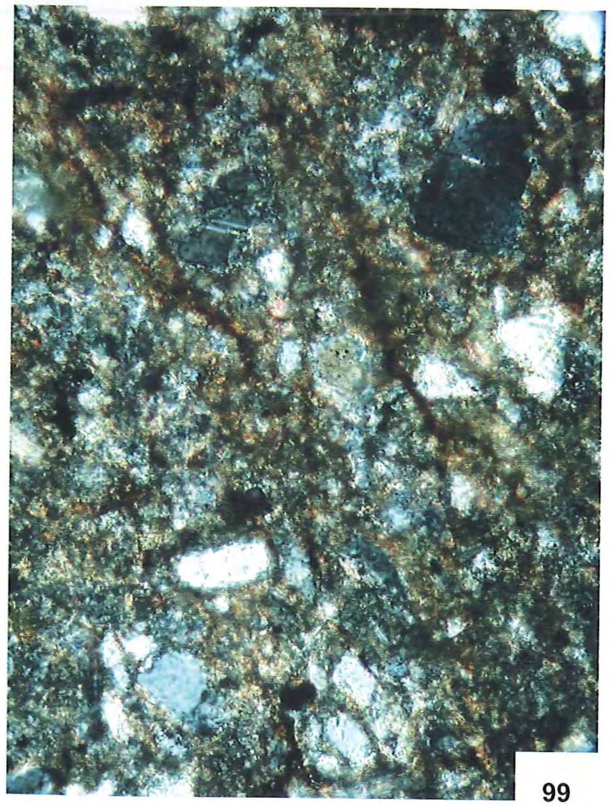
99


100

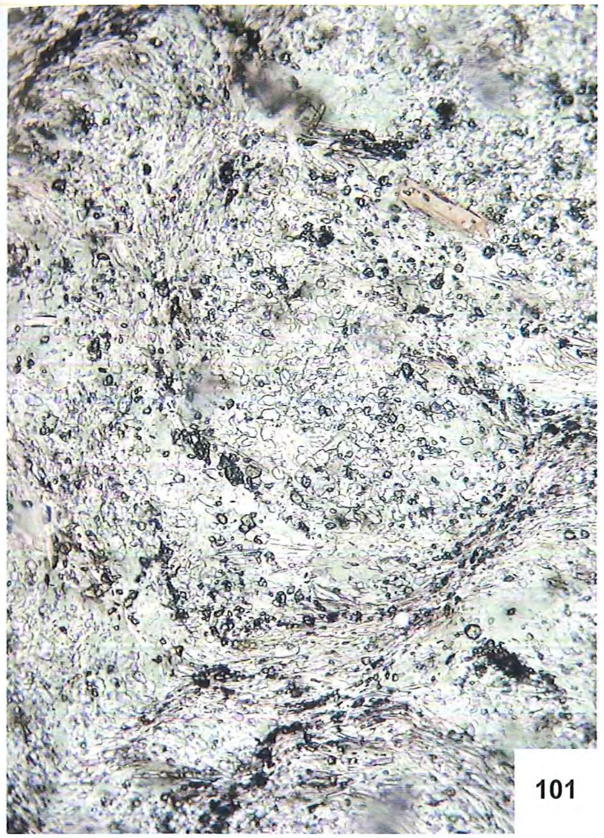
101

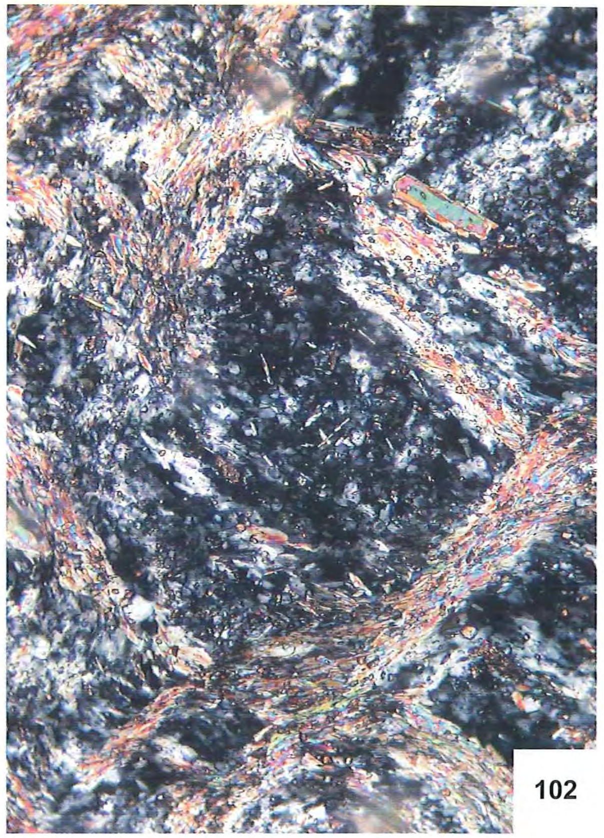
102

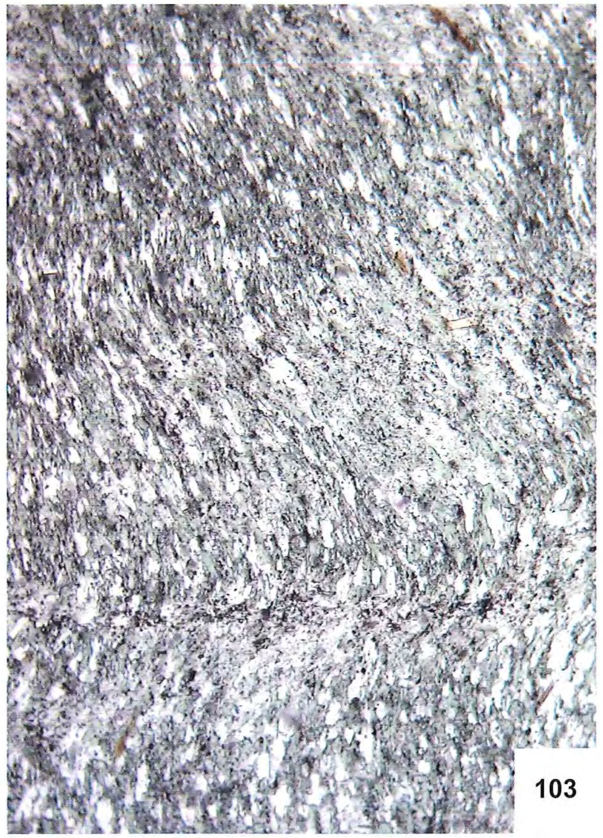
103

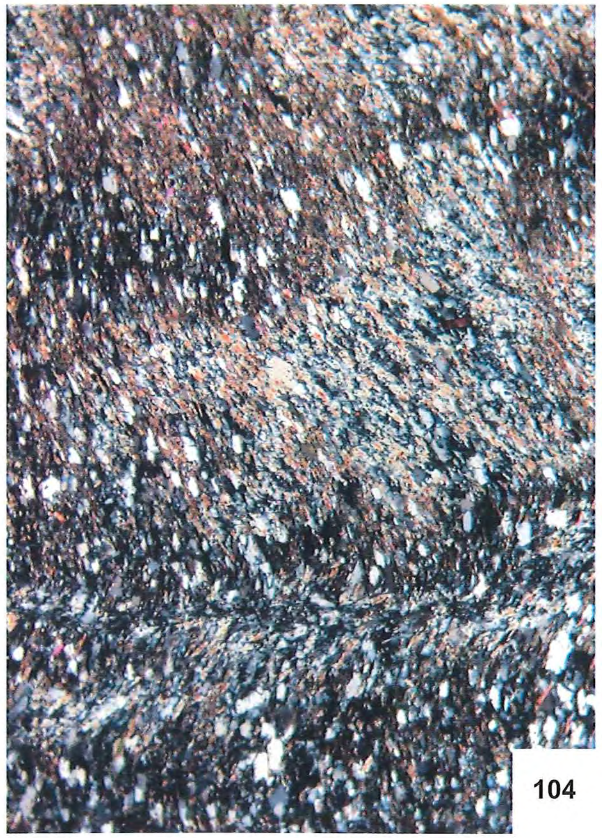
104

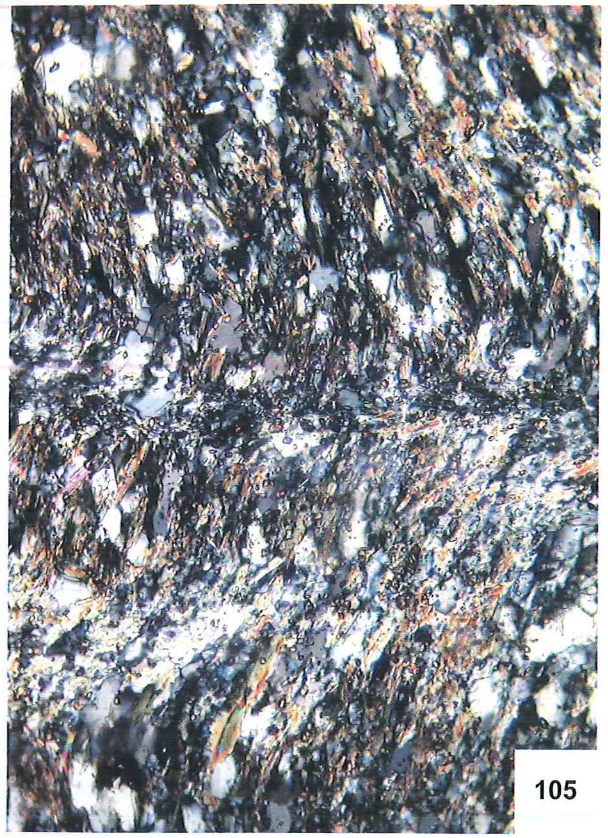
105


106

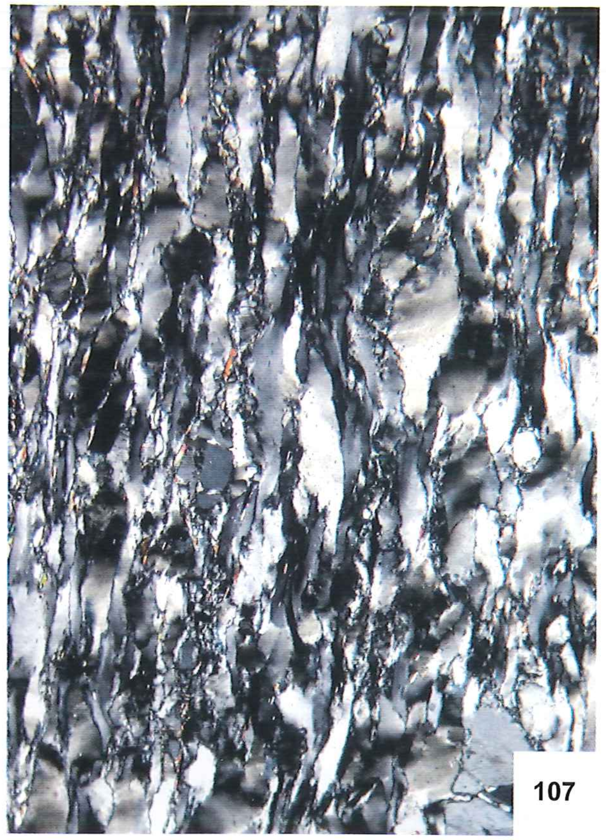
107

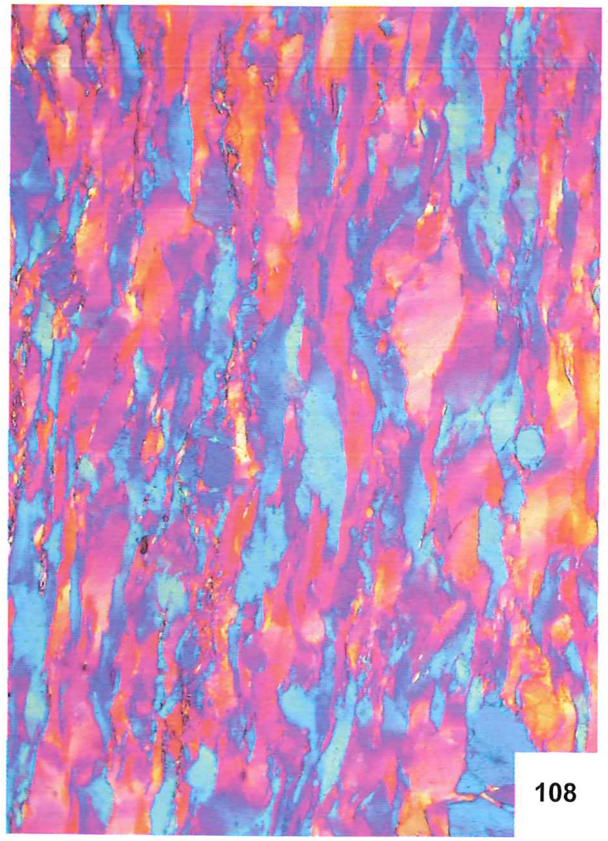
108

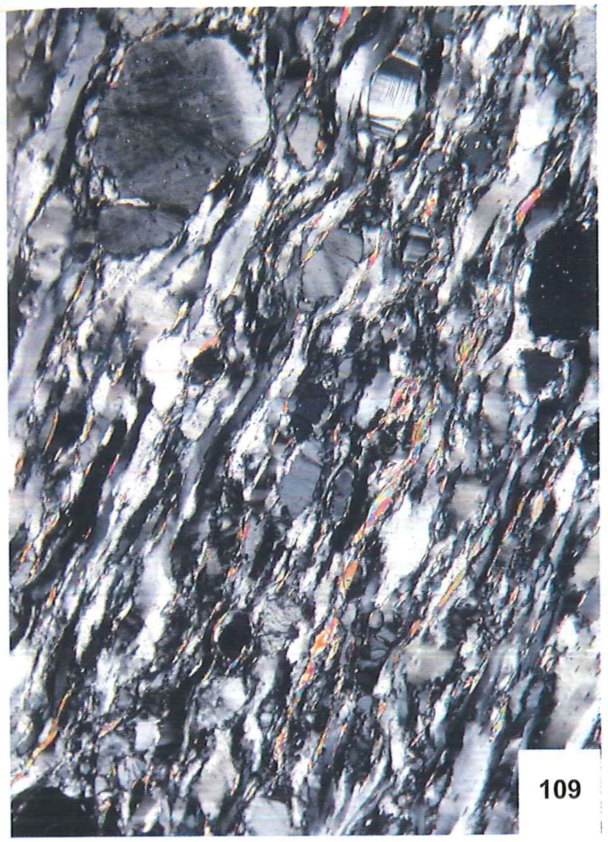
109

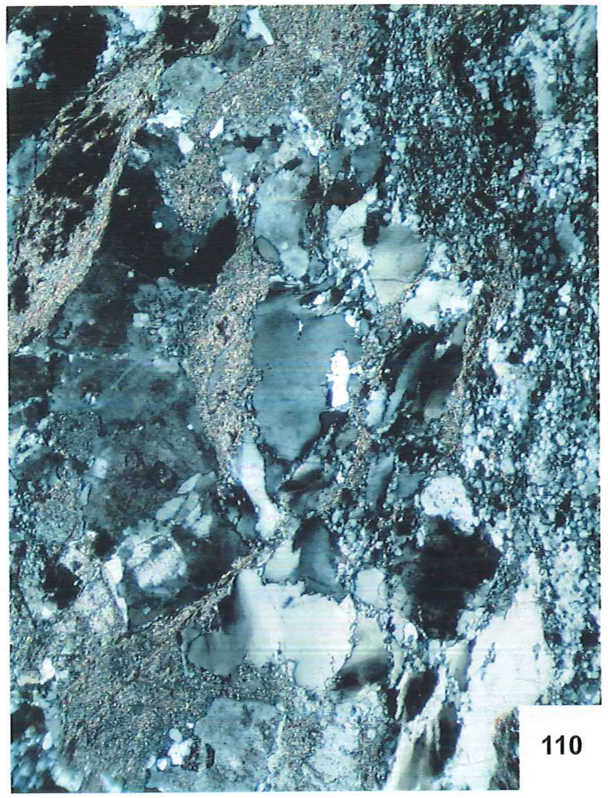
110

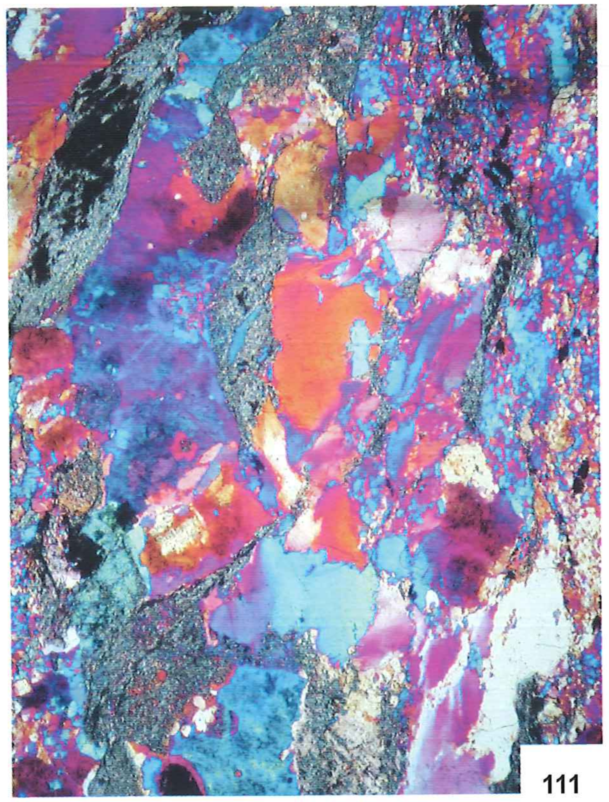
111


112

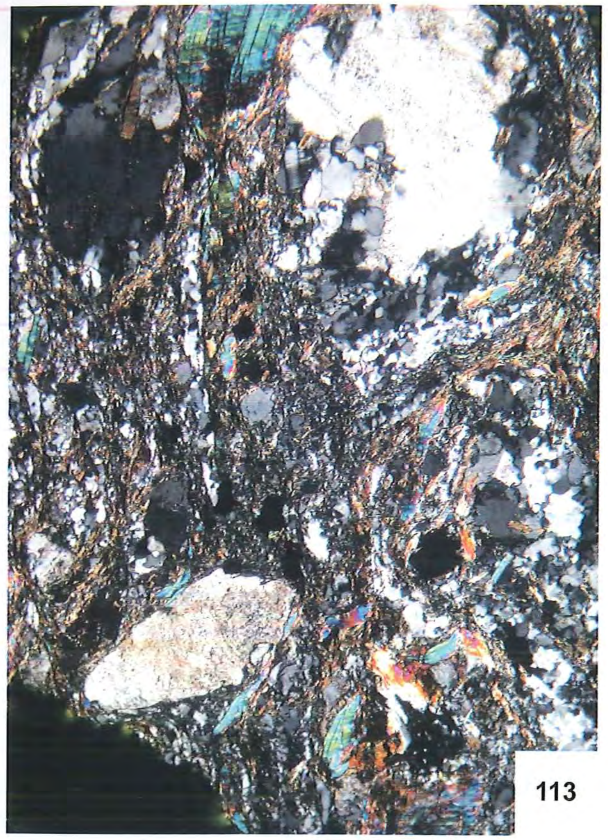
113

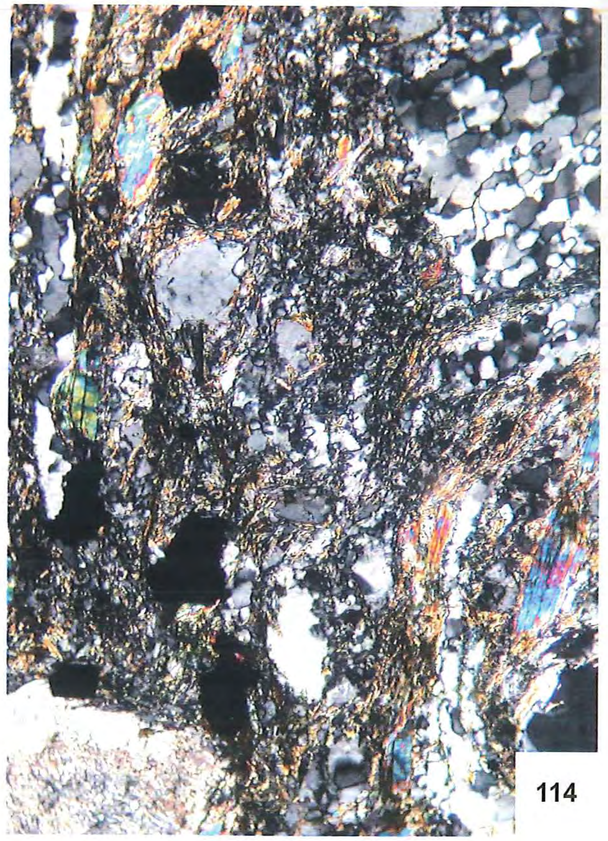
114

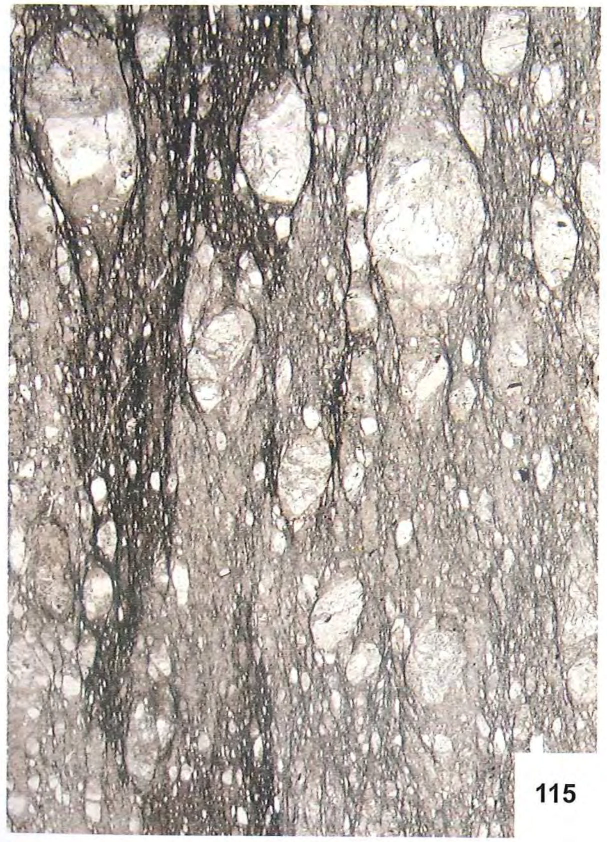
115


116

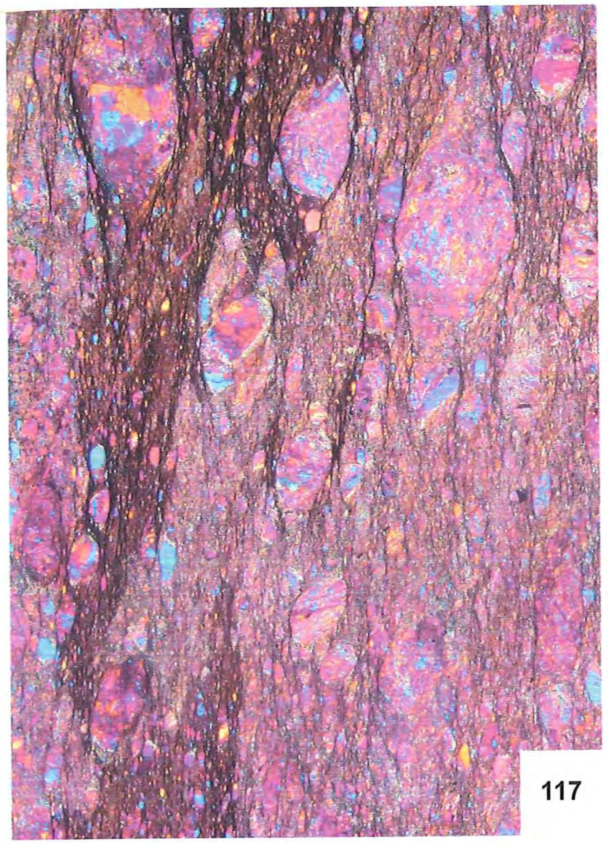
117

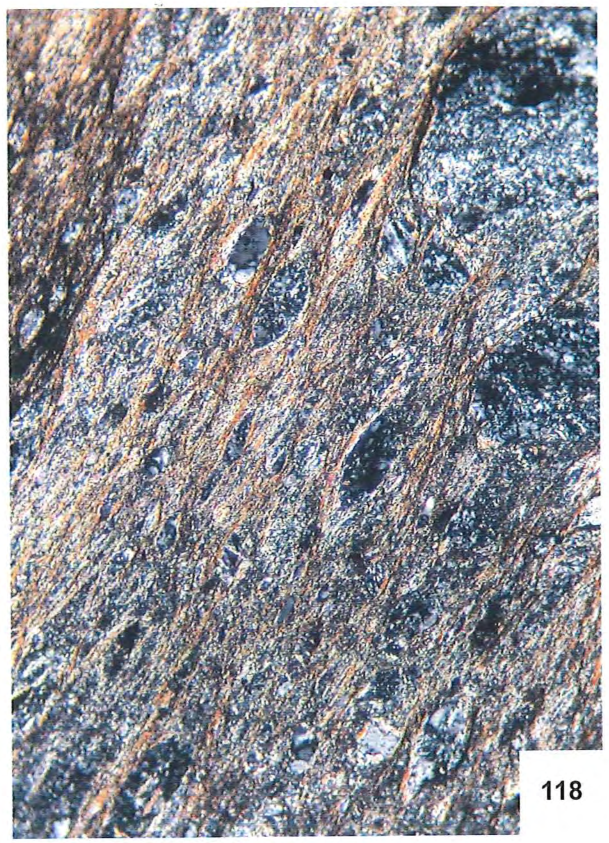
118

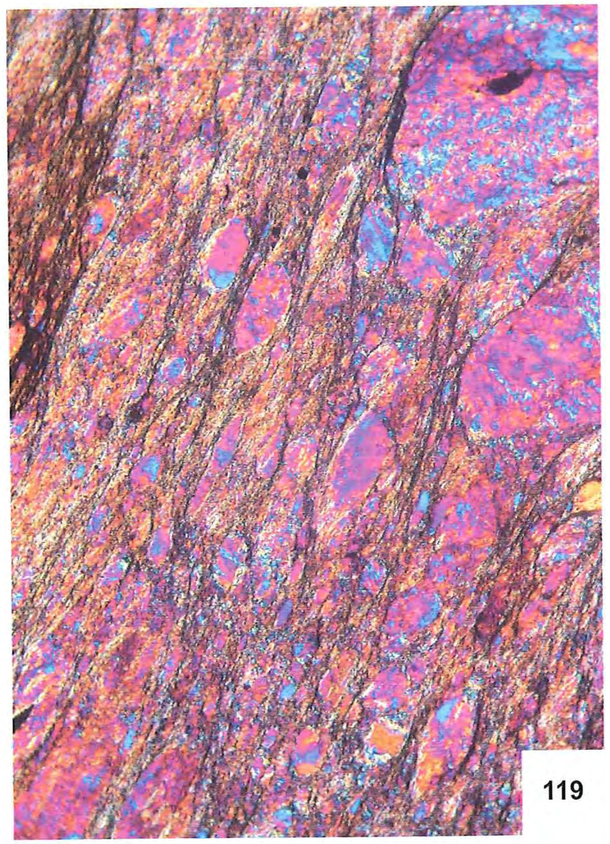
119


120

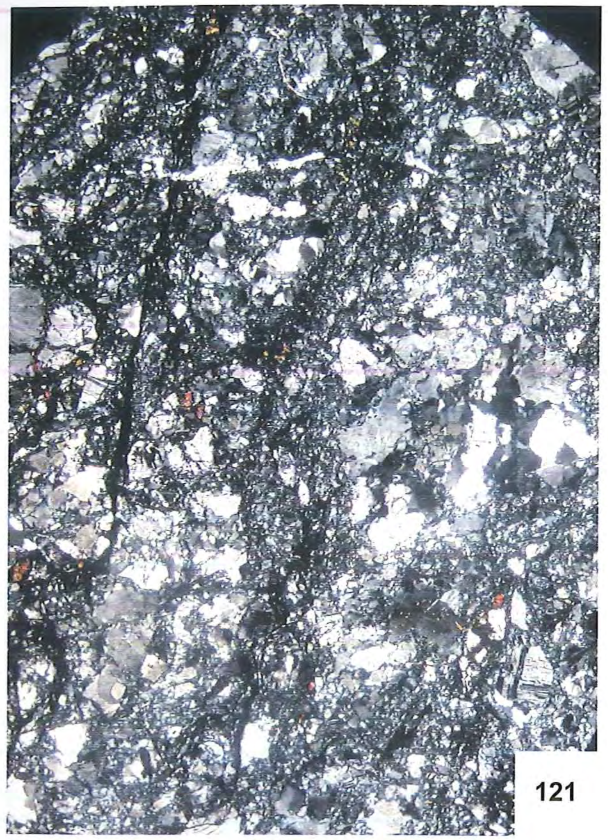
121


122

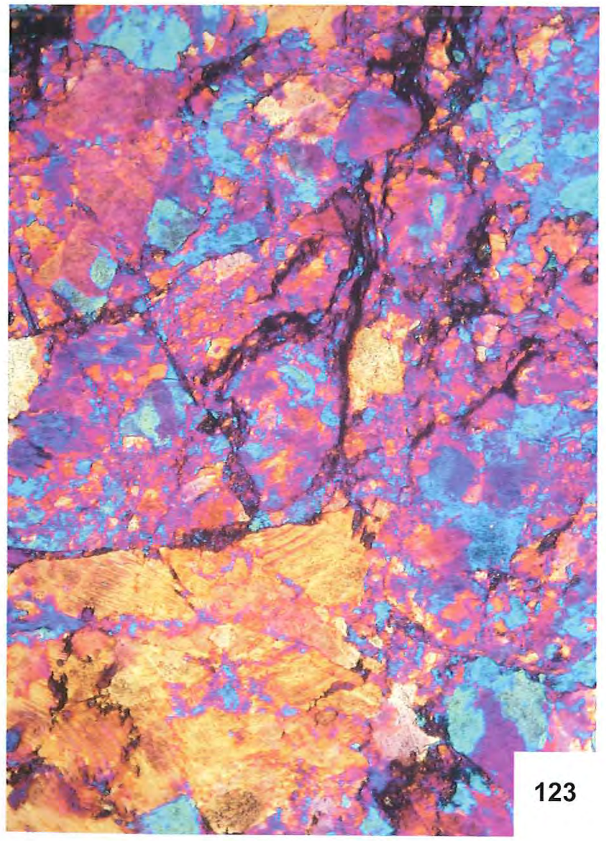
123


124


125

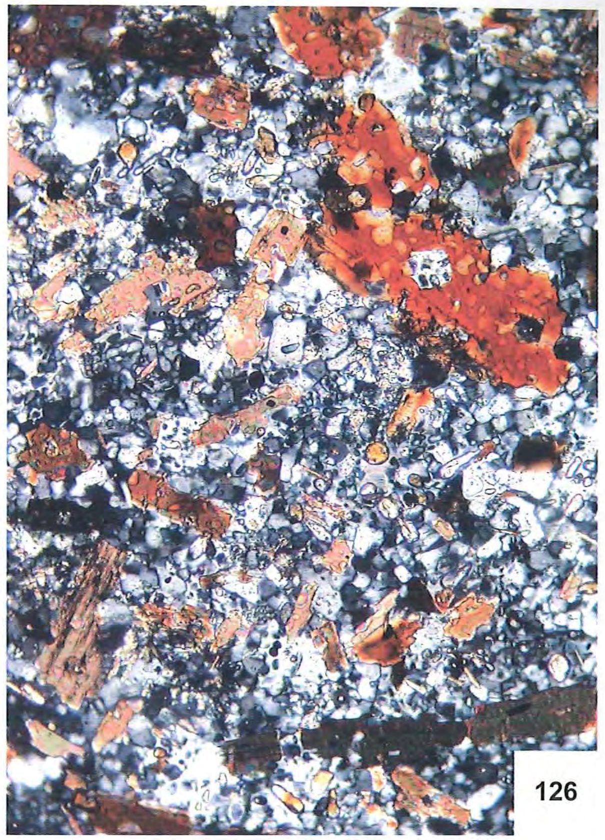
126


127


128

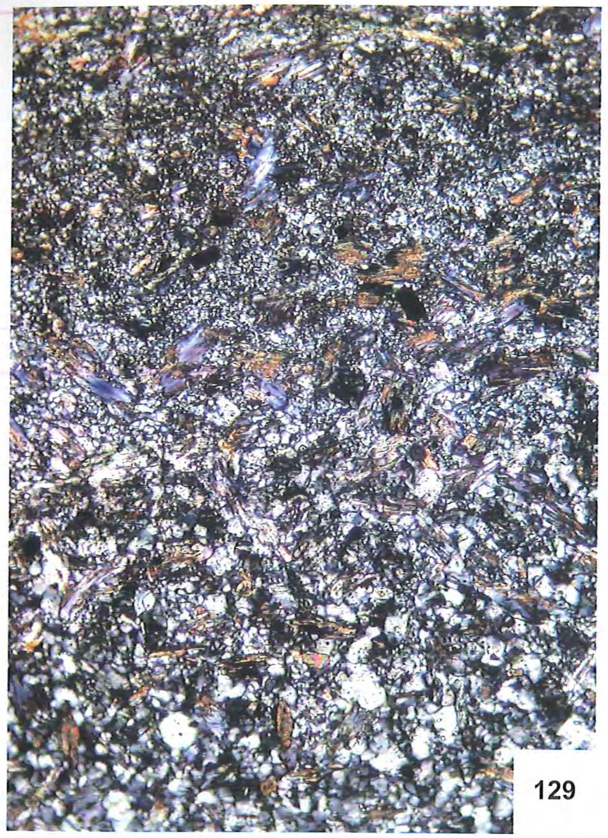

129

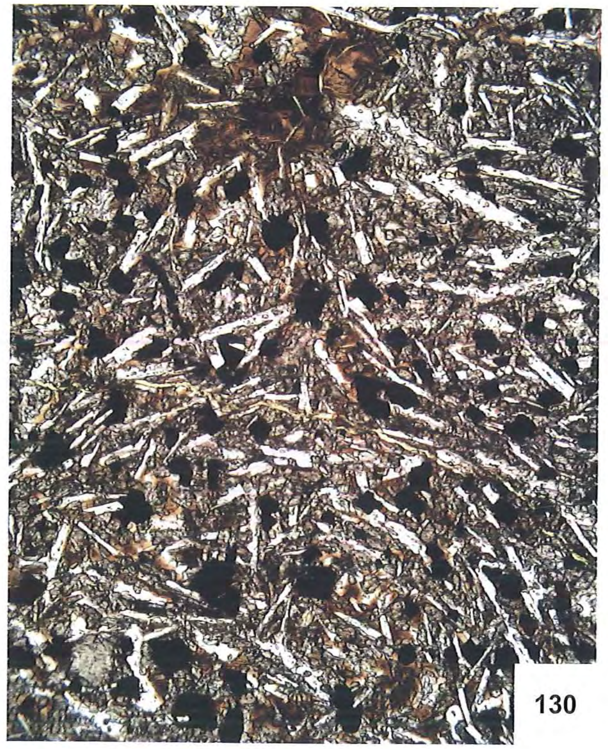

130

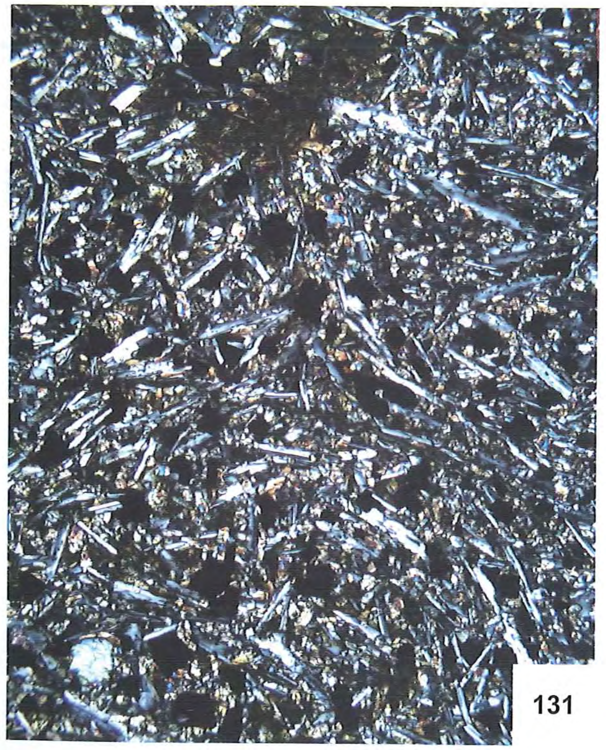

131

132

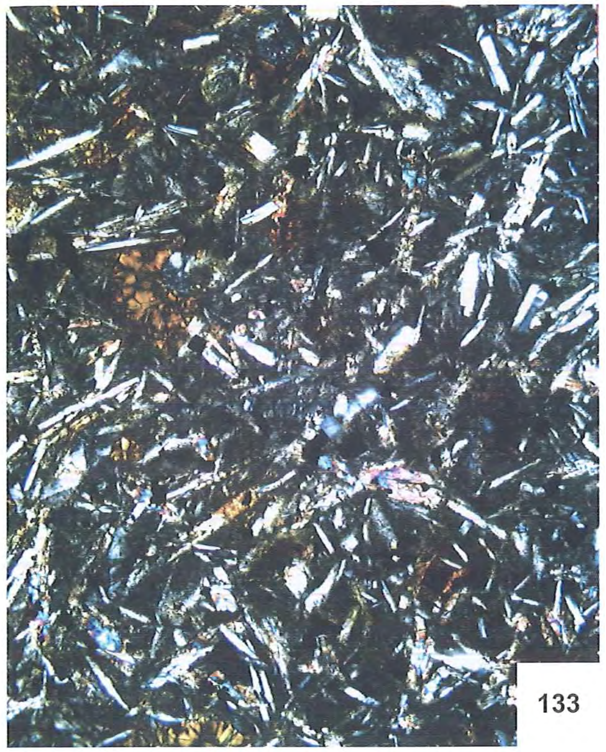

133

134

135

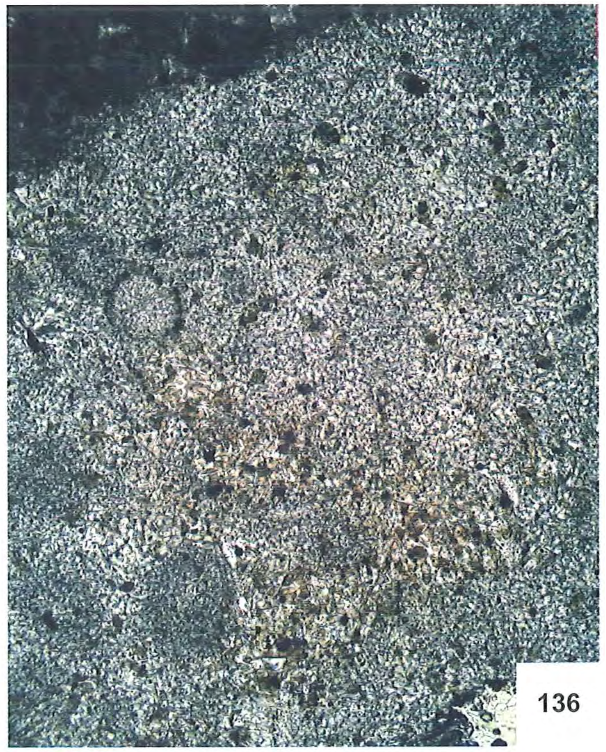

136

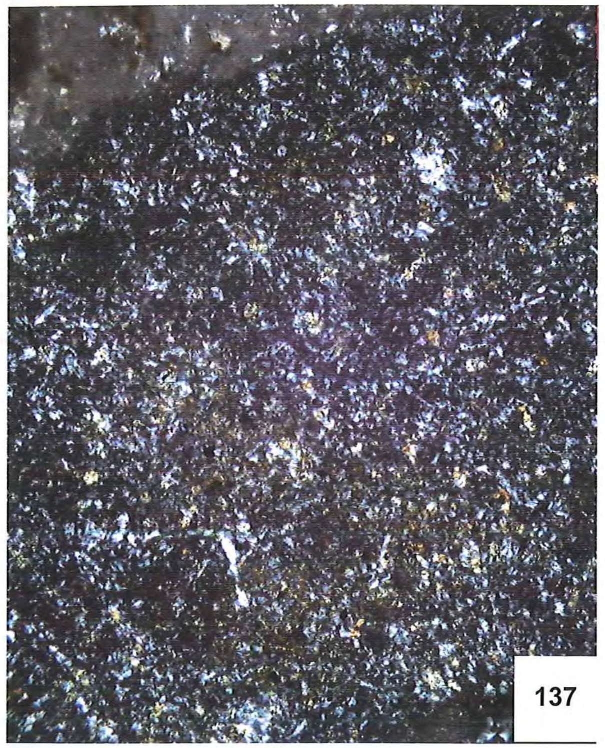

137

138

139

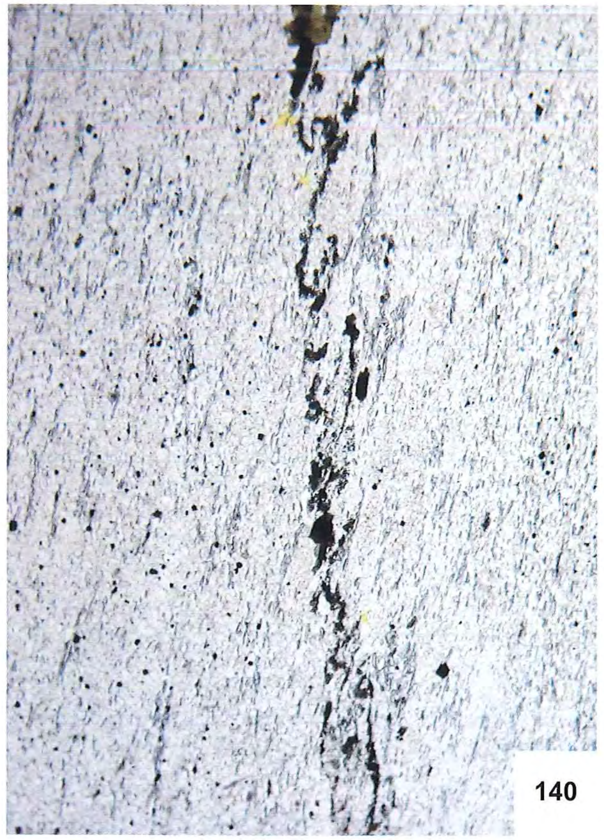

140

141

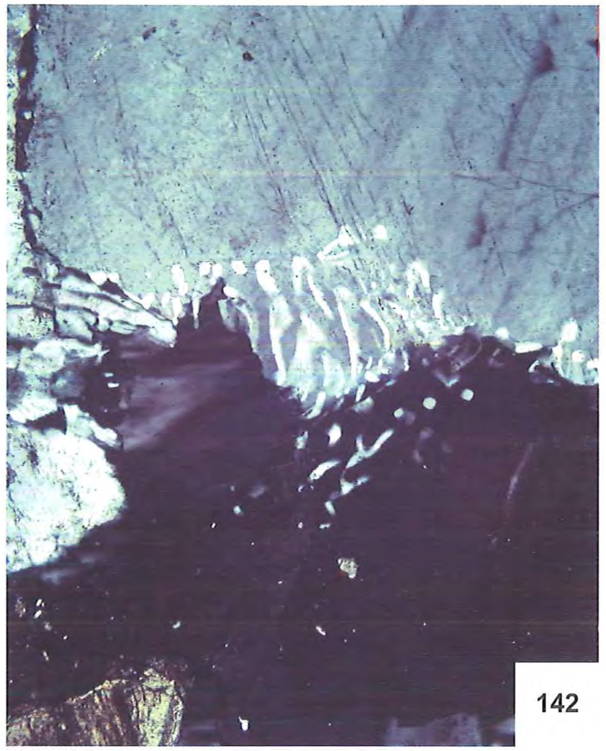

142

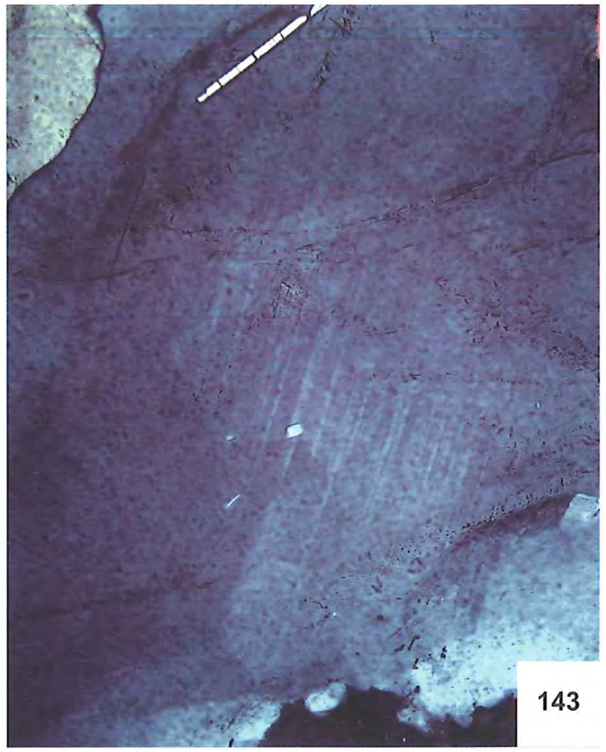

143

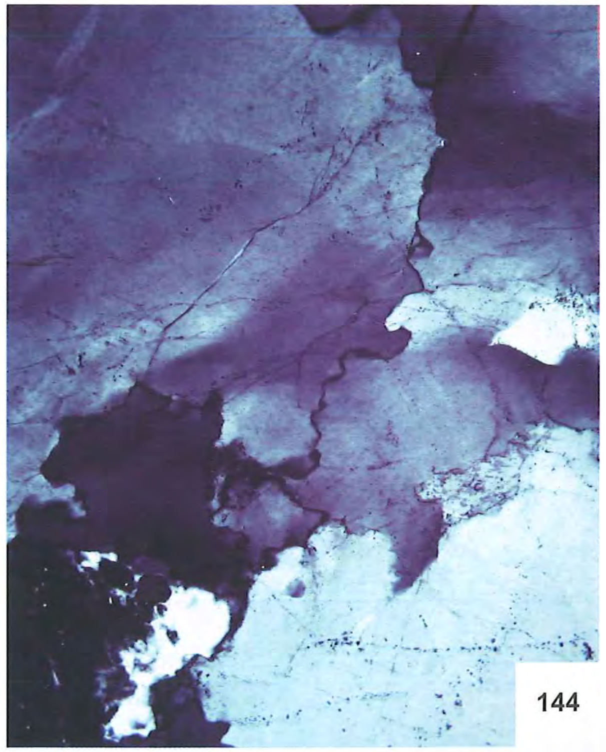

144


145

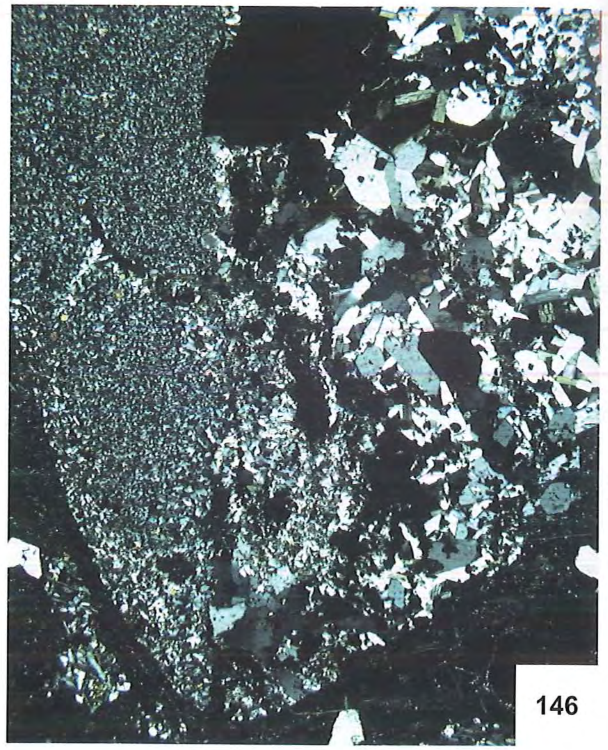
146

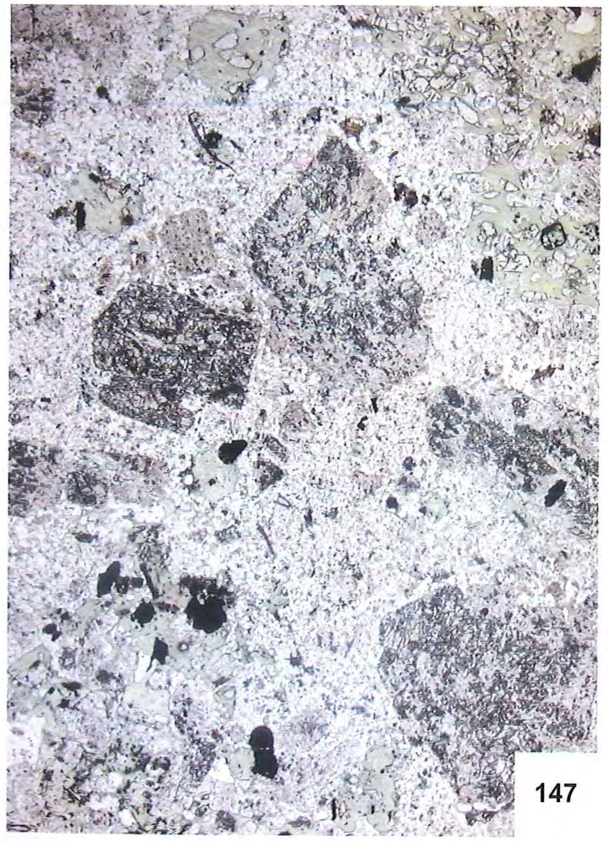
147

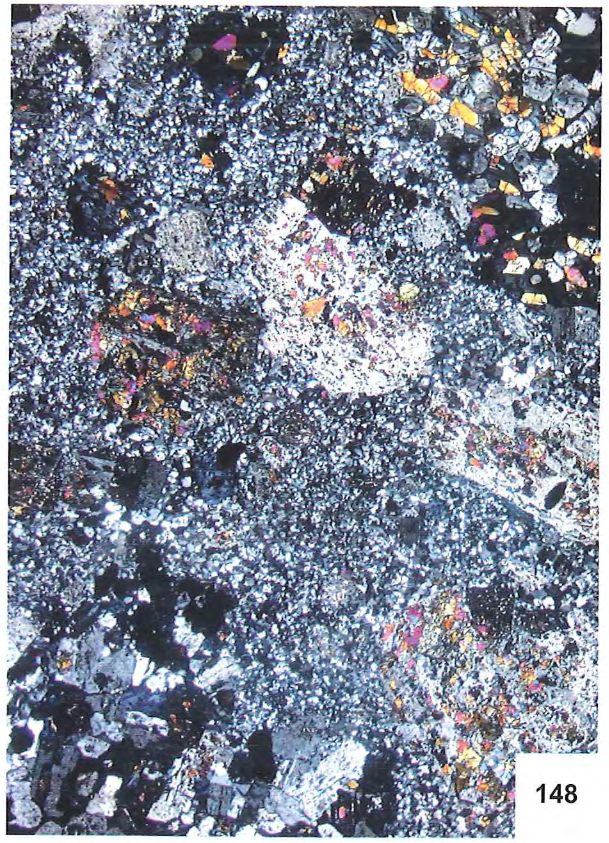
148

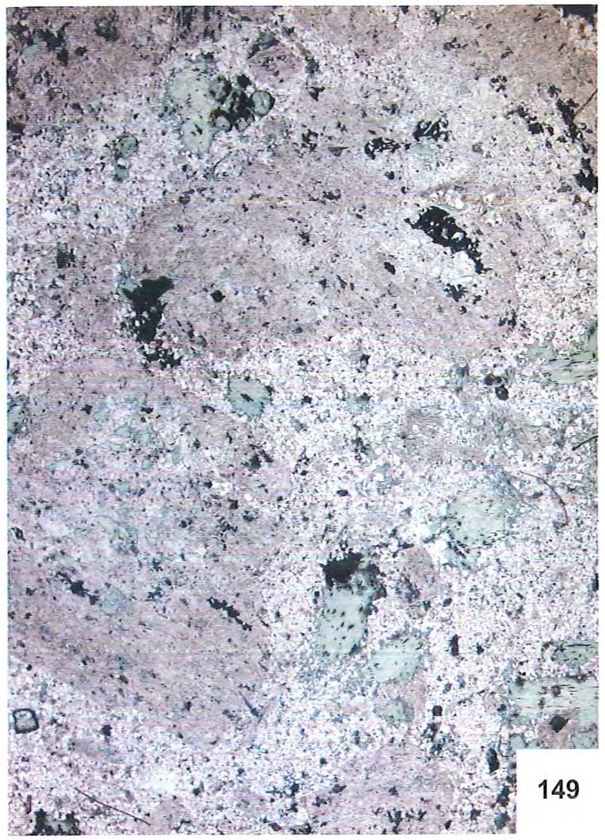
149


150

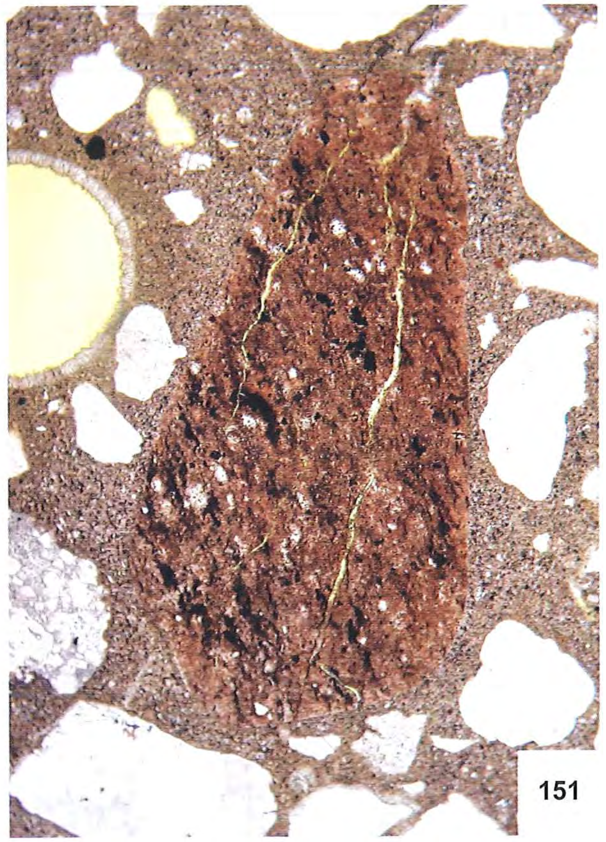
151

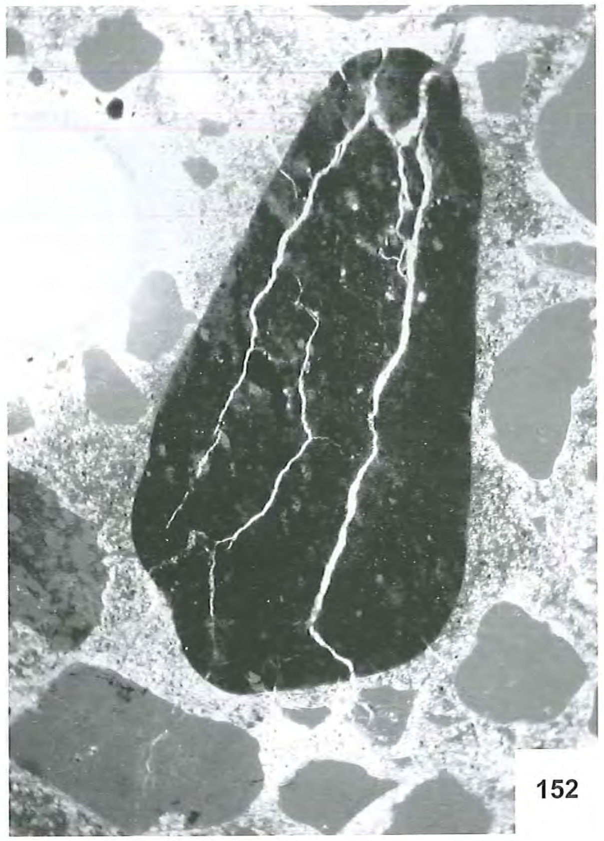
152


153

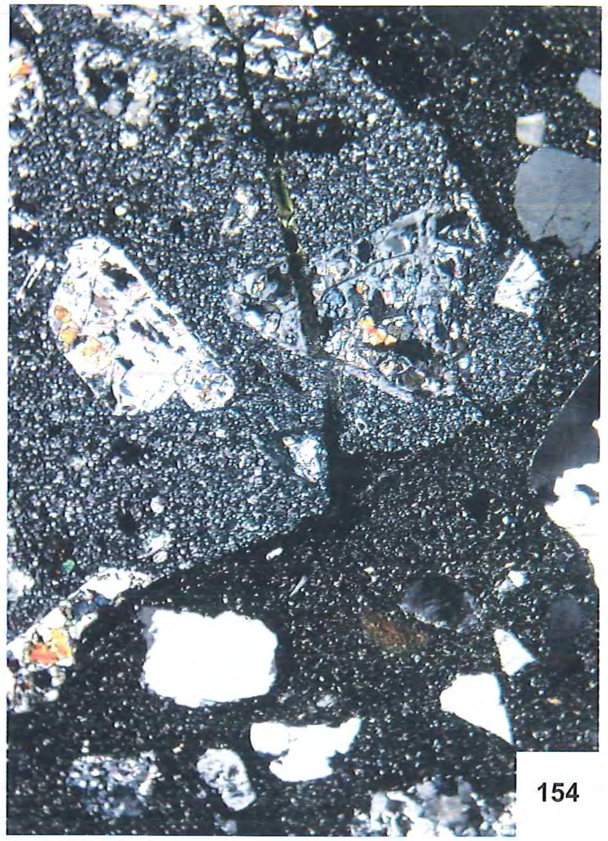
154

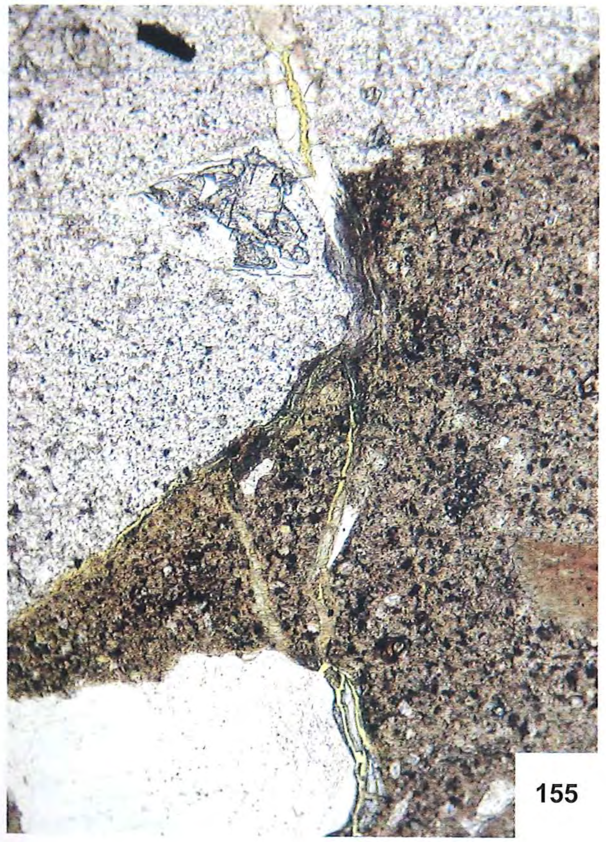
155

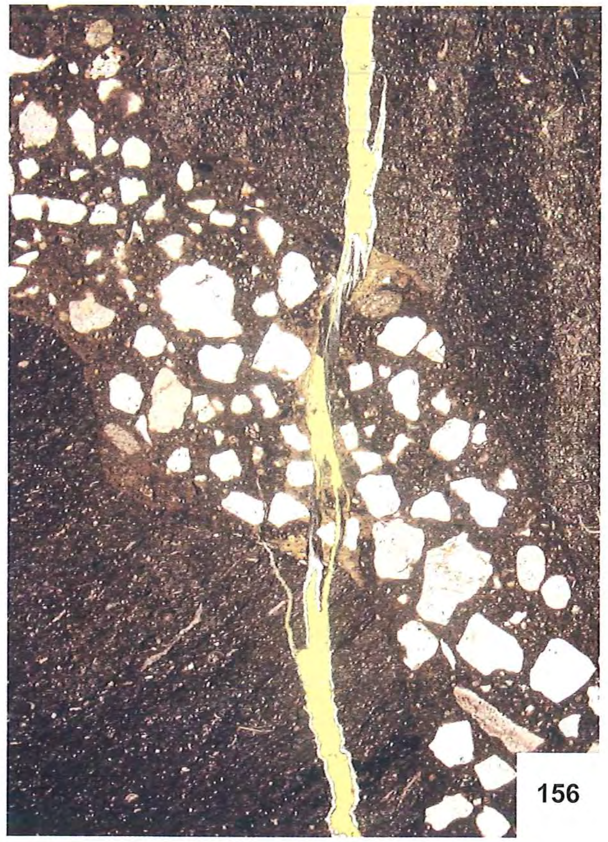
156

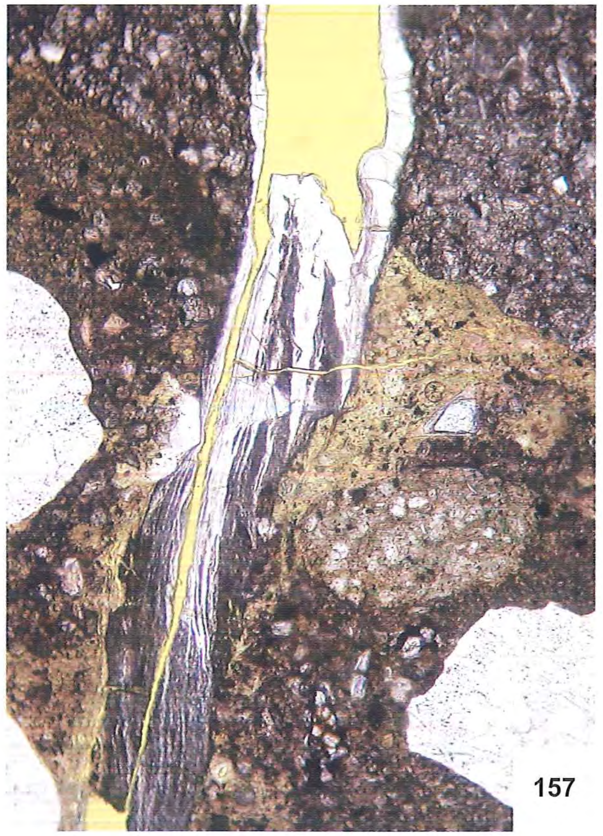
157


158

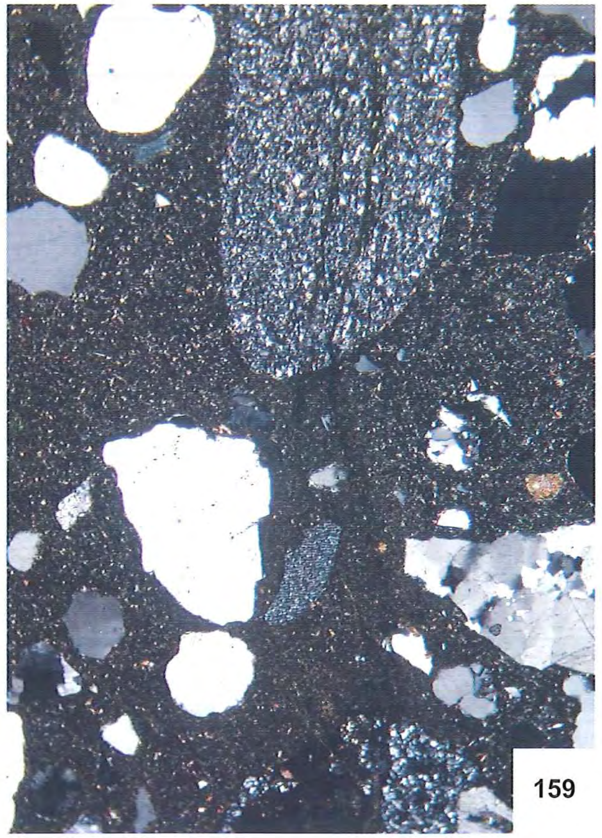
159

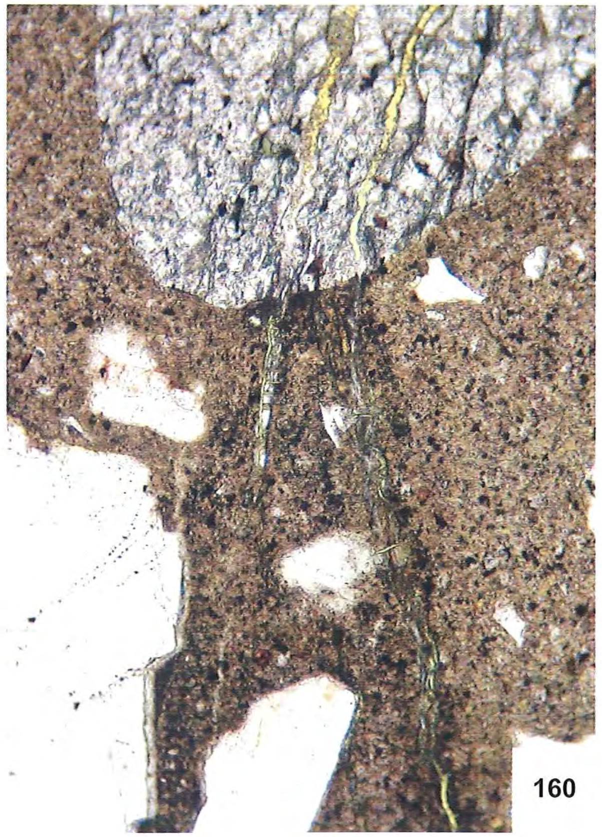
160


161

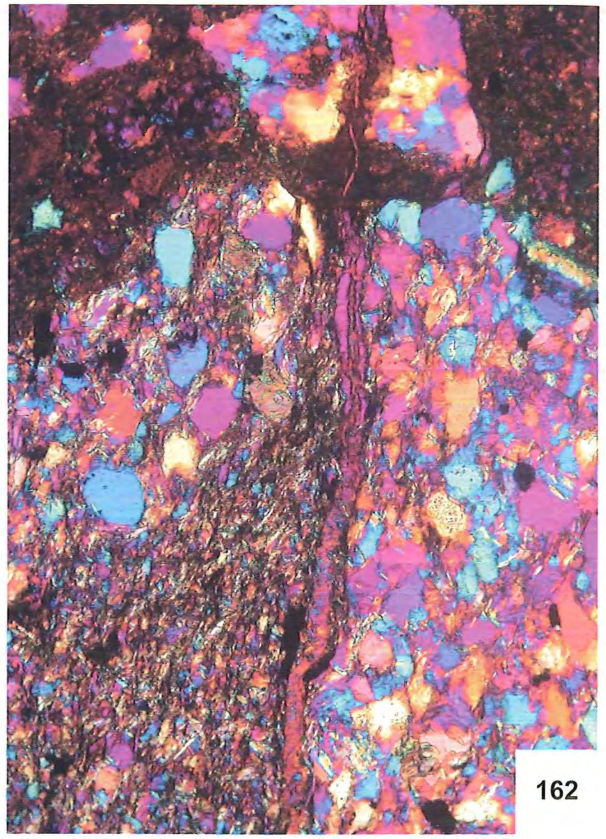
162

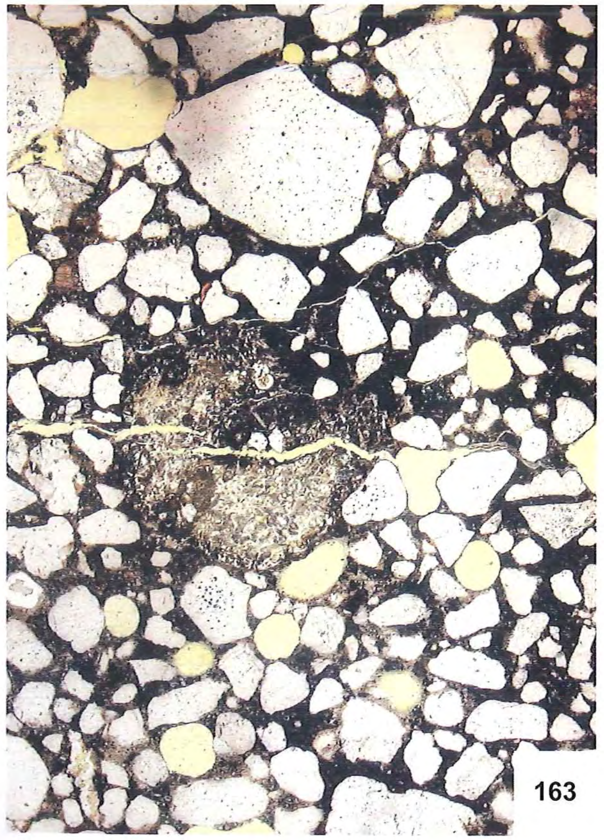
163

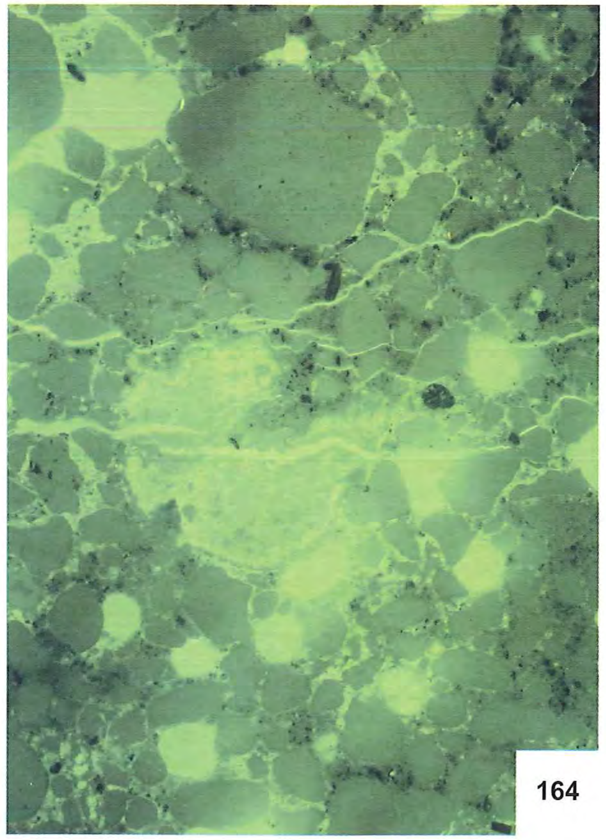
164


165

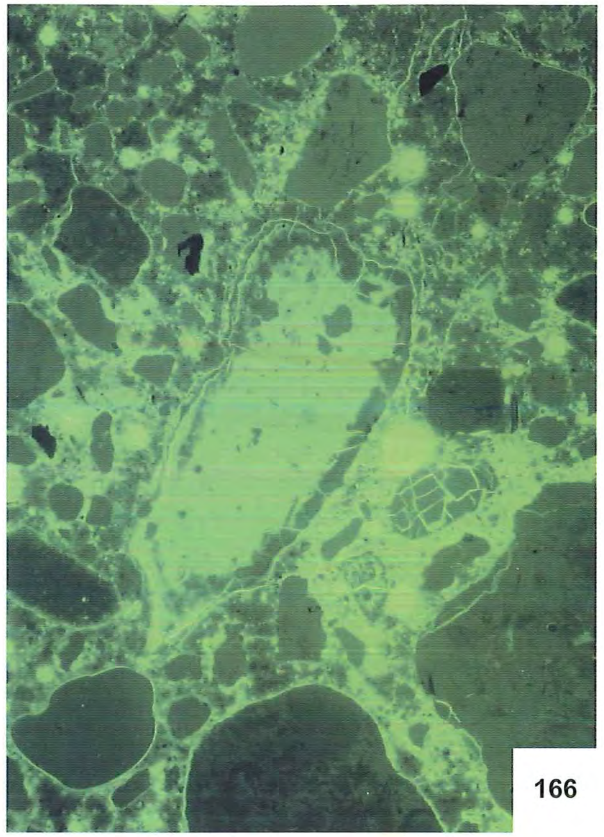
166


167

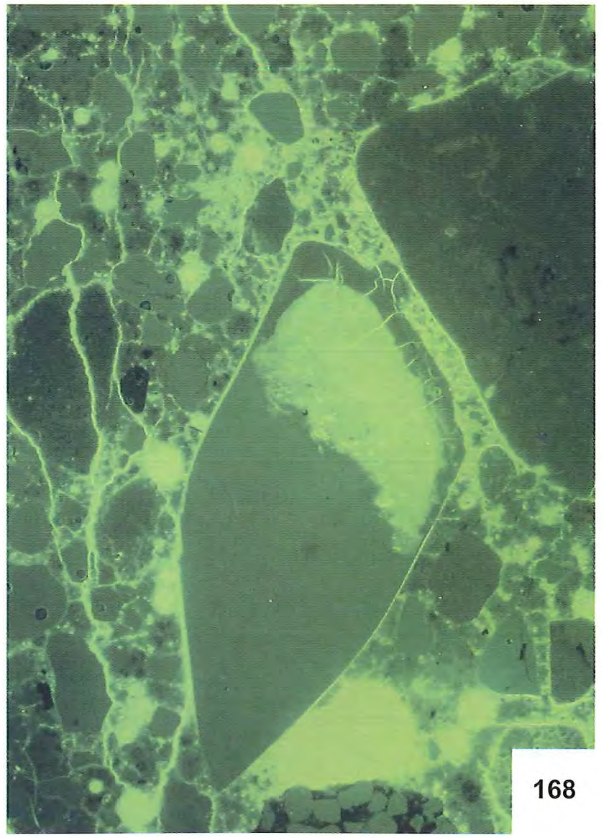
168

169

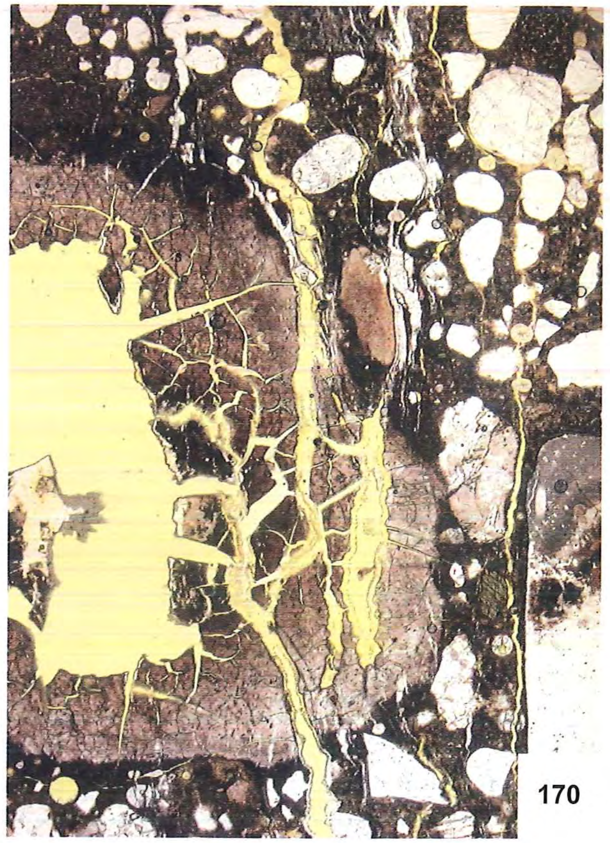

170

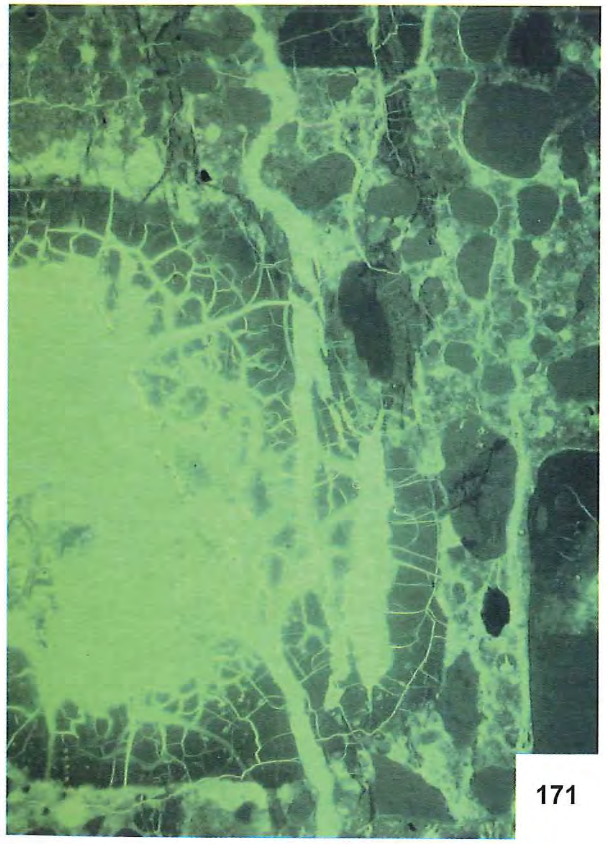

171

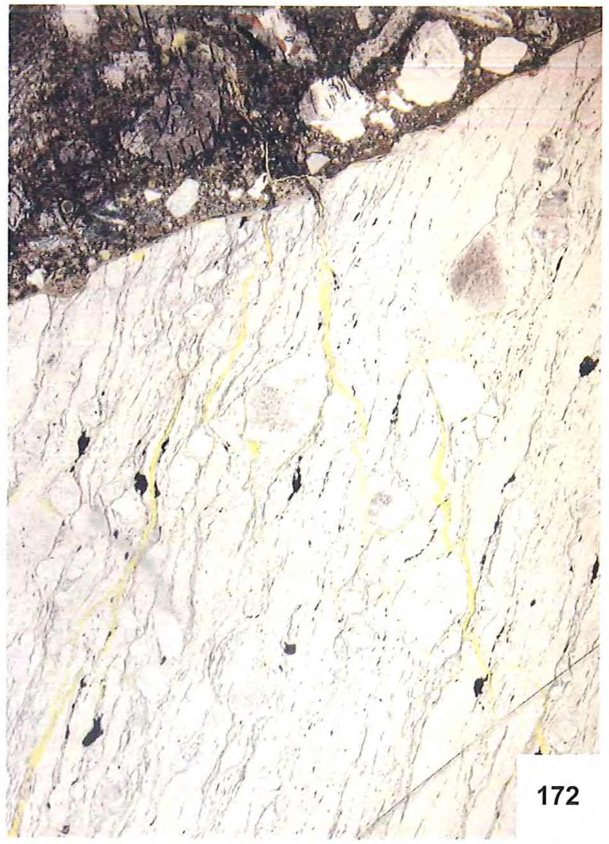

172

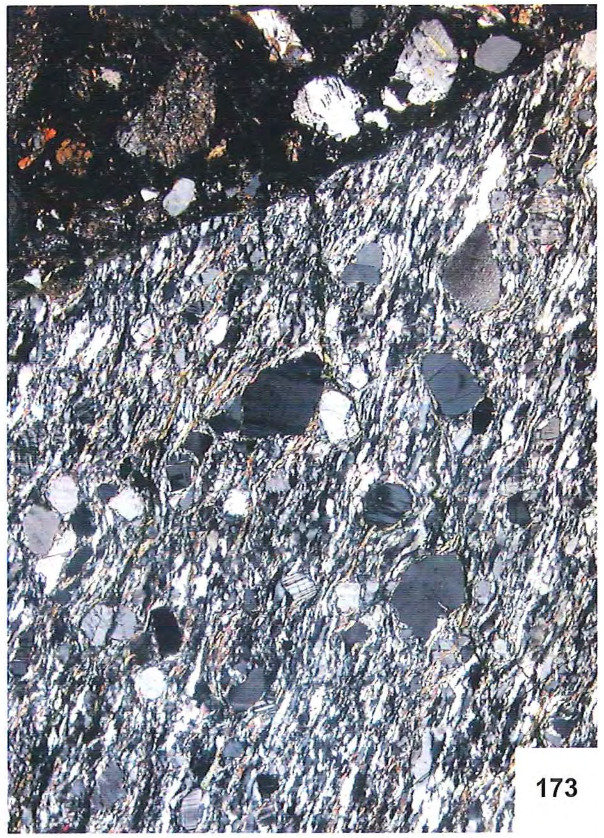

173

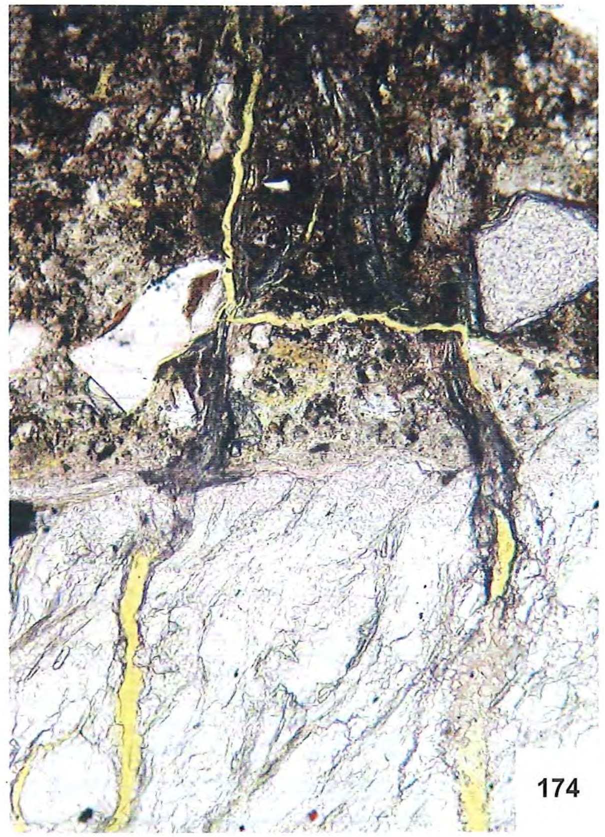

174

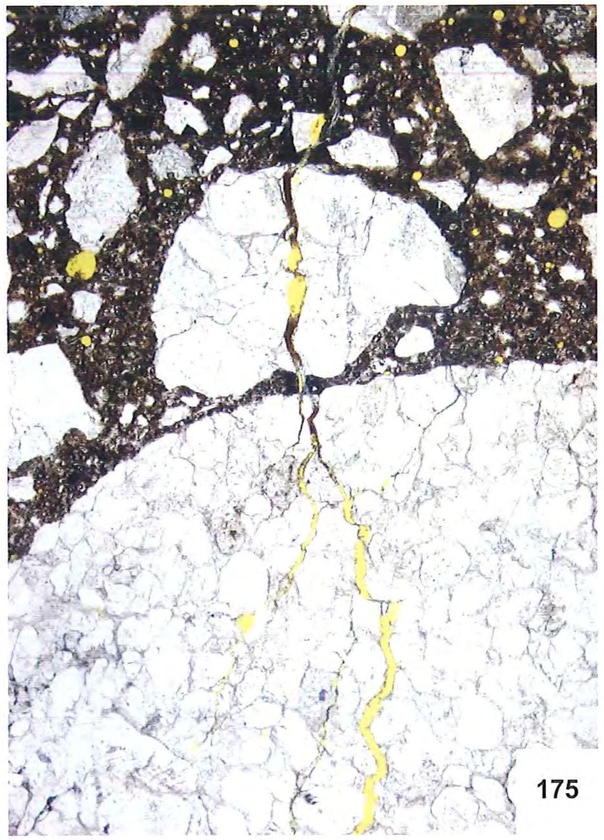

175

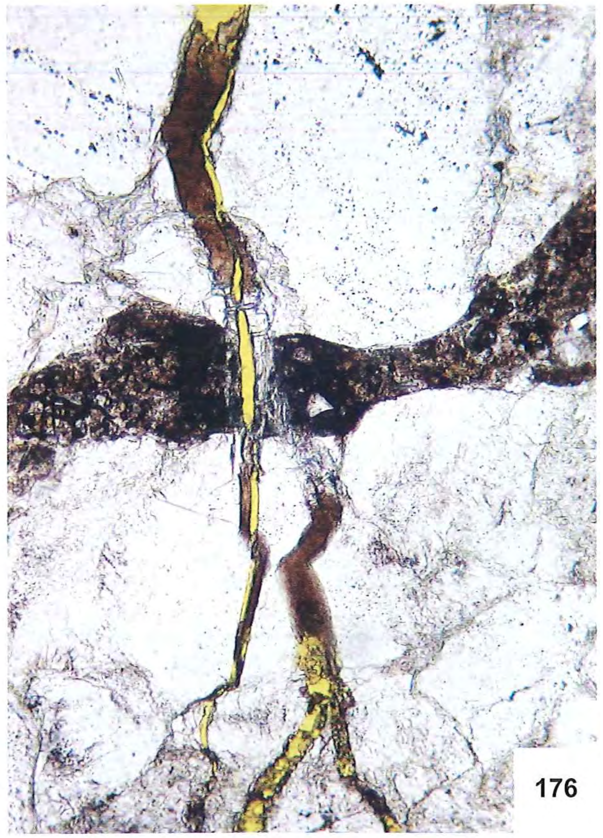

176

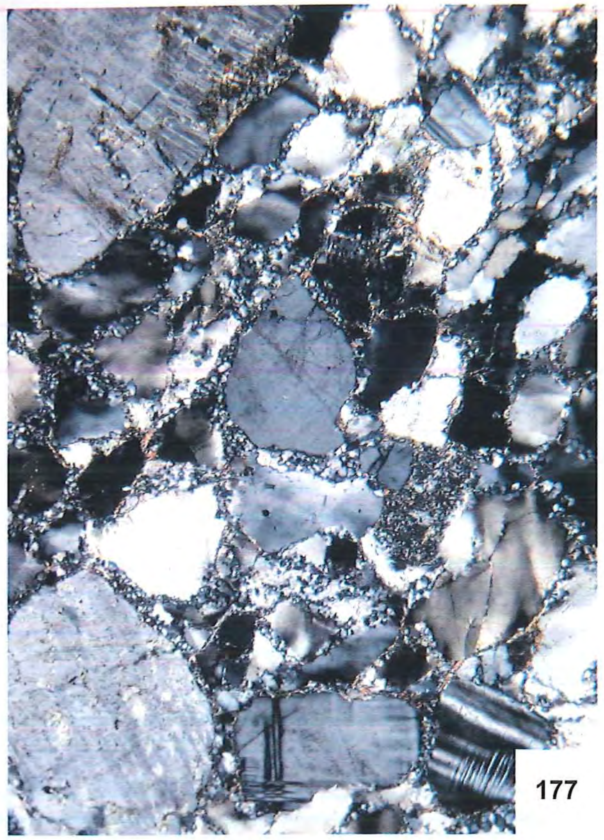
177


178

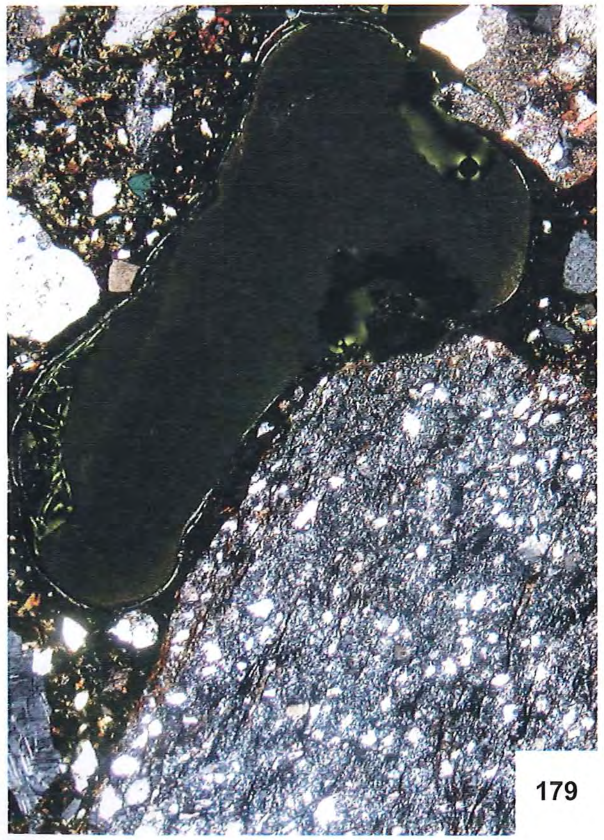
179

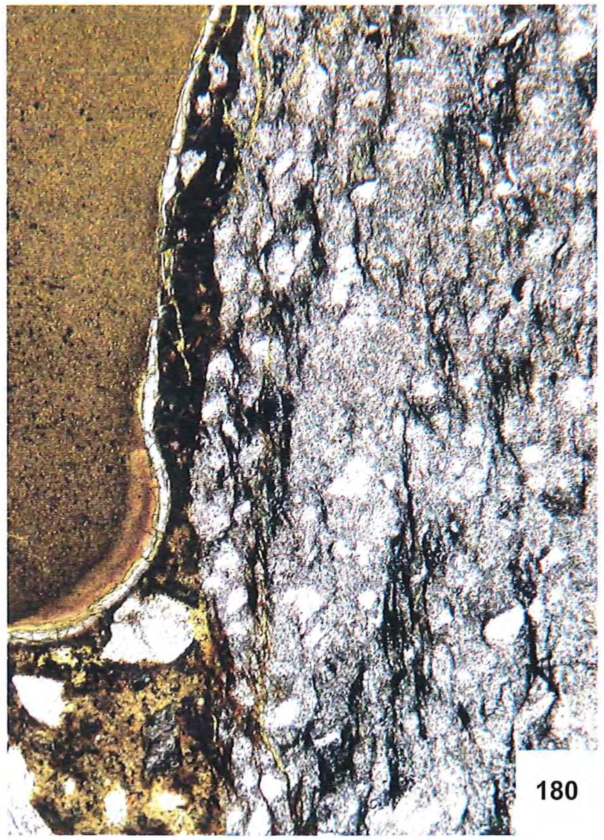
180

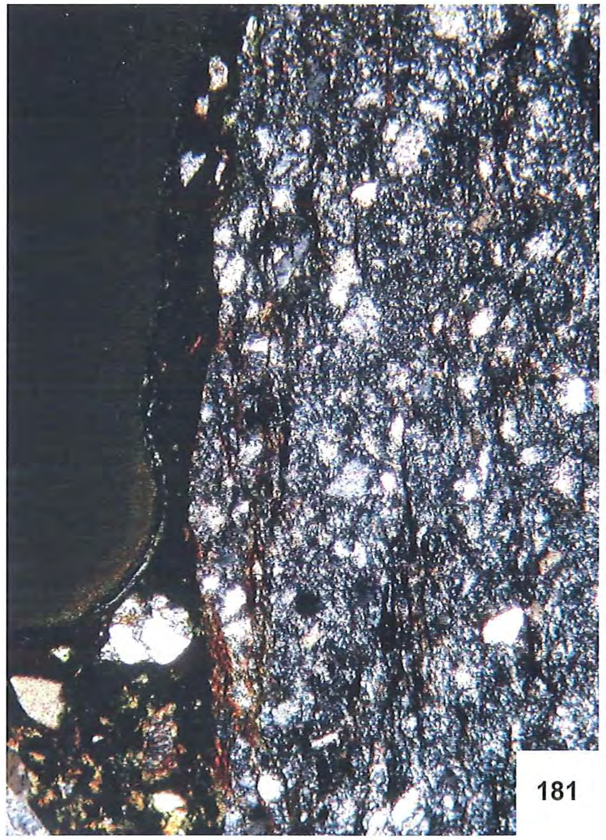
181


182


183

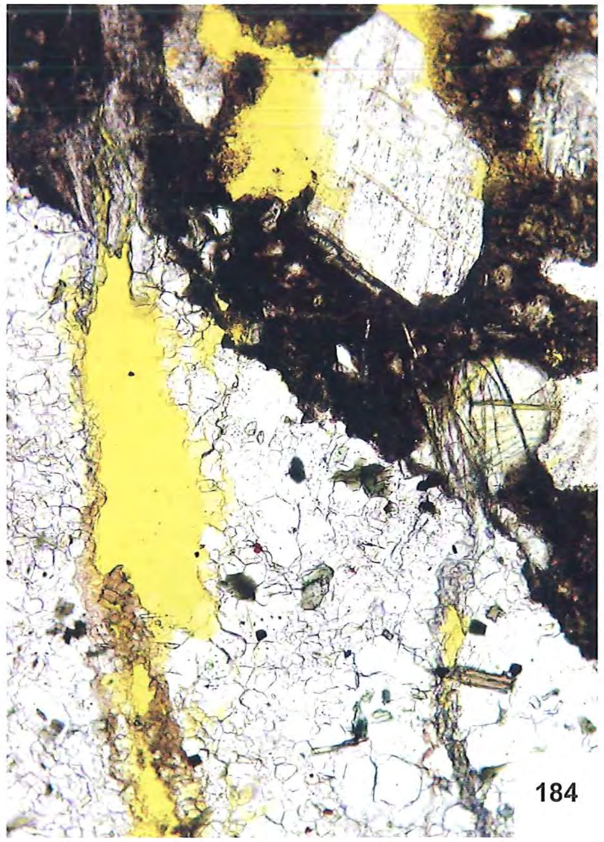
184

185

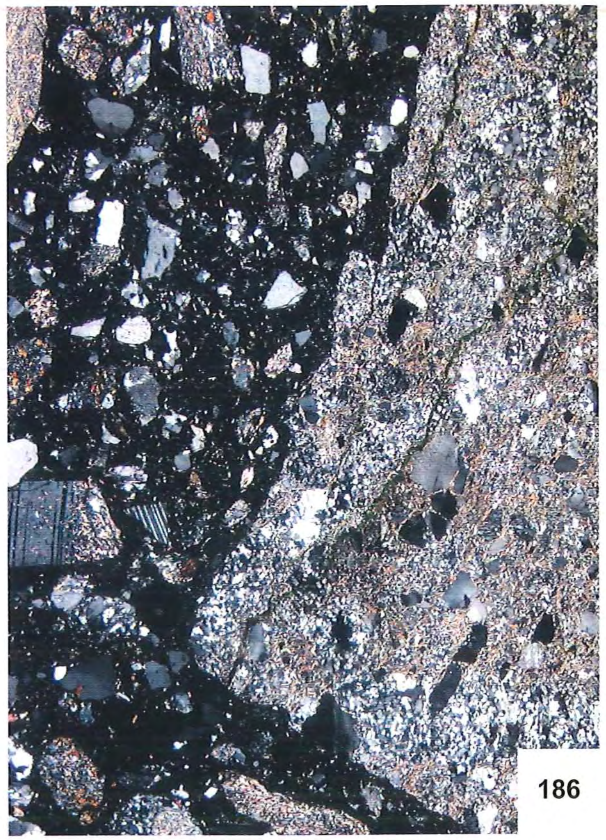

186

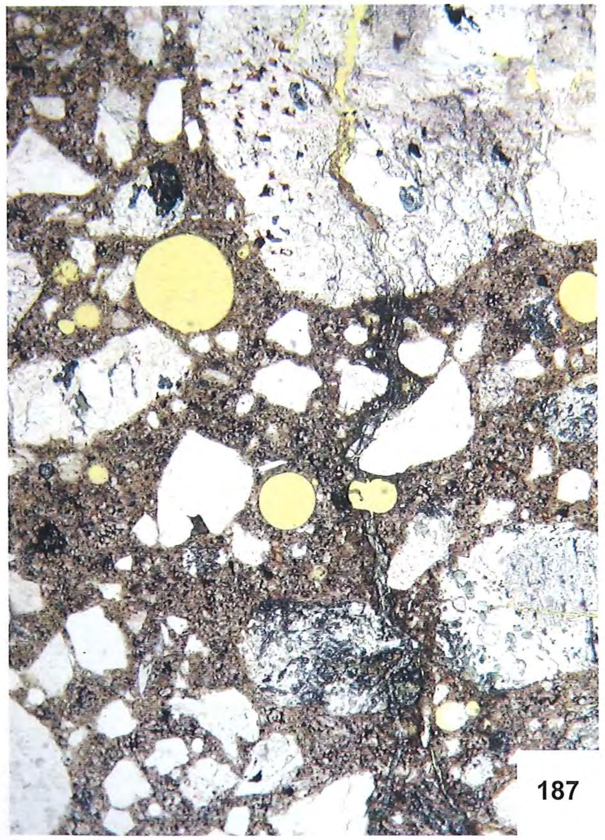

187

188

189

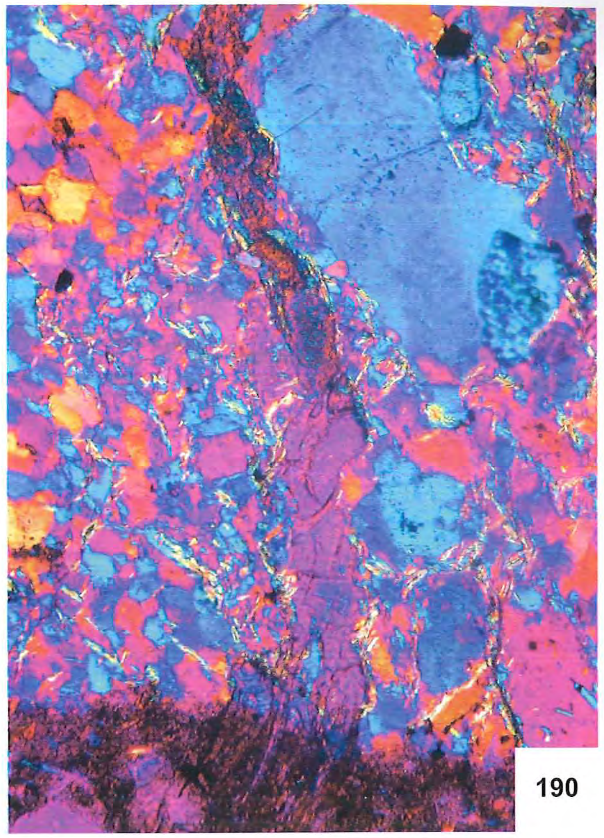

190

191

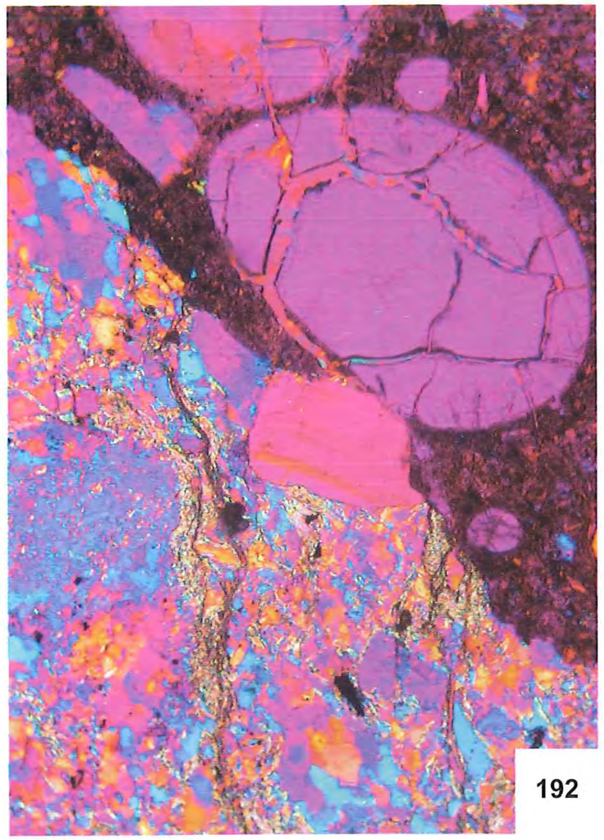

192

Professional Papers of the Geological Survey of Belgium

The series, which started in 1966, welcomes papers dealing with all aspects of the earth sciences, with a particular emphasis on the regional geology of Belgium and adjacent areas. Detailed geological observations are accepted if they are interpreted and integrated in the local geological framework (e.g. boreholes, geological sections, geochemical analyses, etc.). Submitted papers written in English, French, Dutch or German should present the results of original studies. Members of the Geological Survey of Belgium or external reviewers will review each paper.

Editor Geological Survey of Belgium
Jenner str. 13
B-1000 Brussels
Belgium

Guide for authors: see website Geologica Belgica
http://www.ulg.ac.be/geolsed/GB

List of publications and conditions of sale: see website Geological Survey of Belgium
http://www.naturalsciences.be/institute/structure/geology/gsb_website/products/pp
or website Royal Belgian Institute of Natural Sciences
http://www.natuurwetenschappen.be/common/pdf/science/publications/Cata/index.html

ISSN 0378-0902

Impression: Service public fédéral Economie, P.M.E., Classes moyennes et Energie
Drukwerk: Federale Overheidsdienst Economie, K.M.O., Middenstand en Energie

0015-07